

**T.R.**  
**ONDOKUZ MAYIS UNIVERSITY**  
**INSTITUTE OF GRADUATE STUDIES**  
**DEPARTMENT OF NANOSCIENCE AND NANOTECHNOLOGY**



**PHARMACEUTICAL PREPARATION, CHARACTERIZATION  
AND COMPUTATIONAL STUDY FOR PIPENZOLATE  
METHYL BROMIDE AND PHENOBARBITAL NANO-DRUGS  
BY ANTISOLVENT CRYSTALLIZATION METHOD**

Master Thesis

**Marwa Obaid KHALAF**

Supervisor

**Prof. Dr. Müberra ANDAÇ**

This work was supported by the Ondokuz Mayıs University Research Foundation (BAP) Project (PYO.Fen.1904.21.003).

SAMSUN  
2021

## THESIS APPROVAL

By **Marwa Obaid KHALAF**, this study titled “**Pharmaceutical preparation, characterization and computational study for pipenzolate methyl bromide and phenobarbital nano-drugs by antisolvent crystallization method**”, prepared under the consultancy of **Prof. Dr. Müberra ANDAÇ**, was approved by our jury unanimously of votes as a result of the examination held on 18.06.2021 and accepted as a Master Thesis.

	<b>Title Name Surname</b>	<b>University</b>	<b>Department</b>	<b>Signature</b>	<b>Result</b>
<b>Committee Chairman</b>	Asst. Prof. Dr. A. Güralp URAL	Samsun University	Aerospace Engineering Department		<input checked="" type="checkbox"/>
					Accepted
					<input type="checkbox"/>
					Refused
<b>Thesis Advisor</b>	Prof. Dr. Müberra ANDAÇ	Ondokuz Mayıs University	Chemistry Department		<input checked="" type="checkbox"/>
					Accepted
					<input type="checkbox"/>
					Refused
<b>Committee Member</b>	Asst. Prof. Dr. Hilal AY	Ondokuz Mayıs University	Molecular Biology and Genetics Department		<input checked="" type="checkbox"/>
					Accepted
					<input type="checkbox"/>
					Refused

This thesis was approved by the above-named jury members determined by the Institute Administrative Board.

Approved in / /  
Prof. Dr. Ali BOLAT  
Institute Manager

## **ETHICAL STATEMENT**

I declare that all of the information in this dissertation is true and complete, and that it was prepared in accordance with the regulations for Ondokuz Mayıs University Graduate School of Science and thesis writing rules, and that all of the information was referred to and held on the right side of the laws according to scientific ethics while it was being produced.

25/06/2021

Marwa Obaid KHALAF

## **THESIS STUDY AUTHENTICITY REPORT STATEMENT**

**Thesis Title:** Pharmaceutical preparation, characterization and computational study for Pipenzolate methyl bromide and Phenobarbital nano-drugs by Antisolvent crystallization method

As a result of the originality report, which was received from the plagiarism detection program on 20/05/2021 for the thesis work with the above title;

Similarity rate: 23% Select an item.

Single source rate: 2%

25/06/2021

Müberra ANDAÇ

## ABSTRACT

### PHARMACEUTICAL PREPARATION, CHARACTERIZATION AND COMPUTATIONAL STUDY FOR PIPENZOLATE METHYL BROMIDE AND PHENOBARBITAL NANO-DRUGS BY ANTISOLVENT CRYSTALLIZATION METHOD

Marwa Obaid KHALAF  
Ondokuz Mayıs University  
Institute of Graduate Studies  
Department of Nanoscience and Nanotechnology  
Master, June / 2021  
Supervisor: Prof. Dr. Müberra ANDAÇ

A survey revealed that there is currently no efficient method for simultaneously determining the two active pharmaceutical ingredients (pipenzolate and phenobarbital) with proficiency and stability. A new liquid formulation has been invented to treat abdominal spasm in children contains a combination of Pipenzolate methyl bromide and Phenobarbital. So, there must be a necessary to develop a new reliable method and suitable for routine work in pharmaceutical companies

Three main axes have been covered in our project. First part was about computational platforms- based pharmaceutical study of both active pharmaceutical ingredients (Pipenzolate methyl bromide and Phenobarbital) such as molecular docking simulation and Absorption, Distribution, Metabolism, Excretion and Toxicity (ADMET) which represent pharmacokinetics Swiss ADME server. Molecular docking study has been performed by Swiss dock server.

The second part was about quantitative assessment of Pipenzolate methyl bromide and Phenobarbital in liquid dosage form by Reverse Phase-High Pressure Liquid Chromatography (RP-HPLC)-based a new developed method. Validation procedure has been performed to ensure that this method will achieve all requirements according to US pharmacopoeia and International Conference on Harmonization (ICH) guidelines. The validation procedure of developed method demonstrated successfully applied for the quality control routine, also this method exhibits reliable, accuracy, linearity and system suitability results.

The third part regards improve the dissolution rate of Pipenzolate methyl bromide and Phenobarbital in a solid dosage form through synthesizing nanoparticles of by down to up method using antisolvent crystallization technique to prepare colloidal solutions and powders. Several parameters have been optimized to obtain better grade of nanoparticles which included supersaturation solution (concentration), solvent - antisolvent types, solvent - antisolvent ratio, mixing speed, stabilizer, and temperature. An optimum concentration for pipenzolate methyl bromide and phenobarbital for synthesizing nanoparticles has been determined as colloidal solution and powder.

A comparison has been made between colloidal solutions and nanoparticles versus raw active pharmaceutical ingredients in terms of chemical, physical properties, kinetic solubility and characterization depending on FTIR, SEM, TGA, XRD and DSC.

**Keywords:** Pipenzolate MBr, Phenobarbital, Pharmacokinetics, antisolvent crystallization technique, RP-HPLC and stabilizers.

## ÖZET

### ANTİSOLVENT KRİSTALİZASYON YÖNTEMİYLE PİPENZOLAT METİL BROMÜR VE FENOBARBİTAL NANO İLAÇLAR İÇİN FARMASÖTİK HAZIRLAMA, KARAKTERİZASYON VE HESAPLAMA ÇALIŞMASI

Marwa Obaid KHALAF

Ondokuz Mayıs Üniversitesi

Lisansüstü Eğitim Enstitüsü

Nanobilim ve Nanoteknoloji Anabilim Dalı

Yüksek Lisans Tezi, Haziran /2021

Danışman: Prof. Dr. Müberra ANDAÇ

Bir araştırma, iki aktif farmasötik bileşeni (pipenzolat ve fenobarbital) aynı anda yeterlilik ve stabilite ile belirlemek için şu anda etkili bir yöntem olmadığını ortaya koydu. Çocuklarda karın spazmını tedavi etmek için yeni bir sıvı formülasyon icat edilmiştir ve Pipenzolat metil bromür ve Fenobarbital'in bir kombinasyonunu içerir. Bu nedenle ilaç firmalarında rutin işlere uygun, güvenilir ve yeni bir yöntem geliştirilmesi gerekmektedir.

Projemizde üç ana eksen ele alınmıştır. İlk bölüm, farmakokinetiği İsviçre ADME sunucusunu temsil eden moleküler yerleştirme simülasyonu ve Emilim, Dağılım, Metabolizma, Boşaltım ve Toksikite (ADMET) gibi aktif farmasötik bileşenlerin (Pipenzolat metil bromür ve Fenobarbital) her ikisinin de hesaplama platformlarına dayalı farmasötik çalışması hakkındaydı. Moleküler yerleştirme çalışması Swiss dock sunucusu tarafından gerçekleştirilmiştir.

İkinci bölüm sıvı dozaj formunda Pipenzolat metil bromür ve Fenobarbital'in Ters Faz-Yüksek Basınçlı Sıvı Kromatografisi (RP-HPLC) tabanlı yeni geliştirilmiş bir yöntem ile kantitatif değerlendirmesi hakkındaydı. Validasyon prosedürü, bu yöntemin US farmakopesi ve Uluslararası Uyumlaştırma Konferansı (ICH) kılavuzlarına göre tüm gereksinimleri karşılama sağlaması için gerçekleştirilmiştir. Geliştirilen yöntemin validasyon prosedürü kalite kontrol rutini için başarıyla uygulandığını göstermekte, ayrıca bu yöntem güvenilir, doğruluk, doğrusalık ve sistem uygunluğu sonuçları sergilemektedir.

Üçüncü bölüm, kolloidal çözeltiler ve tozlar hazırlamak için antisolvent kristalizasyon tekniği kullanılarak nanopartiküllerin sentezlenmesi yoluyla katı bir dozaj formunda Pipenzolat metil bromür ve Fenobarbitalin çözünme hızının iyileştirilmesi ile ilgilidir. Süperdoyma çözeltisi (konsantrasyon), çözücü - antisolvent türleri, çözücü - antisolvent oranı, karıştırma hızı, stabilizatör ve sıcaklık dahil olmak üzere daha iyi dereceli nanopartiküller elde etmek için çeşitli parametreler optimize edilmiştir. Nanopartiküllerin sentezlenmesi için pipenzolat metil bromür ve fenobarbital için optimum konsantrasyon, kolloidal çözelti ve toz olarak belirlenmiştir.

FTIR, SEM, TGA, XRD ve DSC'ye bağlı olarak kimyasal, fiziksel özellikler, kinetik çözünürlük ve karakterizasyon açısından kolloidal çözeltiler ve nanopartiküller ile ham aktif farmasötik bileşenler arasında bir karşılaştırma yapılmıştır.

**Anahtar Kelimeler:** Pipenzolat MBr, Fenobarbital, Farmakokinetik, antisolvent kristalizasyon tekniği, RP-HPLC ve stabilizatörler.

## ACKNOWLEDGEMENTS

First of all, I would like to thank my supervisor **Prof. Dr. Müberra Andaç** for her support, providing the equipment and devices necessary to complete this work and its success and give them the freedom to work for me and for whom without her good advice and guidance, this work would not have been successful. My supervisor, **Prof. Dr. Müberra ANDAÇ** has been in contact with me throughout all the stages of work and I have been fortunate to be one of her students.

I would also like to express my gratitude and appreciation to **Dr.Prof. Omer ANDAÇ** for his support and participation to get my acceptance in Nanoscience and Nanotechnology department.

I would also like to thank all the members of this department of and engineering faculty of Ondokuz Mayıs University who helped me during the work.

I thank my husband **Mohammed ALSAMARAI**, and my friend **Abdalmohsin AL AIROA** who they helped me in my project.

Finally, I can only offer gratitude and appreciation to my family, without whom I would not have passed all obstacles in my life through their dedicated support to me

## TABLE OF CONTENTS

THESIS APPROVAL .....	i
ETHICAL STATEMENT .....	ii
ABSTRACT .....	iii
ÖZET.....	iv
ACKNOWLEDGEMENTS .....	v
TABLE OF CONTENTS .....	vi
ABBREVIATIONS .....	ix
FIGURES INDEX.....	x
TABLES LIST .....	xii
1. INTRODUCTION .....	1
1.1. Pipenzolate Methyl Bromide (Mbr) .....	1
1.1.1. Antagonists Muscarinic Receptor .....	2
1.1.2. Structure-Activity Relationships (Sar).....	2
1.1.3. Mechanism of Action.....	3
1.2. Phenobarbital.....	3
1.2.1. Anti-Seizure Properties .....	4
1.2.2. Structure-Activity Relationship (SAR).....	5
1.2.3. Mechanism of Action.....	5
1.2.4. Pharmacokinetic Properties .....	5
1.2.5. Toxicity .....	6
2. COMPUTATIONAL ANALYSIS .....	7
2.1. Molecular Docking.....	7
2.2. ADMET Study .....	10
2.3. Chemoinformatic – Based Analysis .....	11
3. QUANTITATIVE ASSESSMENT OF PIPEN AND PHEN .....	13
3.1. Reversed-Phase High-Performance Liquid Chromatography.....	13
3.2. Development Steps of HPLC Method.....	13
3.3. Validation Process for Developed Method .....	15
3.3.1. System Suitability .....	16
3.3.2. Linearity and Concentration Ranges.....	16

3.3.3. Robustness .....	16
3.3.4. Accuracy Test .....	17
3.3.5. Precision Test.....	17
3.3.6. Range .....	18
3.3.7. Detection and Quantitation Limit .....	18
3.3.8. Specificity .....	19
4. NANOTECHNOLOGY AND NANOMATERIALS.....	20
4.1. Nano-Drugs and Their Applications .....	20
4.2. Synthesizing of Drug as Nanoparticles .....	21
4.3. Antisolvent Crystallization Technique.....	22
4.4. Antisolvent Crystallization Parameters and Optimization .....	23
4.4.1. Drug concentration effect .....	23
4.4.2. Stirring Speed Effect.....	23
4.4.3. Flow Rate Effect .....	24
4.4.4. Temperature Effect .....	24
4.4.5. Solvent to Anti Solvent Volume Ratio Effect .....	25
4.5. Colloidal Particles .....	25
5. LITERATURE REVIEW.....	27
6. MATERIALS AND METHODS.....	29
6.1. Computational Studies .....	29
6.1.1. Molecular Docking .....	29
6.1.2. ADMET Analysis .....	30
6.2. Quantitative Assessment of Pipen and Phen by HPLC.....	31
6.2.1. Chromatographic Conditions.....	31
6.2.2. Material And Chemicals Reagent .....	31
6.2.3. Mobile Phase Preparation .....	31
6.2.4. Stock and Test Solutions Preparation .....	31
6.2.5. Calculation .....	32
6.3. Validation of Developed Method .....	32

6.3.1. System Suitability .....	33
6.3.2. Linearity and Concentration Ranges.....	33
6.3.3. Robustness .....	33
6.3.4. Accuracy test.....	33
6.4. Production and Characterization of Nanodrugs in Both Forms (Crystal Powder and Colloidal Solution) .....	34
6.4.1. Materials .....	34
6.4.2. Preparation of Pipenzolate Methyl Bromide and Phenobarbital as Colloidal Particles and Crystal Powder .....	34
6.4.3. Optimization of Antisolvent Crystallization Technique.....	35
6.4.4. Scanning Electron Microscopy (SEM).....	36
6.4.5 Fourier Transform Infrared Spectroscopy (FTIR).....	36
6.4.6. Reverse Phase-High Performance Liquid Chromatography.....	36
6.4.7. X-Ray Diffraction (XRD).....	36
6.4.8. Differential Scanning Calorimetry (DSC) .....	36
6.4.9. Thermogravimetric analysis (TGA).....	37
6.4.10. Image J software .....	37
6.5. Kinetic Dissolution Profile Study .....	37
6.5.1. Preparation of Pipen and Phen-Containing Tablets.....	37
6.5.2. Dissolution Profile Parameters .....	38
7. RESULTS AND DISCUSSION .....	39
7.1. Computational Study .....	39
7.1.1. Docking study .....	39
7.1.2. ADMET Analysis .....	44
7.2. RP-HPLC-Based Quantitative Analysis.....	46
8. CONCLUSION .....	81
REFERENCES.....	82

## ABBREVIATIONS

APIs	Active pharmaceutical ingredients
Pipen	Pipenzolate Methyl Bromide
Phen	Phenobarbital
RP-HPLC	Reverse-Phase High Pressure Liquid Chromatography
ASC	Antisolvent Crystallization
ENs	Engineered nanomaterials
SAR	Structure Activity Relationship
RMS	Root mean square
SEM	Scanning electron microscopy
XRD	X-Ray Diffraction
RMSD	Root mean square distance
ADMET	Absorption Distribution Metabolism Excretion Toxicity
FTIR	Fourier Transform Infra-Red
TGA	Thermal Gravity Analysis
DSC	Differential Scan Calorimetry

## FIGURES INDEX

Figure 1.1. Pipenzolate MBr structure .....	1
Figure 1.2. Phenobarbital structure .....	3
Figure 2.1. Molecular docking steps .....	8
Figure 6.1. Docking requirements and process .....	30
Figure 7.1.A. Native ligand pocket .....	40
Figure 7.1.B. Pipenzolate MBr pocket .....	40
Figure 7.2.A. Native ligand interaction .....	41
Figure 7.2.B. Pipenzolate ligand interaction .....	41
Figure 7.3.A. Native ligand pocket .....	42
Figure 7.3.B. Phenobarbital pocket .....	42
Figure 7.4.A. Native ligand interaction .....	43
Figure 7.4.B. Phenobarbital interaction .....	43
Figure 7.5. Radar plot of Pipenzolate MBr .....	45
Figure 7.7. Chromatogram of std solution for Pipenzolate MBr and Phenobarbital .	50
Figure 7.8. Chromatogram of Spastal drop for Pipenzolate MBr and Phenobarbital	50
Figure 7.9 . Pipenzolate MBr calibration curve .....	51
Figure 7.10. Phenobarbital clibration curve .....	51
Figure 7.11.A. SEM images of Pipenzolate MBr nanoparticles at 30KX .....	60
Figure 7.11.B. SEM images of Pipenzolate MBr nanoparticles at 100KX.....	61
Figure 7.12.A SEM images of Pipenzolate MBr microparticles at 100X Tween20..	61
Figure 7.12.B. SEM images of Pipenzolate MBr microparticles at 100X PVP.....	62
Figure 7.12.C. SEM images of Pipenzolate MBr microparticles at 100X HPMC.....	62
Figure 7.13.A. SEM images of Phenobarbital nanoparticles at 30KX .....	63
Figure 7.13.B. SEM images of Phenobarbital nanoparticles at 50KX.....	64
Figure 7.14.A. SEM images of Pipenzolate MBr microparticles at 100X Tween20.	64
Figure 7.14.B. SEM images of Pipenzolate MBr microparticles at 100X PVP.....	65
Figure 7.14.C. SEM images of Pipenzolate MBr microparticles at 100X HPMC.....	65
Figure 7.15.A. XRD pattern of Pipenzolate MBr raw .....	66
Figure 7.15.B. XRD pattern of Pipenzolate MBr recrystallized .....	66
Figure 7.16. The comparison plot of XRD pattern for Pipenzolate MBr .....	67
Figure 7.17.A. XRD pattern of Phenobarbital raw .....	68
Figure 7.17.B. XRD pattern of Phenobarbital recrystallized .....	68
Figure 7.18. The comparison plot of XRD pattern for Phenobarbital .....	69
Figure 7.19.A. IR chart of Pipenzolate MBr raw .....	70
Figure 7.19.B. IR chart of Pipenzolate MBr recrystallized.....	70
Figure 7.20. IR comparison chart for Pipenzolate MBr.....	71
Figure 7.21.A. IR chart of Phenobarbital raw .....	72
Figure 7.21.B. IR chart of Phenobabitr recrystallized.....	72
Figure 7.22. IR comparison chart for Phenobarbital.....	73
Figure 7.23.A. TG curve of Pipenzolate MBr raw.....	74
Figure 7.23.B. TG curve of Pipenzolate MBr recrystallized .....	74

Figure 7.24.A. TG curve of Phenobarbital raw.....	75
Figure 7.24.B. TG curve of Phenobarbital recrystallized .....	75
Figure 7.25.A. DSC curve of Pipenzolate MBr raw .....	76
Figure 7.25.B. DSC curve of Pipenzolate MBr recrystallized.....	77
Figure 7.26.A. DSC curve of Phenobarbital raw .....	77
Figure 7.26.B. DSC curve of Phenobarbital recrystallized.....	78
Figure 7.27. Comparison dissolution profile of Pipenzolate MBr .....	79
Figure 7.28. Comparison dissolution profile of Phenobarbital .....	80

## TABLES LIST

Table 1. Chromatographic parameters .....	52
Table 2. System suitability of Pipenzolate MBr and Phenobarbital .....	53
Table 3. Linearity data of Pipenzolate MBr and Phenobarbital.....	54
Table 4. Accuracy results of developed method .....	55
Table 5. Repeatability (intra-day)of Pipenzolate MBr and Phenobarbital.....	56
Table 6. Intermediate (inter-day) precision of Pipenzolate MBr and Phenobarbital .	57
Table 7. Intermediate (intra-day)precision of Pipenzolate MBr and Phenobarbital ..	58

# 1. INTRODUCTION

## 1.1. Pipenzolate Methyl Bromide (Mbr)

It is a quaternary ammonium compound (Sweetman, 2009) and anticholinergic agents which block acetylcholine action. It has antimuscarinic actions by targeting a muscarinic receptor of the central nervous system and glandular system similar to other compounds from same pharmaceutical category like Atropine (Vardanyan, 2017), Butylscopolamine, Homatropine methyl bromide, mepenzolate methyl bromide and Anisotropine methyl bromide. It has been used as a cofactor in the medication of flatulent dispepsis and gastrointestinal disorders caused by smooth muscle spasm.

Pipenzolate methyl bromide exerts its action by inhibiting muscarinic (cholinergic) receptors on smooth muscles and prevents the effect of Acetylcholine (muscarinic receptor antagonist). Inhibition of Acetylcholine produces relaxation of smooth muscles of gastrointestinal tract and genitourinary tract and reduces the painful spasm and cramp. It has a structure as shown in figure 1-1 and chemical formula ( $C_{22}H_{28}BrNO_3$ ) with molecular weight 434.4 and CAS number 13473-38-6 (pipenzolate); 125-51-9 (bromide). Synonyms are pipenzolate, methobromide and pipenzolone bromide. The description of Pipenzolate methyl bromide is a white crystalline powder, melting point limit is ( $179^{\circ}C -180^{\circ}C$ ) and freely soluble in water (Moffat et al., 2009). Pipenzolate methyl bromide is not published yet in pharmacopoeia references like USP, BP, EP and JP.

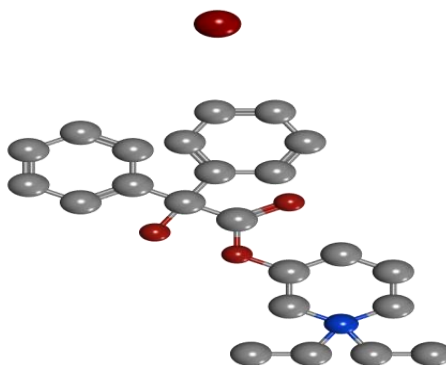


Figure 1.1. Chemical structure of Pipenzolate MBr

### **1.1.1. Antagonists Muscarinic Receptor**

Antagonists' muscarinic receptor includes:

- 1) Scopolamine and atropine are naturally occurring alkaloids.
- 2) Semi-synthetic derivatives of these alkaloids, which differ primarily in their behavior and duration of action in the body from the parent compounds.
- 3) Synthetic derivatives, some of which have muscarinic receptor subtype selectivity (Caulfield et al., 1998).

Homatropine has a shorter duration of action than atropine and methscopolamine, which are quaternized and do not readily cross the blood-brain barrier or membranes, are noteworthy agents in the latter two classes. Muscarinic antagonists generally cause a slight inhibition of nicotinic receptors. On the other hand, quaternary ammonium antagonists exhibit a higher degree of nicotinic blockade and are therefore more likely to interrupt ganglionic or neuromuscular transmission. Methscopolamine bromide, and homatropine methylbromide are all quaternary ammonium derivatives that have had their nitrogen methylated by the addition of a second methyl group (Abrams et al., 2006).

### **1.1.2. Structure-Activity Relationships (Sar)**

Due to the fact that neither the free acid nor the basic alcohol exhibits significant antimuscarinic activity, an intact ester of tropine and tropic acid is needed for antimuscarinic activity. Additionally, the presence of a free OH group is needed for operation in the acyl portion of the ester. When given parenterally, quaternary ammonium derivatives of atropine and scopolamine are usually more active than their parent compounds in blocking muscarinic and ganglionic (nicotinic) receptors. Quaternary derivatives are poorly absorbed and inefficient when taken orally. Both tropic and mandelic acids have an enantiomeric nucleus. Scopolamine is a l-hyoscine analog that is significantly more potent than d-hyoscine. Atropine's antimuscarinic activity is largely due to the naturally occurring l isomer, which is racemized during extraction and is composed of d,l-hyoscyamine. The aromatic acid and bridged nitrogen of tropine are spatially replicated in a wide range of synthetic derivatives. (Birdsall and Lazareno, 2005).

### 1.1.3. Mechanism of Action

Atropine and related compounds compete with acetylcholine (ACh) and other muscarinic agonists for a common binding site on the muscarinic receptor. Due to the competitive nature of atropine antagonism, it can be overcome by adjusting the concentration of ACh at muscarinic receptors in the effector organ. Muscarinic receptor antagonists are less effective at inhibiting responses to postganglionic cholinergic nerve stimulation than injected choline esters. The distinction is clarified by the fact that ACh is released from cholinergic nerve terminals very close to receptors, resulting in extremely high transmitter concentrations at the receptors (Carmin and Brogden, 1985).

### 1.2. Phenobarbital

It has a structure illustrated in figure 1-2 and the chemical formula is  $C_{12}H_{12}N_2O_3$  with molecular weight 232.2, CAS number 50-06-6. Synonyms are phenobarbitone, phenobarbital, phenobarbitalum and phenylethylbarbituric acid (Sweetman, 2009). The description is slightly hygroscopic crystals or white powder which may exhibit polymorphism, melting point limit is (174°C-178°C) and soluble 1g in 1000ml of water, 1g in 8ml of ethanol, 1g in 40ml of chloroform, 1g in 13ml of ether, and 1g in about 700 ml of benzene (Moffat et al., 2009).

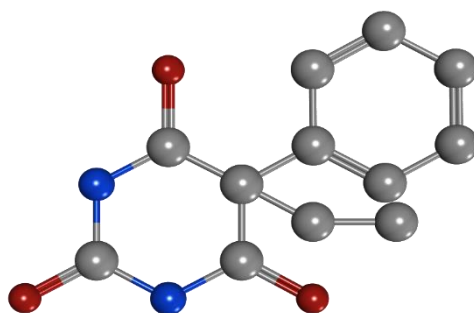


Figure 1.2. Chemical structure of Phenobarbital

Barbituric acid is a commonly used in a variety of chemical fields. While it has no medical benefit, its derivatives, when the two hydrogen atoms at the C-5 position are replaced with alkyl or aryl groups, belong to a significant class of drugs with CNS activity.

They're used as hypnotics to treat insomnia, as well as to alleviate anxiety and provide sedation prior to surgery. Barbiturates can cause a variety of CNS depressions, ranging from mild sedation to deep coma and even death, depending on the dosage. (Neels et al., 2004). Phenobarbitone is used as an antiepileptic to control partial and generalized tonic-clonic seizures. Barbiturates are a part of complex mixtures used to treat weaker forms of pain. Headaches and other types of pain are treated with phenobarbital, acetylsalicylic acid, codeine, or caffeine combinations. Phenobarbital is used to treat neurosis, cardiovascular problems, and hypertension when combined with herbal compounds (Kosior et al., 2006).

Phenobarbital (phenobarbitone), a nonselective central nervous system depressant, is commonly used as an antiepileptic treatment due to a number of benefits, including availability, affordability, a broad range of action, and ease of administration. Additionally, it is used to treat partial and generalized tonic-clonic seizures. Hauptmann discovered its anticonvulsant properties by chance when using it as a hypnotic for his epilepsy patients. (Semah et al., 1994).

As cognitive and behavioral side effects of phenobarbital, fatigue, weakness in adults, insomnia, hyperkinesia, and violence in children (and sometimes in the elderly) have been reported. Additionally, all age groups can experience moderate mood, memory, and learning disturbances. The first effective organic anti-seizure agent was phenobarbital (LUMINAL, others). Due to its low toxicity and low cost, it remains one of the most effective and widely used medications (Livanainen and Savolainen, 1983).

### **1.2.1. Anti-Seizure Properties**

The majority of barbiturates have antiseizure properties. Only a few of these drugs, such as phenobarbital, exert maximal anti-seizure activity at doses lower than those needed for hypnosis, severely restricting their clinical efficacy as anti-seizure medications. Although phenobarbital is relatively nonselective, it is successful in the majority of anti-seizure animal studies. It prevents tonic hind limb extension, pentylenetetrazol-induced clonic seizures, and kindled seizures in the maximal electroshock model (Farwell et al., 1990).

### **1.2.2. Structure-Activity Relationship (SAR)**

Barbiturates' structure-activity relationships have been thoroughly researched. When one of the carbon 5 substituents is a phenyl group, the anti-seizure activity is at its peak. While the 5,5-diphenyl derivative has less anti-seizure efficacy than phenobarbital, it lacks hypnotic activity. Convulsions are caused by 5,5-dibenzyl barbituric acid, on the other hand (Macdonald and Greenfield, 1997).

### **1.2.3. Mechanism of Action**

Potential of synaptic inhibition through an action on the GABAA receptor is most likely the mechanism by which phenobarbital prevents seizures. Phenobarbital enhances the responses of mouse cerebral or neurons in the spinal cord to iontophoretically applied GABA, according to intracellular recordings. These effects were observed at therapeutically important phenobarbital concentrations. Phenobarbital increased the GABAA receptor-mediated current by increasing the length of bursts of GABAA receptor-mediated currents without raising the frequency of bursts, according to studies of single channels in the neurons of spinal cord in mouse isolated from outside-out patches (Twyman et al., 1989). Phenobarbital limits repeated regular firing at levels above therapeutic doses, which may explain several anti-seizure results of increased phenobarbital concentrations obtained during status epilepticus therapy.

### **1.2.4. Pharmacokinetic Properties**

Phenobarbital is fully absorbed but at a sluggish rate; peak plasma concentrations occur several hours after a single dose. It binds to plasma proteins 40-60% and tissues, including the brain, to a similar degree. Near to 25% of a dose is eliminated unchanged in the urine through pH-dependent renal excretion; the remainder is inactivated by hepatic microsomal enzymes, mainly CYP2C9, with some CYP2C19 and CYP2E1 metabolism. Phenobarbital induces the uridine diphosphate glucuronosyltransferase (UGT) enzymes, and also the CYP2C and CYP3A subfamilies. When these enzymes are co-administered with phenobarbital, drugs metabolized by these enzymes will degrade more quickly; specifically, oral contraceptives are metabolized by CYP3A4 (Macdonald and Greenfield, 1997).

### **1.2.5. Toxicity**

Sedation, phenobarbital's most common adverse effect, is apparent in all patients at the beginning of treatment, but tolerance increases over time. Excessive dosage causes nystagmus and ataxia. In infants, phenobarbital can cause irritability and hyperactivity, while in the elderly; it can cause agitation and confusion.

Phenobarbital is added as a synergistically agent with pipenzolate methyl bromide for increasing the spasmolytic action (Abo-Talib and El-Ghobashy, 2009). Pipenzolate methyl bromide is present in combination with phenobarbital as a liquid pharmaceutical formulation (oral drops) in middle east markets under trade mark (Babytal drops) in Egypt and (Piplar drops) in India.

A several spectrophotometric methods are suggested for the determination of pipenzolate methyl bromide alone by UV-spectrophotometer or by HPLC or within a combination of other active pharmaceutical ingredients like chlordiazepoxide by UV-spectrophotometer, but doesn't have the required accuracy and stability when validation protocol has been applied because of the phenobarbital and pipenzolate methyl bromide peaks are merging or just one peak or no peak appears under chromatographic parameters they suggested. Pipenzolate methyl bromide is not official yet in a different pharmacopoeia reference.

## **2. COMPUTATIONAL ANALYSIS**

### **2.1. Molecular Docking**

Over the past few decades, several experimental and high-throughput screening methods have been used in drug production. Historically, developing new medicinal drugs was prohibitively expensive, time consuming, and unsuccessful.

To overcome the shortcomings of traditional methods, more effective and logical methods based on virtual screening have been introduced. Depending on the availability of structural data, the virtual screening approach may be classified as structure-based or ligand-based. The structure-based approach emphasizes molecular docking, while the ligand-based approach emphasizes quantitative structure-activity relationships and pharmacophore modeling. The availability of structural information about proteins and protein-ligand complexes through chemical synthesis, purification, X-ray crystallography, and Nuclear Magnetic Resonance Spectroscopy (NMR) has resulted in the identification of a diverse array of therapeutically important molecular targets (Meng et al. 2011).

The ligand-target molecule interaction is determined by the molecular docking method. It determines the preferred orientation of the ligand's minimum free binding energy in order to form a stable complex with the protein (Ferreira et al., 2015).

This interaction involves non-covalent interactions such as hydrogen bonds, ionic bonds, hydrophobic interactions, and van der Waals interactions. A docking analysis between a protein and another protein, a protein and a ligand, or a protein and a nucleotide is possible (Rangaraju and Rao, 2013). The steps in the molecular docking method include the preparation of three-dimensional structures of proteins, the preparation of ligands, the calculation of the binding energy of the protein-ligand complex, and the analysis of the effects, as shown in Figure 2-1 below (Mukesh and Rakesh, 2011).

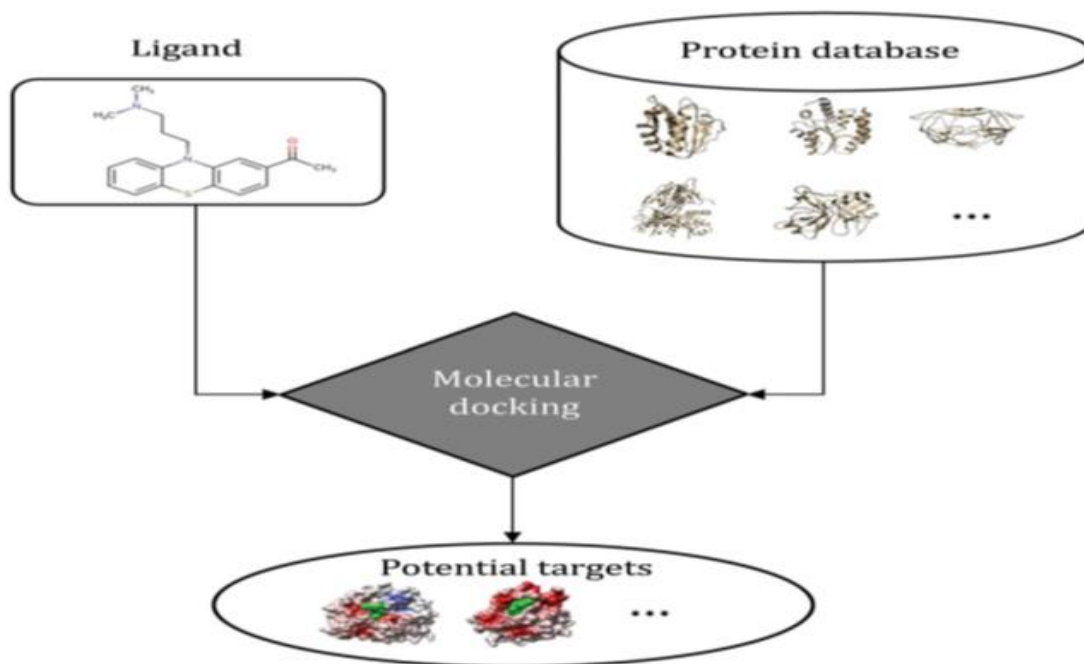


Figure 2.1. Molecular docking steps

The protein and the ligand are physically separated in this method, and the ligand eventually makes its way into the protein's active site after a certain number of "moves" in its conformational space. Internal ligand shape changes, such as torsion angle rotations, as well as rigid body alterations such as translations and rotations, are included in the motions. Each of these alterations to the ligand's conformation space results in a cumulative energetic value for the system, so the total energy of the system is measured after each change. Different scoring functions, such as force-field based functions, empirical scoring functions, knowledge-based scoring functions, Consensus scoring, and descriptor-based scoring functions, are used to calculate the interaction between ligand and receptor in terms of minimal binding free energy. (Kitchen et al. 2004).

The benefit of the simulation approach is that it is more amenable to modeling ligand versatility, while shape complementarity techniques need some ingenious methods to do so. Additionally, the mechanism is physically more similar to what occurs in reality when the protein and ligand meet one another following molecular recognition. A simple drawback of this technique is that it requires more time to determine the correct binding pose since it must traverse a relatively broad energy landscape.

However, grid-based approaches and rapid optimization techniques have greatly alleviated these issues.

Covalent docking of irreversible inhibitors on a target receptor has been published in recent studies. Due to the creation of a tight linkage between the electrophile (ligand) and the nucleophile, covalent docking results in highly potent and selective chemical probes (protein). Numerous FDA-approved drugs have been discovered to contain covalent bonds, including aspirin, warfarin, azacitidine, and isoniazid. Covalent bonding can be used to benefit virtual screening, lead optimization, QSAR analysis, and molecular dynamics simulation (Kumalo et al., 2015; London et al., 2014).

Molecular docking can be performed manually or automatically. After identifying the binding groups on the ligand and binding site, the ligand is manually docked with the binding site's complementary group. The bonding distance between each possible interaction is calculated.

The software repositions the molecule inside the binding site in order to find the best fit as defined by the operator. The paired groups are not directly overlaid, but rather fitted together to achieve the desired bonding distances. Docking can be performed automatically, with the software determining how the ligand should be docked. The docking software serves a dual purpose.

- I. The ligand must be placed in various orientations or binding modes inside the active site.
- II. It must score the various binding modes in order to determine which are the strongest.

The order of complexity may be (a) rigid bodies for both the ligand and the target; (b) rigid bodies for the target but flexible bodies for the ligand; and (c) flexible bodies for both the target and the ligand.

Molecular docking can lead to the discovery of therapeutic drugs in a variety of ways, including:

- I. Target identification
- II. Drug screening for potent activators/inhibitors against specific diseases
- III. Lead optimization in the development of new drugs
- IV. Prediction of active site existence and binding mode
- V. Chemical compound synthesis in a shorter amount of time (Anushree and Krishna, 2017).

## 2.2. ADMET Study

In Silico ADMET prediction is a critical component of pharmaceutical research and development. Last year, the FDA authorized 59 new molecular entities, with small molecules accounting for 64% of approved therapies. Pharmacokinetic properties estimation has been critical in guiding hit-to-lead and lead optimization activities during the early stages of drug production. Due to the extreme complexity of the current R&D model, drug discovery companies have concentrated their efforts on molecular modeling techniques for detecting trends in ADMET data and converting them to knowledge. The field has advanced in lockstep with chemoinformatics, which has advanced from traditional chemometric techniques to advanced machine learning techniques.

Drugs with a high potency, affinity, and selectivity for their molecular target, as well as adequate absorption, distribution, metabolism, excretion, and tolerable toxicity, have a balanced property in terms of pharmacodynamics (PD) and pharmacokinetics (PK) (Ferreira and Andricopulo, 2019).

Coordination of the optimization of these interdependent variables is a significant challenge in drug growth (Segall, 2014). To that end, unprecedented efforts have been made to develop technologies capable of forecasting PD and PK endpoints during hit-to-lead and lead optimization programs (Cheng et al., 2013; González et al., 2017).

Over the last decade, pharmacokinetic properties have had less of an effect on drug R&D attrition rates, despite the increasing prevalence of efficacy and safety concerns (Waring et al., 2015). This reduction is the result of enhanced pharmacokinetic monitoring programs and their earlier integration into the research pipeline. By simultaneously targeting several PK parameters, fully integrated ADMET prediction platforms can easily eliminate unsuitable compounds, reducing the number of synthesis evaluation cycles and reducing the number of more expensive late-stage failures. As the market's demand for innovative products has increased in lockstep with increasing risks and costs associated with research and development, ADMET's prediction has become commonplace. 90 percent dropout rates between clinical trials and marketing authorization, as well as estimated costs of

\$2.6 billion per new chemical entity (NCE), demonstrate the gravity of the situation (Fleming, 2018).

The pharmaceutical industry needs powerful cheminformatics tools for comparing the molecular structure, physicochemical properties, and ADMET endpoints of compounds (Ferreira and Andricopulo, 2019).

### **2.3. Chemoinformatic – Based Analysis**

Without the appropriate tools, it's difficult to deal with a massive amount of molecular data. In this paper, we discuss the need for directed virtual libraries and how to build them in order to design efficient molecules and optimize them for lead generation. Rather than their structures, experimental chemists and biologists are more concerned with the properties of chemicals and their interactions with biological systems, both beneficial and detrimental. Chemoinformatics was designed with the aim of associating newly discovered chemical structures with their predicted action, property, or toxicity. Property prediction software saves time, money, and the lives of laboratory animals.

They aid in making informed decisions, especially in cases involving pharmacodynamic studies of drug molecules in humans, which inevitably involve ethical and safety concerns. Property prediction is a necessary component of virtual screening, which is central to drug design and in which chemoinformatics plays a critical role. Agrochemicals and environmental science, specifically pollutant toxicity and biodegradability prediction, are two additional fields in which structure–activity relationship-based principles are applicable to virtual screening. Chemoinformatics can demonstrate how to develop software tools for constructing virtual libraries based on a set of molecules with similar properties, fragments, or bioactivity continuums (Karthikeyan and Vyas, 2014).

Chemical properties, bioactivities, and data on toxicity derived from the scientific literature or experimental results are used to create predictive models using sophisticated statistical methods or machine learning techniques, based on the principle that "similar structures have similar properties" (Hansch et al., 1990).

The performance of a predictive model is heavily influenced by the choice of suitable molecular descriptors and the precision of experimental findings (Tropsha et al., 2003). Molecular descriptors are structural features that encode independent properties such as action, property, and toxicity. The aim of computing binary fingerprints and descriptors from a molecular graph and its three-dimensional (3D) chemical structure is to investigate the relationship between structure and property (Seybold et al., 1987).

Descriptors are properties that allow a molecule to be classified based on its physicochemical properties, such as melting or boiling points, or on algorithms, such as two-dimensional (2D) fingerprints (Todeschini and Consonni, 2009). A variety of molecular descriptors and features are used to define structure–property relationships. The constitution, surface, molecular connectivity, electrostatics, shape, geometry, quantum chemical, physico-chemical, and hybrid properties, as well as other molecular descriptors, are all inextricably linked (Karelson, 2000).

The most fundamental and widely used descriptors are constitutional descriptors, which essentially include information about a molecule's chemical composition. Topological descriptors, which encode a molecule's surface properties, are used to determine a drug's solubility and permeability. Electrostatic descriptors such as polarizability, dipole moment, and ionization energy are used to predict crystalline density. Geometrical or three-dimensional descriptors based on XYZ coordinates provide more information about the position of a molecule in space than other types of descriptors and are therefore more accurate at predicting biological activity (Balaban, 2006).

### **3. QUANTITATIVE ASSESSMENT OF PIPEN AND PHEN**

#### **3.1. Reversed-Phase High-Performance Liquid Chromatography**

RP-HPLC is used to separate molecules based on their hydrophobicity. The separation is dependent on the solute molecule's hydrophobic interaction with the immobilized hydrophobic ligands on the stationary phase, i.e., the sorbent. The solute mixture is initially added to the sorbent in the presence of aqueous buffers, and the solutes are eluted from the mobile phase by adding organic solvent.

Elution may take place under isocratic conditions, under which the concentration of organic solvent remains constant, or under gradient elution, under which the amount of organic solvent gradually increases over time. Thus, the solutes are eluted in ascending order of molecular hydrophobicity. Due to a variety of reasons, RP-HPLC is a very effective technique for the study of pharmaceuticals, peptides and proteins. These factors include the following:

- 1- The excellent resolution that can be obtained for quite closely related molecules as well as structurally very distinct molecules under a wide variety of chromatographic conditions.
- 2- The ease with which chromatographic selectivity can be manipulated experimentally by modifying the mobile phase characteristics.
- 3- The relatively high rate of recovery and, consequently, the high rate of productivity.
- 4- The high reproducibility of repeated separations over an extended period of time, which is due in part to the sorbent materials' stability under a wide variety of mobile phase conditions (Aguilar and Hearn, 1996).

#### **3.2. Development Steps of HPLC Method**

In the pharmaceutical industry, analytical method creation is a crucial task. It's important to create an analytical method because there are numerous column forms, operating parameters, mobile phase composition, diluent composition, and pH values available. A good analytical method should be easy, with a common column, mobile phase, and buffer. It's easy to do step by step.

The steps for developing an HPLC system are as follows:

- Selection of method
- Selection of chromatographic conditions
- Optimization of parameters

**1. Choosing an HPLC Analytical Method:** First, look at the product literature.

It will assist you in comprehending the essence of the commodity, which will aid in the selection of the various parameters.

**A. Sample Preparation:** To make a simple solution for HPLC analysis, select an appropriate method for sample preparation based on the sample's solubility, filtration, extraction, or other special requirements.

**B. Chromatography:** For most samples, reverse phase chromatography is used, but when acidic or basic molecules are present, reverse phase ion suppression (for weak acid or base) or reverse phase ion pairing (for strong acid or base) should be used. It's best if the stationary step is C18 bonded. When it's necessary to distinguish product isomers, normal phase is used for analytes with a low to moderate polarity. For normal phase separations, use cyano bonded phase. For inorganic anion or cation analysis, ion exchange chromatography is the best choice. Size exclusion chromatography is the safest method to use if the analyte has a high molecular weight.

**C. Gradient HPLC (also known as isotonic HPLC):** It is useful for analyzing complex samples with multiple components. It will help in achieving higher resolution than isotonic HPLC, which has a constant peak width while the peak width increases with retention time in isotonic HPLC. Gradient HPLC has an excellent sensitivity, especially for products with longer retention periods.

**D. Column Size:** The majority of the tests are run on 100-150 mm columns.

It cuts down on the time it takes to create a system and analyze a sample.

For complex samples that take longer to separate, larger columns are used. Initially, a flow rate limit (0.8 - 1.5) ml/min and a column particle size of 3 to 5 m should be maintained.

**E. HPLC Detectors:** If the analyte contains chromophores that allow UV detection, it is preferable to use a UV detector. UV detectors are often preferred over other types of detectors. Fluorescence and electrochemical detectors can be used for trace analysis. High-concentration samples can be tested using refractive index detectors.

**F. The wavelength at which the sample is most sensitive to UV light is max.** It detects chromophores present in sample components.

A wavelength greater than 200 nm has a greater sensitivity than a wavelength shorter than 200 nm. Wavelengths shorter than 200 nm generate much more noise and should be avoided.

**2. Chromatographic Conditions Selection:** After selecting an analytical method, a variety of chromatographic conditions are selected.

The solvent concentration in the mobile phase has an effect on the analytes' movement through the column. Typically, the retention time is determined by the solvent concentration. The pH of the mobile phase and the ion pairing reagents also affect the retention time of the sample. The gradient method is used to analyze samples containing a large number of components in order to avoid an extended retention time, while the isotonic system is used to analyze samples containing only one or two components.

**3. Parameter Optimization:** Some parameters, such as column dimensions, particle size, run time, and flow rate, are optimized after taking the same sample runs. It is achieved in order to achieve the highest resolution and the shortest possible run time. After the research method has been properly optimized, it is checked to ensure that the analytical method is consistent. All regulatory agencies now require that analytical methods be validated.

### **3.3. Validation Process for Developed Method**

Following the development of an analytical method, it is critical to ensure that the procedure reliably produces the desired precise outcome with a high degree of accuracy. The process should produce a particular result that is unaffected by outside factors. This necessitates the validation of the analytical procedures.

Analytical method validation is the process by which we can make sure that all suggested parameters of the procedure meet the requirements through laboratory studies for the intended analytical applications.

Validation process must be performed for a new analytical method or for existing methods when the formula changes are made for the pharmaceutical products and synthesis of the drugs substances.

The validation is performed according to US pharmacopoeia (Pharmacopeia, 2016) and International Conference on Harmonization (ICH) guidelines as shown in the validation of analytical procedures and methodology of ICH Q2A&B (Borman and Elder, 2018). Each validation process consists of the next steps:

### **3.3.1. System Suitability**

Numerous analytical techniques incorporate device suitability testing into their workflow. The tests are based on the concept that the equipment, electronics, analytical procedures, and samples to be studied are all components of a broader system that can be assessed. The criteria for the device suitability test for a particular procedure are determined by the type of procedure being validated. They are especially applicable in the chromatographic techniques.

### **3.3.2. Linearity and Concentration Ranges**

Linearity refers to the ability of method to generate test results that are proportional to the concentration of the analyte within a specified range, either directly or through a well-defined mathematical transformation. It can be calculated visually by observing a chart of signals as a function of the concentration of the substance analyte. If a linear relationship tends to exist, statistical approaches may be used to evaluate the test results. The degree of linearity can be calculated using the regression line data.

### **3.3.3. Robustness**

The robustness of an analytical method refers to its ability to remain unaffected by small but deliberate adjustments to the methodological parameters stated in the procedure report, and it indicates the procedure's suitability for routine use. The robustness of an analytical procedure can be calculated during its growth. If measurements are subject to changes in analytical parameters, the conditions must be properly controlled or the protocol should include a precautionary statement. A set of device suitability parameters (resolution test for example) should be developed as a result of the robustness assessment to ensure that the analytical procedure's validity is preserved whenever it is used.

Examples of common variations in liquid chromatography include:

- pH value of mobile phase.
- The mobile phase components.
- Different columns.
- Temperature.
- Flow rate.

#### **3.3.4. Accuracy Test**

Accuracy is an empirical process that determines the degree to which the test results obtained using the suggested procedure are identical to the true value. According to ICH guidelines, accuracy of suggested method is determined using three different concentrations at mg/ mL of APIs with at least duplicate at each concentration.

#### **3.3.5. Precision Test**

The precision of the suggested method is the closeness of replicate results acquired from the same homogeneous sample analysis. When an analytical method is repeated on multiple samplings of a homogeneous sample, the precision is the degree of agreement among individual test results. The standard deviation or relative standard deviation of measurements sequence is commonly used to express the accuracy of an analytical method. Precision is measured on three different scales: repeatability, reproducibility, and intermediate precision.

##### **A. Repeatability**

The use of an analytical technique inside a laboratory for a short period of time by the same analyst using the same equipment is referred to as repeatability. A minimum of nine determinations covering the procedure's defined spectrum should be used to determine repeatability (three concentrations with three replicates per each concentration, or at least six determinations at 100% of the test concentration).

##### **B. Reproducibility**

It refers to the uniformity of laboratory findings like collaborative experiments, which are often used to standardize methods. An inter-laboratory trial is commonly used to show reproducibility.

### **C. Intermediate Precision**

The effects of laboratory variations due to random events such as application in different days, another equipment and another analyst are referred to as intermediate precision. For each form of precision examined, the standard deviation value, relative standard deviation value and confidence interval value should all be recorded.

#### **3.3.6. Range**

The range of an analytical procedure is the distance between the upper and lower levels of analyte sample that have been demonstrated to be measured with a sufficient precision degree accuracy, and linearity degrees using the procedure as written. Typically, the spectrum is measured in the same units as the test results for the analytical process.

Consider the following minimum defined ranges:

- Drug assay: The limit should be (80 – 120) % of the labeled amount.
- Impurity determination: The limit should be (50 – 120) % of the acceptance criterion.
- Uniformity of content: (70 – 130) % of the test concentration, unless broader or more appropriate range is justified by the design of the dosage type.
- Dissolution rate:  $\pm 20\%$  over the indicated range if the acceptance limits for a controlled-release product include a range of 20% after one hour to 90% after 24 hours, the validated range will be (0 - 100) % of the label claim.

#### **3.3.7. Detection and Quantitation Limit**

The Detection Limit of an analyte is the least concentration of the sample that can be determined in a sample but not quantified. The Quantitation Limit is the least concentration of the sample that can be determined with adequate precision and accuracy under the defined operating conditions of the analytical procedures.

The following are several methods for determining the Detection and Quantitation Limits:

## **A. Visual Evaluation**

Non-instrumental approaches may benefit from visual evaluation. The detection limit for non-instrumental procedures is usually calculated by analyzing samples with known concentrations and determining the lowest amount at which the analyte can be reliably detected. The quantitation limit is usually established by analyzing samples with known analyte concentrations and determining the lowest level at which the analyte can be measured with sufficient accuracy and precision. Instrumental approaches can also be used in conjunction with the visual evaluation approach.

## **B. Signal to Noise**

This technique is applicable only to analytical procedures that generate baseline noise. The signal-to-noise ratio is determined by comparing measured signals from samples with known concentrations to those from blank samples and calculating the minimum concentration at which can be correctly detected and quantified for the Detection Limit and Quantitation Limit. The detection limit is normally estimated using a signal-to-noise ratio of 3 or 2:1, whereas the quantitation limit is determined using a normal signal-to-noise ratio of 10:1.

### **3.3.8. Specificity**

Specificity refers to the ability to measure the analyte of interest accurately and precisely in the presence of other components present in the sample matrix, such as impurities, degradation products, and matrix components. The existence of related materials like impurities and/or excipients must be shown to have no impact on the analytical process.

When conducting recognition tests, the method must be able to differentiate between potentially present compounds with identical structures. If the assay and impurity are identical, the resolution of the two components is closest to one another shows specificity.

It is not always possible to establish the uniqueness of an analytical method for a particular analyte (complete discrimination). Combining two or more analytical methods is recommended in this case to achieve the desired degree of discrimination.

## **4. NANOTECHNOLOGY AND NANOMATERIALS**

Nanotechnology refers to the analysis and manipulation of materials at the nanoscale, which are usually smaller than 100 nanometers in dimension. (Betle, 2012). Nanoparticles are used in a variety of ways, depending on their scale, orientation, and physical properties, which can affect the fabric's performance (Daniel and Astruc, 2004). It's also rapidly gaining traction in a variety of fields, including healthcare, devices, biomedical applications, pharmaceutical industries, drug delivery and catalysis (Colvin et al., 1994). Nanomaterials are the basic building blocks of nanotechnology, with measurements less than 100 nanometers on their shortest dimension or structures of such small dimensions that they can be incorporated into larger materials (Bleeker et al., 2012). Nanomaterials are often made from existing chemical materials or completely new chemical compounds, as well as from the synthesis of one or more components. Nanotechnology offers many advantages in various fields of science. In this regard, nanoparticles are the essential building blocks of nanotechnology. Recent advances in nanotechnology have proven that nanoparticles acquire a great potential in medical applications (Yetisgin et al., 2020).

### **4.1. Nano-Drugs and Their Applications**

Pure drug crystals with particle sizes less than a few hundreds of nanometers are known as drug nanocrystals (Lu et al., 2015; Lu et al., 2016). As the size of a particle is reduced to the nanometer scale, the surface area increases dramatically, making dissolution easier. Nanocrystal formulations were primarily created to improve oral bioavailability and reduce pharmacokinetic variability in poorly soluble drugs (Xie et al., 2018). Oral drug products based on nanocrystals have been commercialized in large numbers. The majority of these drugs use drug nanocrystals made by milling larger drug crystals from the top down. Surfactants are often used to treat the surface of nanocrystals in order to minimize their size and preserve their size distribution, which raises safety issues due to surfactant-induced side effects (Pramanick et al., 2013).

Furthermore, the use of stabilizer materials raises the total chemical pressure on the patient; as a result, drug loading is minimized, potentially exacerbating toxic reactions (Ren et al., 2019).

There is a growing interest in nanotechnology and its applications in a variety of fields, especially medicine for diagnostic, therapeutic, and research biomedical tools. It can be described as any method or technique for producing nanoscale materials with particle sizes ranging from 1 to 100 nanometers. Nanomedicine is the use of nanotechnology to improve human health. As a result, nanotechnology has firmly established itself in the field of drug delivery, with the aim of maximizing drug therapeutic activity while minimizing undesirable side effects. In this paper, we discuss nanoparticles and nanofibers, as well as their medical applications. Nanoparticles have special properties due to their small size and high surface area, resulting in higher particle numbers than those prepared using traditional methods. Nanoparticles may also be used to enhance drug bioavailability by enhancing biodegradability and biocompatibility. Water filtration, tissue engineering scaffolds, wounds, fiber composites, drug release, and protective clothing are just some of the applications (Ibrahim, 2020). Nanoparticles combined with the therapeutic agents overcome problems associated with conventional therapy; however, some issues like side effects and toxicity are still debated and should be well concerned before their utilization in biological systems. It is important to understand the specific features of therapeutic nanoparticles and their delivery strategies (Yetisgin et al., 2020).

#### **4.2. Synthesizing of Drug as Nanoparticles**

Nanoparticles can be obtained either by top-down approach or bottom-up approach (Zhang et al., 2009). The top-down approach involves the mechanically reduction of previously formed larger particles by the technologies available like; jet milling, pearl mill, spiral media milling technology, and high-pressure homogenization. However, these techniques are not efficient due to high energy input and denaturation during the milling process (Cho et al., 2010). In contrast, the approach known as “bottom up” which includes anti solvent precipitation technology is rarely applied. As compared to milling and high-pressure homogenization (top-down approach), anti-solvent crystallization (“bottom up” approach) is simple, cost effective, and easy to scaleup (Kakran et al., 2012).

Nanoparticle preparation can be divided into two categories: top-down and bottom-up (Shegokar and Müller, 2010). Top-down methods are used to create nanoparticles, which involve the breakdown of large particles into smaller particles

through high-energy processes such as wet milling and high-pressure homogenization (Gao et al., 2008). Bottom-up approaches, on the other hand, begin at the molecular level and work their way up. Precipitation/crystallization can be used to make nanoparticles in this process (Thorat and Dalvi, 2012).

### **4.3. Antisolvent Crystallization Technique**

At the research scale, an anti-solvent crystallization method is being used to produce nanoparticles or microparticles for drugs that are poorly soluble in water. This approach is capable of altering the solid-state properties of pharmaceuticals, such as crystal formation and particle size distributions.

Anti-solvent crystallization is a technique that can be used in place of cooling or evaporative crystallization. Antisolvent crystallization has the potential to modify the physical properties of pharmaceutical compounds, such as crystal formation and particle size distributions. Antisolvent crystallization can be used in the production of submicronic particles of pharmaceutical compounds as well as in the manufacture of crystals that require an enhanced drug release rate. Indeed, the polycrystalline drug particles with higher amorphous portions exhibit a faster dissolution rate in solutions. In general, three types of fluids: gas, liquid, and supercritical fluids can be employed as anti-solvents. Additionally, water can be used as an anti-solvent due to its low solubility in the majority of drug compounds and relative miscibility with a small number of polar solvents (Kurup and Arun, 2016).

The compound is dissolved in an organic solvent and then precipitated with the addition of an antisolvent. Crystal growth following precipitation is one of the most serious problems associated with nanoparticles. (Sinha et al., 2013).

The presence of a stabilizer may be more effective in preventing crystal growth and nanoparticle aggregation. A hydrophilic stabilizer may also improve the wettability of hydrophobic products, improving their water solubility and oral bioavailability. Combining bottom-up and top-down techniques has been used recently to track particle size and prevent nanocrystals in suspension from aggregating (Thorat and Dalvi, 2012).

## **4.4. Antisolvent Crystallization Parameters and Optimization**

### **4.4.1. Drug concentration effect**

The precipitated particles have a size that is inversely proportional to the drug concentration. The amount of precipitated drug particles decreases as the drug concentration increases. This proportion reflects the nucleation rate's dependence on the concentration of the substance in the solution from which it crystallizes. The degree of supersaturation will affect the nucleation rate, which is dependent on the concentration of the drug solution. The rapid rate of nucleation results in the formation of a large number of nuclei, which increases the number of crystals and hence the size of each crystal.

They discovered that up to a certain concentration of the drug solution had no effect on the crystal habit of Roxithromycin (Park and Yeo, 2010). However, as the concentration is increased further, the resulting particles begin to agglomerate together during the precipitation process, resulting in a poor distribution of the final product's size and shape.

This phenomenon may be explained by the formation of nuclei at the solvent/antisolvent interface and the effect of drug concentration on viscosity. The presence of a large number of nuclei inhibits diffusion from solvent to anti-solvent, resulting in particle aggregation (Kakran et al., 2012; Wang et al., 2007; Li et al., 2011).

Increased viscosity in the drug solution impedes drug diffusion between solution and anti-solvent, resulting in non-uniform super saturation and agglomeration. Kakran et al. found a reversal of this pattern when the stirring speed was increased to 1000 rpm and the concentration was increased from 5 to 15 mg/ml. As a result of this observation, it can be concluded that as mixing increases, the super saturation effect of drug concentration outweighs the agglomeration effect. As a result, even at higher drug concentrations, the smaller particles are formed at the higher stirring speed.

### **4.4.2. Stirring Speed Effect**

The stirring speed is critical because it affects the mixing phenomena between solvent and anti-solvent, which results in a decrease in the solubility of the solute in the solvent.

A general effect of increasing the stirring speed is that the particle size decreases due to the intensification of micro mixing (mixing at the molecular level) between the multiphases.

Increased micro mixing efficiency enhances mass transfer and diffusion between multiphases, resulting in a high homogeneous super saturation that promotes rapid nucleation and the formation of smaller drug particles. As the stirring speed is increased, the high-intensity speed produces a large amount of heat energy, raising the temperature and causing the nanoparticle size to expand (Zhang et al., 2009).

#### **4.4.3. Flow Rate Effect**

The rate at which the solution and antisolvent are mixed (injection rate) determines the particle size. The mixing of the two-liquid media at a faster and slower rate creates smaller and larger crystals, respectively. At low flow rates, the solvent/antisolvent mixing efficiency decreases, prolonging the crystal growth phase and resulting in the creation of larger crystals.

In comparison, increasing the flow rate increases the amount of solvent/antisolvent mixed per unit time, resulting in the shortest possible time for crystal growth and the formation of smaller crystals.

On the other hand, they observed no noticeable decrease in the diameter of the curcumin particle as the flow rate increased, owing to the fact that curcumin crystallizes in one direction, resulting in needle-shaped crystals. (Kakran et al., 2012; Liu et al., 2010; Li et al., 2011).

#### **4.4.4. Temperature Effect**

According to crystallization theory, the nucleation rate is inversely proportional to temperature. Thus, temperature is regarded as a critical governing factor because it has the ability to influence the final particle size and distribution.

When crystallization occurs at higher temperatures, larger crystals are formed. Zhang et al. found that the precipitated particles had a mean size of approximately 2 microns at 30 °C and an irregular flake-like morphology, while the particles collected at 3 °C had a rod-like morphology and a diameter of approximately 240nm.

The solubility of the drug in the solvent-antisolvent mixture decreases at low temperatures, resulting in a higher supersaturation state. As a result, low temperatures slow diffusion and growth at the crystal boundary layer interface. As a result, at low temperatures, smaller drug particles are obtained.

#### **4.4.5. Solvent to Anti Solvent Volume Ratio Effect**

The volume ratio of solvent to antisolvent is a critical parameter that affects the particle size. The particle size decreases dramatically as the ratio increases. When the drug solution is added to the anti-solvent, the concentration of the drug rapidly decreases as the amount of anti-solvent increases, precipitating the drug into nanoparticles. Additionally, a higher anti-solvent concentration results in a faster nucleation rate, which results in smaller nuclei and simultaneous growth. The greater the anti-solvent number, the greater the diffusion distance for growing species, and thus diffusion becomes the limiting stage for growth nuclei (Kakran et al., 2012; Li et al., 2011).

Unlike crystal growth, nucleation is more dependent on super saturation and has a major effect on the final particle size distribution. There is an inverse relationship between the critical size and the logarithm of the super saturation ratio. Tiny particles are produced as a result of the large number of nuclei formed in a high super saturation state (Paulino et al., 2013).

#### **4.5. Colloidal Particles**

Colloidal particles are pervasive in everyday life. Numerous foods, pharmaceuticals, cosmetics, coating materials, and printer inks, for example, contain colloidal particles (Matsuoka et al., 1985).

Colloidal particles are tiny particles that remain stable in a fluid phase. Their sizes range from ten nanometers to several microns. This reduces the size of the particles to the level that they can be suspended in the fluid through thermal motion, given that the buoyancy mismatch between the particles and the fluid is not excessive. Colloidal suspensions are important in the technical world because they permit the movement of solid particles in the same way as liquid particles do. They are extremely precise; colloidal particles with a size polydispersity of less than 3%, as measured by the standard deviation of the particle radii distribution, are possible.

Additionally, by controlling the colloids' interparticle interactions, their interfacial properties can be precisely tuned. The interaction potential can be strongly repulsive or strongly attractive, and it can contain both repulsive and attractive components; however, the interaction potential can span distances up to two orders of magnitude smaller than the particle diameter.

On the other hand, colloidal particles are intrinsically only kinetically stable due to their composition of a scattered solid phase with a lower energy than a simple solid. Thus, a repulsive energy barrier must exist in all cases to avoid irreversible particle aggregation, which is often caused by van der Waals attractions. Colloidal particles are an incredibly useful model system for the analysis of a number of different types of behavior due to their precise regulation of their size and interaction potential. Typically, in this situation, the properties of the particles themselves are at stake. The fluid heats the particles, allowing them to equilibrate and sample the complete phase space.

Due to the phase behavior of the particles, colloidal suspensions are extremely interesting to research. The use of colloidal particles to model more conventional atomic or molecular solids is an enthralling example. Colloidal particles exhibit phase behavior somewhat close to that of atomic or molecular samples. The motion of individual particles in colloidal samples can be visualized and monitored using tools like laser scanning confocal fluorescence microscopy. (Lu and Weitz, 2013).

## 5. LITERATURE REVIEW

Numerous current and new drugs are underutilized due to their low bioavailability in aqueous media (Biopharmaceutics Classification System drug classes II and IV). An antisolvent precipitation method does not involve usage of traditional volatile organic solvents to accelerate the dissolution of these types of poorly water-soluble drugs. To demonstrate this technique, ultrafine rifampicin particles were prepared using a room temperature ionic liquid (1-ethyl-3-methylimidazolium methyl-phosphonate) as an alternative solvent and a phosphate buffer as an antisolvent (Viçosa et al., 2012).

Carbamazepine was crystallized from organic solutions using an antisolvent crystallization technique. Carbamazepine was dissolved in ethanol and antisolvent was sterile water. Until injecting the carbamazepine into the antisolvent, it was dissolved in the solvent, resulting in particle precipitation. During the crystallization experiments, the effects of process parameters such as solution concentration, temperature, injection rate of the solution, and the presence of ultrasound were examined. According to an analysis of the formed particles, external characteristics such as particle size and distribution were a significant feature of the process parameters, while internal structures such as crystallinity and thermal stability remained nearly unchanged. As solutions containing large concentrations of drugs were used, smaller particles were collected. Higher temperatures resulted in larger crystals. The rate at which the drug solutions were injected also had an effect on particle size. The size of carbamazepine particles was significantly reduced when an ultrasonic wave was applied selectively to them (Park and Yeo, 2012).

Improved drug bioavailability is one of the most important issues in the pharmaceutical industry. These drugs can now be prepared as nanoparticles or microparticles using cutting-edge formulation techniques. Numerous essential pharmaceutical properties are influenced by a compound's size and morphology. To meet biopharmaceutical and processing criteria, the drug delivery system must have a uniform particle shape and a limited particle size distribution, ideally an engineered drug particle. Antisolvent crystallization is being used at the laboratory scale to prepare nanoparticles or microparticles for drugs that are insoluble in water.

This method can be used to alter the solid-state properties of pharmaceutical compounds, such as crystal formation and particle size distributions (Lonare and Patel, 2013).

Colloidal particles are solid microscopic particles that can suspend in a liquid. Colloids are small enough that thermal energy powers their dynamics and maintains their equilibrium with the suspending fluid, but large enough that optical techniques may be used to precisely determine their positions and motions. Colloidal suspensions are an ideal model system for studying other condensed matter physics phenomena since the solid particles' collective phase behavior is comparable to that of other condensed systems. (Lu and Weitz, 2013).

The insoluble and dissolvable nature of hydrophobic drugs has become a major impediment to pharmaceutical development. Drug nanoparticles have gained widespread acceptance as a solution to this issue. The aim of this study was to synthesize celecoxib nanoparticles using antisolvent precipitation and high-pressure homogenization techniques in combination with various concentrations of soluplus® as a hydrophilic stabilizer. Celecoxib nanoparticles were prepared using two methods: antisolvent crystallization followed by freeze drying (CRS-FD) and antisolvent crystallization followed by high pressure homogenization and freeze drying (HPH-FD) (Homayouni et al., 2014). There has been a surge in interest in nanocrystal research and development for the delivery of poorly water-soluble drugs that can be manufactured directly from solution. Drug nanocrystals avoid potential side effects caused by carrier polymers and the low stability problems associated with encapsulation as compared to conventional carrier-based or encapsulation designs.

The processing of carrier-free nanocrystals necessitates meticulous nucleation control and, as a result, a detailed understanding of the metastable zone of the appropriate solution. A solution will become metastable if it remains supersaturated without forming nuclei. The metastable zone width is the maximum degree of supersaturation. When nucleation occurs directly from the metastable region, it aids in the formation of homogeneous nuclei that result in uniform nanocrystals (Ren et al., 2019).

## **6. MATERIALS AND METHODS**

### **6.1. Computational Studies**

#### **6.1.1. Molecular Docking**

##### **A- Ligand preparation (Pipenzolate MBr and Phenobarbital)**

The 3D structures of tested APIs were downloaded from the PubChem website (<https://pubchem.ncbi.nlm.nih.gov/>), and prepared by protonation (Adding hydrogen atoms followed by energy minimization process to get the final geometry of both APIs before docking process as shown in figure 6.1.

##### **B- Target protein preparation**

This process must be performed because any extracted and crystallographic protein and elucidated by X-ray diffraction will have some separated amino acids with broken bonds. Hydrogen atoms in protein data sites would be removed for facilitating upload and download for this reason protonate 3D then energy minimization processes should be performed. All water molecules must be removed from protein structure except active site.

The crystal structure of the human M1 muscarinic acetylcholine receptor was download from the Protein Data Bank (PDB ID: 5CXV) for Pipenzolate MBr while the crystal structure of the MMP-9 active site mutant with barbiturate inhibitor was download from the Protein Data Bank (PDB ID: 2OVX) for Phenobarbital. Both of proteins were protonated by adding hydrogen atoms with standard 3D geometry fixation by correcting the broken bonds and other errors via Swiss dock server.

Target protein prediction was performed by Swiss target prediction website (<http://www.swisstargetprediction.ch/>) for the of both APIs. The most probability target has been identified depending on the similarity between native small molecule of target protein and APIs structure of our interest.

##### **C- Docking process**

Rigid docking will be used where binding sites at protein are not alter their internal geometry by toggle the receptor strength value to (5000). For ligands (Pipen and Phen) we used them as MDB file to retrieve it in docking process. We used two scoring functions (London dG and GBVI/WSA dG). The resulting poses ranked and saved in MDB file to view all poses an make a comparison among them.

Docking process was performed by Swiss dock prediction website (<http://www.swissdock.ch/>).

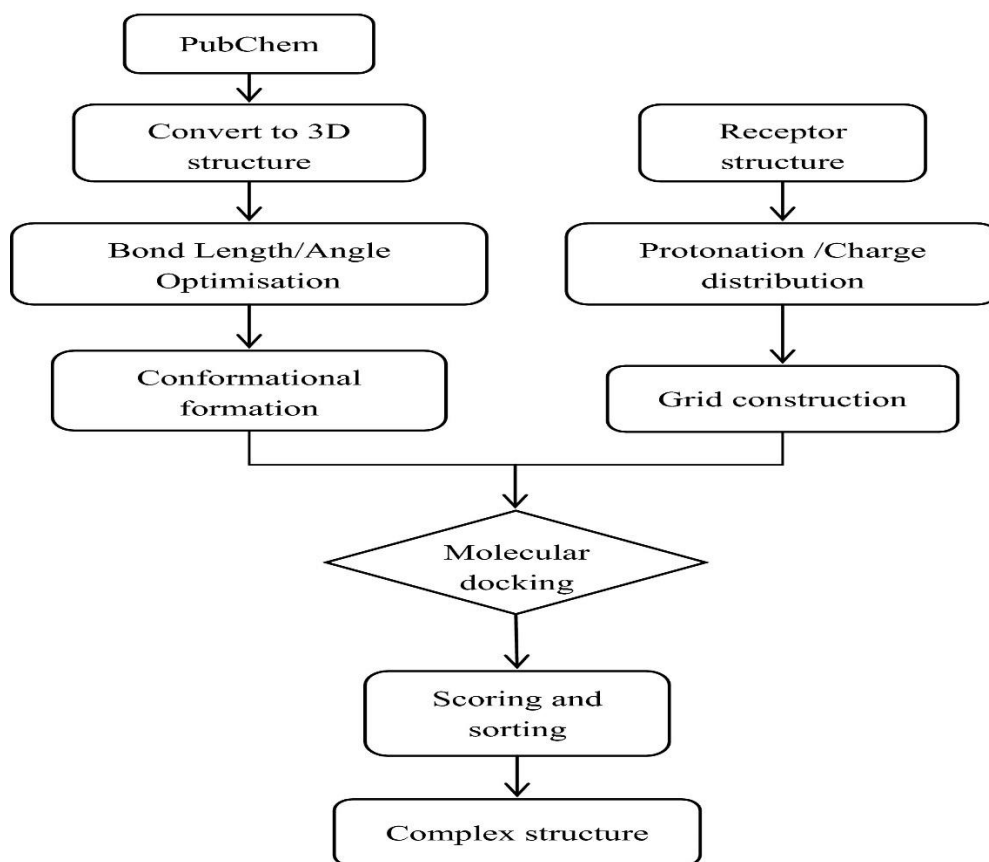


Figure 6.1. Docking requirements and process

### 6.1.2. ADMET Analysis

In order to study our APIs computationally in terms of pharmacokinetic behavior we used In Silico platform (Swiss ADME) (<http://www.swissadme.ch/index.php>) to predict the Absorption, Distribution, Metabolism, Excretion and toxicity.

## **6.2. Quantitative Assessment of Pipen and Phen by HPLC**

### **6.2.1. Chromatographic Conditions**

The HPLC system (Shimadzu instrument, Model LC 2040 with photo diode array detector) used in an isocratic mode. The suggested chromatographic conditions included a mobile phase that encompass volumes (55:10:35) of 10 mM phosphate buffer, methanol and acetonitrile respectively, 20  $\mu$ l volume injection loop, MACHEREY-NAGEL-Germany (C18, 5  $\mu$ m, 25 cm x 4.6 mm) column, 1 mL/min as flow rate, 230 nm as detection wavelength and ambient temperature.

### **6.2.2. Material And Chemicals Reagent**

Monobasic potassium phosphate, dibasic sodium phosphate and octane sulfonic acid sodium salt were supplied from Sigma Aldrich-Germany as analytical reagent grade. Deionized water, methanol, acetonitrile and orthophosphoric acid were HPLC grade. Pipenzolate bromide (100.5% purity) supplied by Olon company, Italy while phenobarbital (99.8% purity) supplied by Harman Finochem Ltd, India.

### **6.2.3. Mobile Phase Preparation**

In order to prepare solution A, (0.60) g of monobasic potassium phosphate and (0.82) g of dibasic sodium phosphate was weighted and transferred to 1 Liter volumetric flask, then (1.25) g of octane sulfonic acid sodium salt was added with about 500 mL of water and shaken, the volume has been completed to 1000 mL and pH was adjusted to 5.75 with orthophosphoric acid. The prepared solution was filtered through 0.45 $\mu$ m nylon filter. The mobile phase solution was prepared from a mixture of solution (A), methanol and acetonitrile (55:10:35) V/V/V% respectively.

### **6.2.4. Stock and Test Solutions Preparation**

The diluent consists of methanol and water (50:50) V/V has been prepared.

Stock standard solution of phenobarbital (A) was prepared by dissolving (240) mg of phenobarbital in diluent to make (100) mL of solution.

Stock standard solution of Pipenzolate methyl bromide (B) was prepared by dissolving (160) mg of Pipenzolate methyl bromide in diluent to make (100) mL of solution.

Standard Solution was prepared by transferring 5 mL of each stock standard solution (A) and (B) into 50 mL volumetric flask. The volume has been completed with diluent then filtered through 0.45µm nylon filter.

Test Solution was prepared by transferring 2mL of Spastal drops (equivalent to 12 mg from phenobarbitone and 8 mg from pipenzolate methyl bromide) into 50 mL volumetric flask, volume has been completed with diluent.

### 6.2.5. Calculation

Calculate the percentage of (Pipenzolate MBr & Phenobarbital) assay using the following equation:

$$A\% = \frac{Ab.sp}{Ab.st} \times \frac{Wt.st}{100} \times \frac{5}{50} \times \frac{50}{V.sp} \times \frac{1}{L.C} \times \frac{100 - Wc}{100} \times P \times 100 \quad (6.1)$$

Where as

Ab.sp = Area response of phenobarbital & pipenzolate MBr due to test preparation.

Ab.st = AVG. area response of phenobarbital & pipenzolate MBr due to standard solution.

Wt.st = Weight of the phenobarbital & pipenzolate MBr standard.

V.sp = Volume of the sample.

L.C= Label Claim in mg of phenobarbital & pipenzolate MBr

W.C=Water content of phenobarbital & pipenzolate MBr standard.

P=potency of phenobarbital & pipenzolate MBr standard.

### 6.3. Validation of Developed Method

The validation procedure was conducted by calibrated HPLC instruments (Shimadzu LC 2040-with UV-VIS detector and photodiode array detector), standard solution of Pipenzolate MBr has a potency (100.5) % with water content (0.4) %, standard solution of Phenobarbital has a potency (99.8) % with water content (0.21) %.

The validation was performed according to US pharmacopoeia (Pharmacopoeia, 2016) and International Conference on Harmonization (ICH) guidelines as shown in the validation of analytical procedures and methodology of ICH Q2A&B (Borman and Elder,2018).

The suggested method was developed for quantifying Pipenzolate MBr and Phenobarbital in Spastal drops with greater precision and accuracy. Separation was performed with (C18, 250 × 4.6 mm, 5 $\mu$ m) (MN) HPLC column in isocratic mode, mobile phase consisting of buffer pH 5.75, methanol and acetonitrile (55:10:35) v/v/v%, flow rate was 1.0 mL/min and detection wave length at 230 nm.

### **6.3.1. System Suitability**

To ensure the validity of the suggested method, a system suitability test has been conducted. Data from five injections of 20  $\mu$ L of the standard solution containing (0.16) mg / mL of Pipenzolate MBr and (0.24) mg / mL of Phenobarbital were used for evaluating the system suitability parameters, such as retention time, response, tailing factor, theoretical plates, resolution, asymmetry, and resolution.

### **6.3.2. Linearity and Concentration Ranges**

As recommended by ICH guidelines the linearity of analytical method should be determined at least by five different concentrations range as follows (0.120 - 0.192 - 0.240 - 0.288 - 0.384) mg/ mL of Phenobarbital and (0.080 - 0.128 - 0.160 - 0.192 - 0.256) mg/ mL of Pipenzolate MBr were conducted. We obtained standard calibration graphs for both APIs by plotting peak areas and analyzing them using regression analysis.

### **6.3.3. Robustness**

Robustness is a critical criterion for determining the method's capability since it ensures that the results do not dramatically change when the pH is changed ( $\pm 0.1$ ), the same column has a different lot number (different origins), the column temperature is set to 5 $^{\circ}$ C, the wavelength is set to 1 nm, the mobile phase contains  $\pm 2\%$  acetonitrile, and the flow rate is set to  $\pm 0.2$  mL/min.

### **6.3.4. Accuracy test**

Accuracy is an analytical process that determines the degree to which test results obtained using the suggested method are identical to the true value. According to ICH guidelines, the suggested method's accuracy was calculated using three separate concentrations of Pipenzolate MBr (0.08 - 0.16 - 0.256) mg/mL and (0.12 - 0.24 - 0.384) mg/mL of Phenobarbital, with at least one repeat at each concentration.

Three concentration samples (standard solutions) were analyzed, and the values obtained from the respective peak areas were compared to the linearity range (50-160) percent.

#### **6.3.5. Precision test**

Precision was determined using two criteria: repeatability and intermediate precision. The term "repeatability" (intra-day precision) refers to the precision obtained over a short period of time while maintaining the same chromatographic conditions. Precision is sometimes referred to as repeatability inside an assay. Multiple injections (6 replicate injections) of the sample at concentrations of (0.16) mg/mL Pipenzolate MBr and (0.24) mg/mL Phenobarbital were performed. Intermediate precision (inter-day precision) was determined by evaluating the same sample on different days under the same conditions (two days).

### **6.4. Production and Characterization of Nanodrugs in Both Forms (Crystal Powder and Colloidal Solution)**

#### **6.4.1. Materials**

Pipenzolate bromide (100.5% purity) supplied by Olon company, Italy while phenobarbital (99.8% purity) supplied by Harman Finocem Ltd, India. Ethanol absolute and Methyl Ethyl Ketone (2-Butanone) were obtained from BDH-England. Deionized water was purified through a Milli-Q water purification system from Thermo Scientific Smart 2Pure (Sweden).

#### **6.4.2. Preparation of Pipenzolate Methyl Bromide and Phenobarbital as Colloidal Particles and Crystal Powder**

APIs crystal powder and colloidal particles were prepared using the antisolvent precipitation technique. For Pipenzolate MBr, three samples were prepared. One sample contained water as solvent while Methyl Ethyl Ketone (2-Butanone) as antisolvent without stabilizer and the other two samples contained 1% of (tween 20 and PVP k30) as stabilizers. Pipenzolate MBr supersaturated solution (125mg/ml) was prepared and filtered through 0.45 $\mu$ m (HPLC inlet filter) then injected into a beaker contains Methyl Ethyl Ketone (2-Butanone). The ratio of solvent: antisolvent was 1:3. The drug particles were beginning to form after half quantity of

solvent solution has been consumed, then we conserved this solution for colloidal particles characterization.

For crystal powder production, the suspension was centrifuged till only precipitate layer was completely formed. Supernatant was neglected and then repeatedly washed with Methyl Ethyl Ketone (2-Butanone) for 3-4 times then centrifugation at (10000 rpm) for 30 minutes has been applied after each wash process and the colloidal particles were sonicated by ultrasonic apparatus for 15 seconds then freeze-dried.

For Phenobarbital, four samples were prepared. One sample contained Ethanol absolute as solvent while deionized water as antisolvent without stabilizer and the other three samples contained 1% of (tween 20, HPMC E6 and PVP k30) as stabilizers. Phenobarbital supersaturated solution (40mg/ml) was prepared and filtered through 0.45 $\mu$ m (HPLC inlet filter) then injected into a beaker contains deionized water. The ratio of solvent: antisolvent was 1:3. The drug particles were beginning to form after half quantity of solvent solution has been consumed, then we conserved this solution for colloidal particles characterization.

For crystal powder production, the suspension was centrifuged till only precipitate layer was completely formed. Supernatant was neglected and then repeatedly washed with deionized water for 3-4 times then centrifugation at (10000 rpm) for 30 minutes has been applied after each wash process and the colloidal particles were sonicated by ultrasonic apparatus for 15 seconds then freeze-dried.

#### **6.4.3. Optimization of Antisolvent Crystallization Technique**

The optimum conditions for the preparation of APIs, colloidal particles, and crystal powder were determined using single-factor experiments. In a preliminary experiment, four variables were analyzed: the concentration drug, the volume ratio of solvent to antisolvent, the mixing speed, and the temperature.

Only one element was modified in this process, while the others remained unchanged. The same method as above was applied to study the other factors. The effects of drug concentrations at 125, 250, 500 mg/ml for Pipenzolate MBr and 20, 30, 40mg/ml for Phenobarbital, solvent - antisolvent ratio (1:3, 1:5, and 1:7), mixing speed at (200, 500 and 700 rpm) and the temperature at (25, 50, and 80) °C were examined. Finally, the optimal conditions for each factor were calculated using the water solubility, supersaturation, and crystallization of the gained APIs.

#### **6.4.4. Scanning Electron Microscopy (SEM)**

SEM was used to identify the shapes of raw, colloidal particles, and recrystallized powders (Jeol JSM7001F model). Direct deposition of powder and crystal samples onto a carbon tape mounted on the surface of an aluminum stub was used to prepare the powder and crystal samples, while the colloidal particles were prepared by drying under vacuum. Morphology and particle size of fabricated crystals has been detected.

#### **6.4.5 Fourier Transform Infrared Spectroscopy (FTIR)**

The chemical compositions of raw APIs, colloidal particles, and re-crystallized powders were determined using FTIR spectroscopy with an IRAffinity-1S spectrophotometer. Every sample was directly analyzed by put a tiny quantity in specific holder. With a resolution of  $4\text{ cm}^{-1}$ , the scanning range was  $4000\text{--}400\text{ cm}^{-1}$ . We obtained spectra using LabSolution LC software version 5.92

#### **6.4.6. Reverse Phase-High Performance Liquid Chromatography**

The raw APIs and APIs crystal powders after processing were analyzed according to prescribed preparation method of solutions in **6.2.4 section**. All samples were detected by HPLC. Spectra were obtained using the LabSolution LC software version 5.97 (Shimadzu Corporation, Kyoto, Japan).

#### **6.4.7. X-Ray Diffraction (XRD)**

The raw APIs and APIs crystal powders after processing were detected using Rigaku Smart Lab XRD with Cu\_K-beta filter; none diffracted beam mono, SC-70 detector and continuous scan mode. The samples were scanned from (0 – 60) minutes and measured with a voltage of 40 kV and 30 mA.

#### **6.4.8. Differential Scanning Calorimetry (DSC)**

A sample of 7.80000 mg, 7.10000 mg of raw powder and 7.70000 mg, 6.40000mg of recrystallized powders for Pipenzolate MBr and Phenobarbital respectively were analyzed by DSC Q2000 V24.11 Build 124 Standard Cell RC at an increasing temperature heating rate of  $10\text{ }^{\circ}\text{C}/\text{min}$  from  $25\text{ }^{\circ}\text{C}$  to  $300\text{ }^{\circ}\text{C}$ .

#### **6.4.9. Thermogravimetric analysis (TGA)**

A sample of 5.70700 mg, 6.78700 mg of raw powder and 5.72800 mg, 6.63400mg of recrystallize powders for Pipenzolate MBr and Phenobarbital respectively were analyzed by TG analyzer SDT Q600 V20.9 Build 20. In open aluminum pans, both samples were weighed. The test conditions were as follows: 50 mL/min nitrogen flow rate. The percentage weight loss of the samples was tracked as they were heated from 10 to 900 °C at a rate of 10 °C per minute.

#### **6.4.10. Image J software**

Image J software version 1.52 used to measure the particle size of the synthesized colloidal particles and APIs crystal powders after processing. These measurements have been performed through images that captured by SEM.

### **6.5. Kinetic Dissolution Profile Study**

#### **6.5.1. Preparation of Pipen and Phen-Containing Tablets**

Raw and recrystallized powders of PIPEN and PHEN were compressed into tablets based on specific formulations of generic products under trade name (Piptal tablets containing 5mg of Pipenzolate MBr and Barabital tablets containing 15mg of Phenobarbital).

##### **A- For Piptal tablets**

Each tablet consists of (Pipenzolate methyl bromide as API, Aerosil 130 V as glidant, maize starch dried as diluent, Polyvinyl pyrrolidone as binder, Talc as lubricant, Magnesium stearate as lubricant and lactose monohydrate as filler. The tablet formulation ingredients were blended for 10 minutes at 100 rev/min in a blender, then compressed into 120 mg tablets using an ERWEKA tablet unit (Hamburg, Germany).

##### **B- For Barabital tablets**

Each tablet consists of (Phenobarbital as API, maize starch dried as diluent, Polyvinyl pyrrolidone as binder, Talc as lubricant, Magnesium stearate as lubricant and lactose monohydrate as filler. All ingredients for the tablet formulation were blended for 10 minutes at 100 rev/min in a blender, then compressed into 120 mg tablets using an ERWEKA tablet unit (Hamburg, Germany).

## **6.5.2. Dissolution Profile Parameters**

### **A- For pipenzolate MBr**

This test has been done according to In House method (IH). One tablet Piptal was added into each glass vessel (6 vessel) of dissolution tester device. Each vessel contains media (500 ml) of distilled water. Standard solution of Pipenzolate MBr was prepared by weighting 10 mg of raw and recrystallized powder crystal powder were added into volumetric flask (100 mL) of the dissolution medium (water), then withdraw 1 mL into volumetric flask (10 mL) of the dissolution medium (water). The temperature, paddle speed and time were set at 75 r/minute,  $37 \pm 0.5$  °C, and 60 minutes respectively. Aliquots of 5 mL at 5, 10, 15, 30, 45 and 60 minutes were withdrawn from vessels and filtered using a 0.22 mm micro syringe filter.

### **B- For Phenobarbital**

This test has been done according to standards parameters of United States Pharmacopeia 2020 (USP 42). One tablet Barabital was added into each glass vessel (6 vessels) of dissolution tester device. Each vessel contains media (900 ml) of deionized water. Standard solution of Phenobarbital was prepared by weighting 16.6 mg of raw and recrystallized powder crystal powder were added into the dissolution medium (water), then withdraw 1 mL into volumetric flask (10 mL) of the dissolution medium (water). The temperature, paddle speed and time were set at  $37 \pm 0.5$  °C, 50 r/minute and 45 minutes respectively. Aliquots of 5 mL at 5, 10, 15, 30 and 45 minutes were withdrawn from vessels and filtered using 0.22 mm micro syringe filter. Each of standard and test solutions were injected and performed according to prescribed parameters in **6.2.1 section**.

## **7. RESULTS AND DISCUSSION**

### **7.1. Computational Study**

#### **7.1.1. Docking study**

Usually in each protein, there are more than pocket and chain so we have to choose the suitable pocket and chain depending on native small molecule (ligand), consequently the consumed time for preparation and docking process will decrease. we selected one pose for each one where the free binding energy and RMSD values are the least, in other word more stable pose will represent the optimum structure of the ligand–protein complex. All water molecules must be removed from protein structure except active site because it improves pose prediction. Without neglected water molecules, it causes deleterious effect by giving false energetic stability for the protein-ligand complex. Scoring functions will ranking the resulting poses based on RMSD and energy values. More than one scoring function type employed for each pose to eliminate positive false.

When we compared Pipenzolate MBr interaction inside the pocket with the native ligand in figure 7-1 there was a similar connection with a crucial amino acid (Asparagine 382) by hydrogen bond donor and acceptor with hydroxyl and carboxyl groups. This pose showed the lowest energy (S value = -9.3889) and (RMSD value = 1.7382) which represented the correlation distance between the original ligand and the Pipenzolate MBr inside the pocket, the smaller distance indicates that the binding site of them is almost the same and thus the effectiveness is better., consequently the least S value refers to the most stable pose inside the pocket as shown in figure 7-2.

When the connection between certain drug and the protein is achieved, the shape of the protein will change and thus the pharmacological action of the drug will occur. So, the medicinal chemists and biologists are depending on what will find out inside the target protein in terms of pocket and native ligands to design a novel drug for this protein.

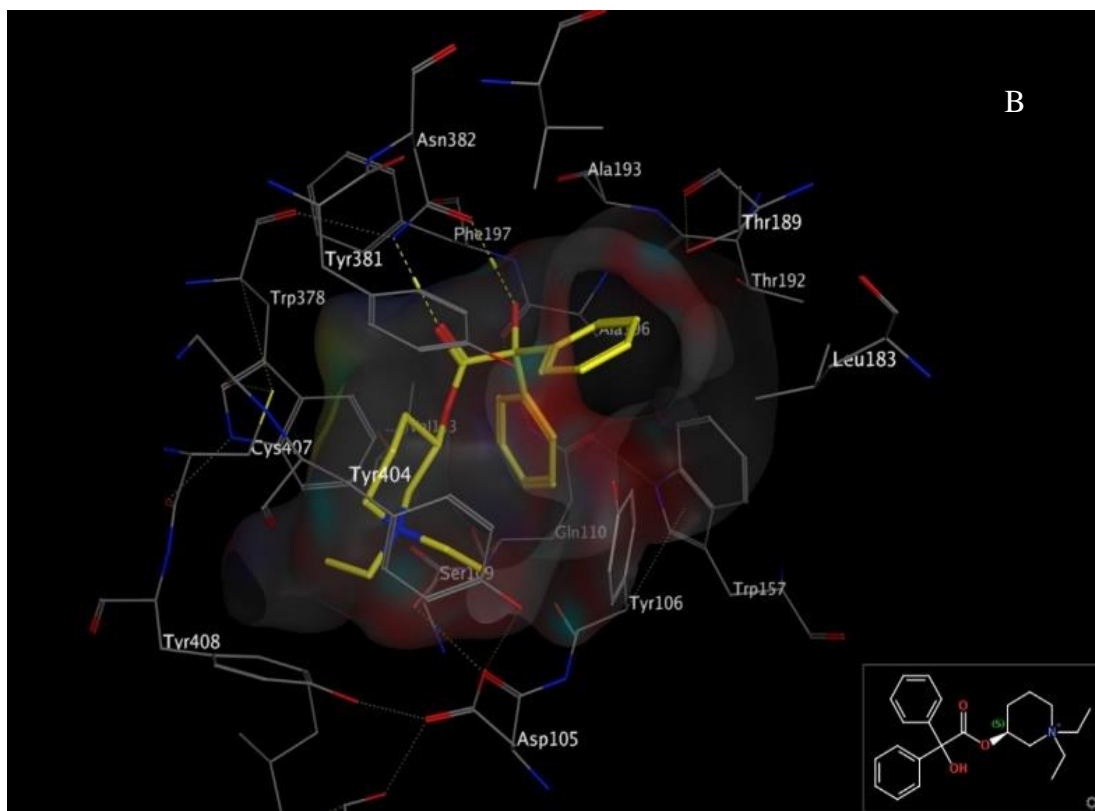
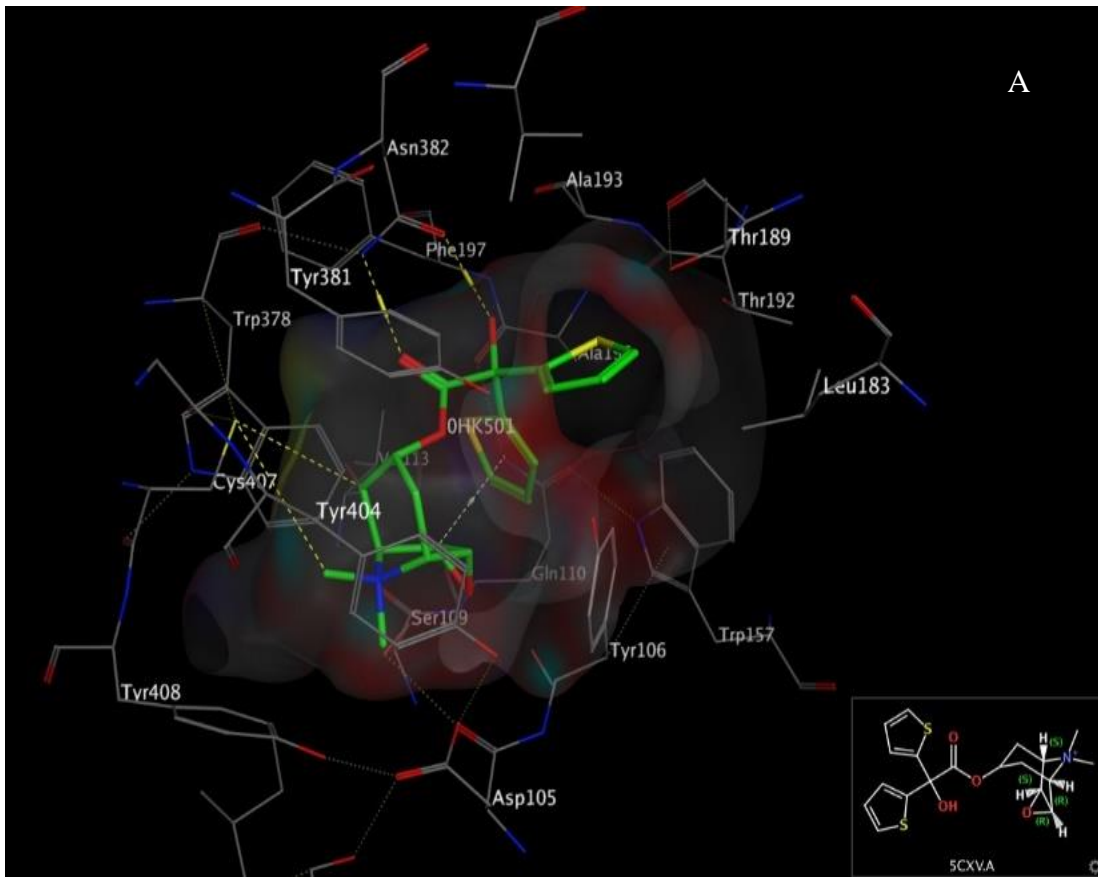


Figure 7.1. (A) Native ligand pocket, (B) Phenobarbital pocket

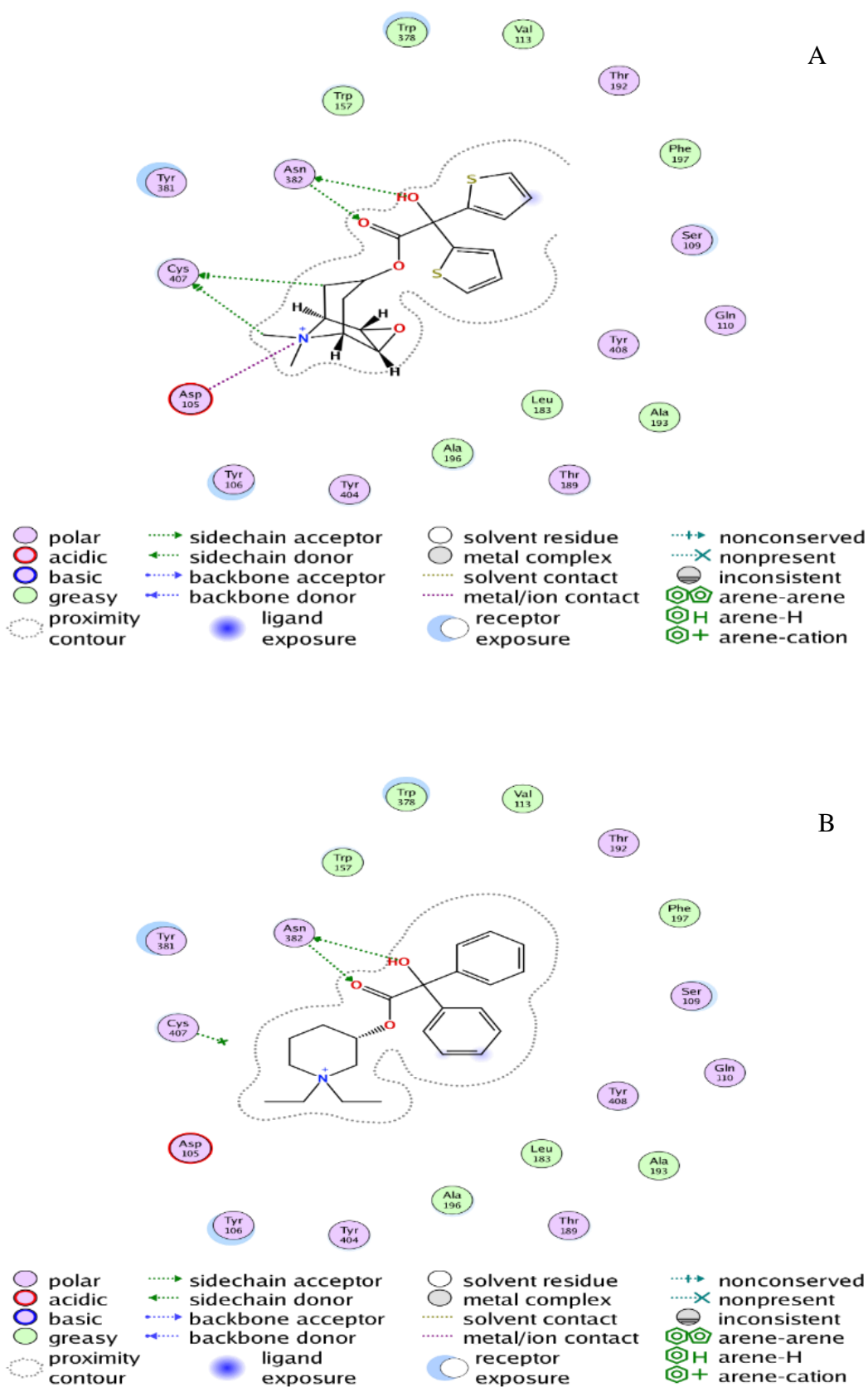


Figure 7.2. (A) Native ligand interaction, (B) Pipenzolate MBr interaction

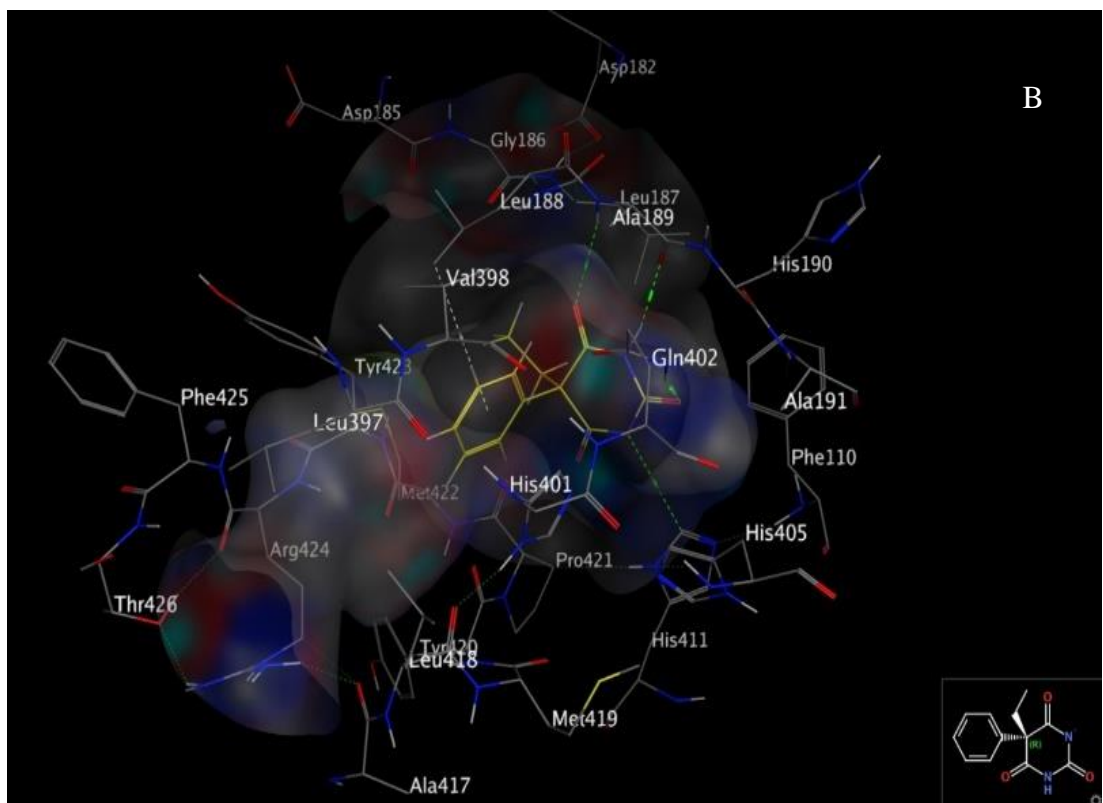
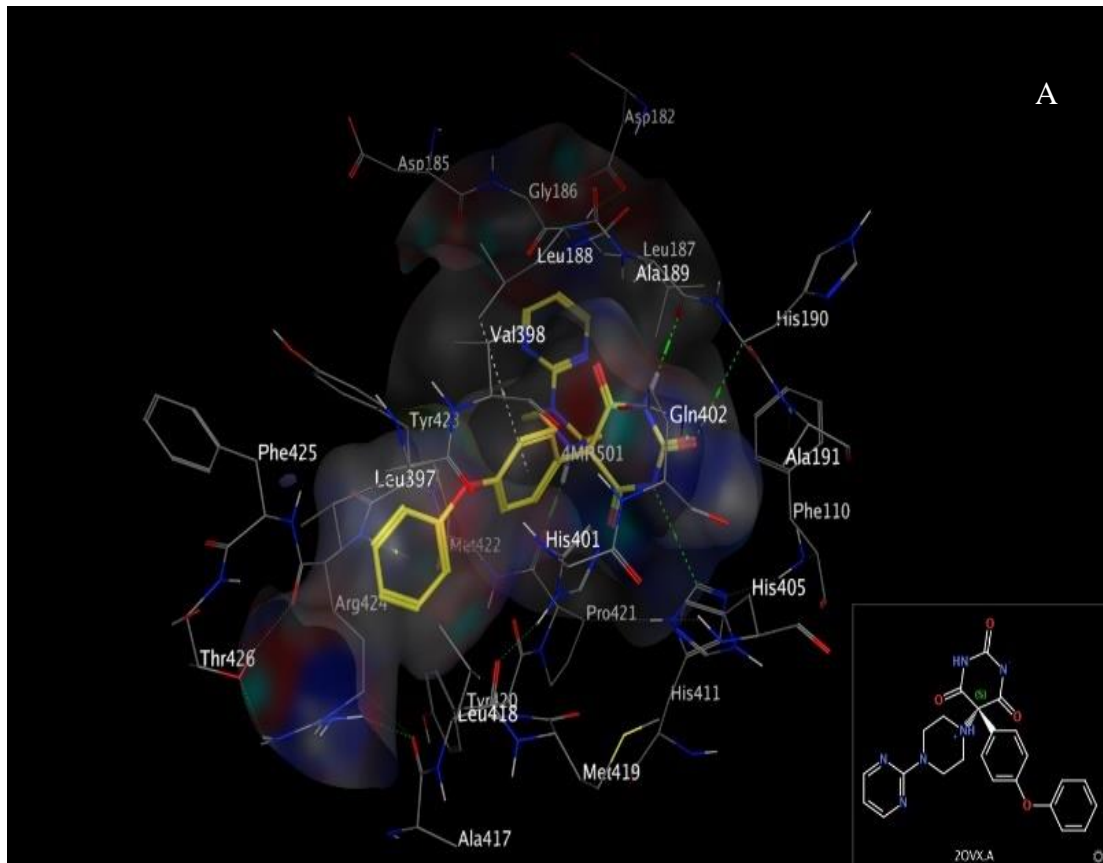
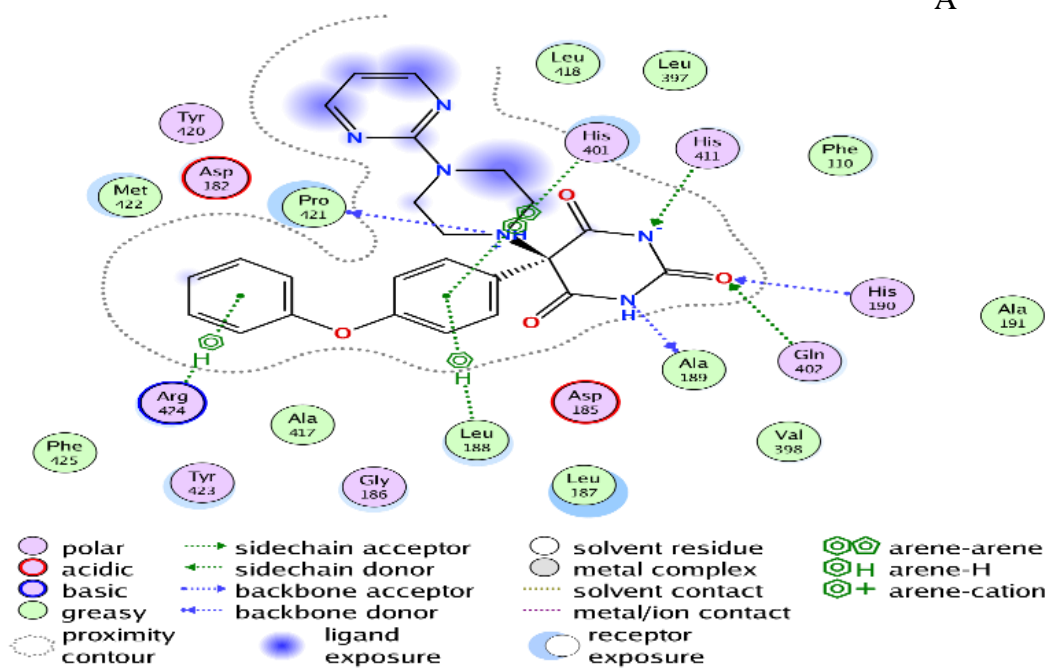


Figure 7.3: (A) Native ligand pocket, (B) Phenobarbital pocket

A



B

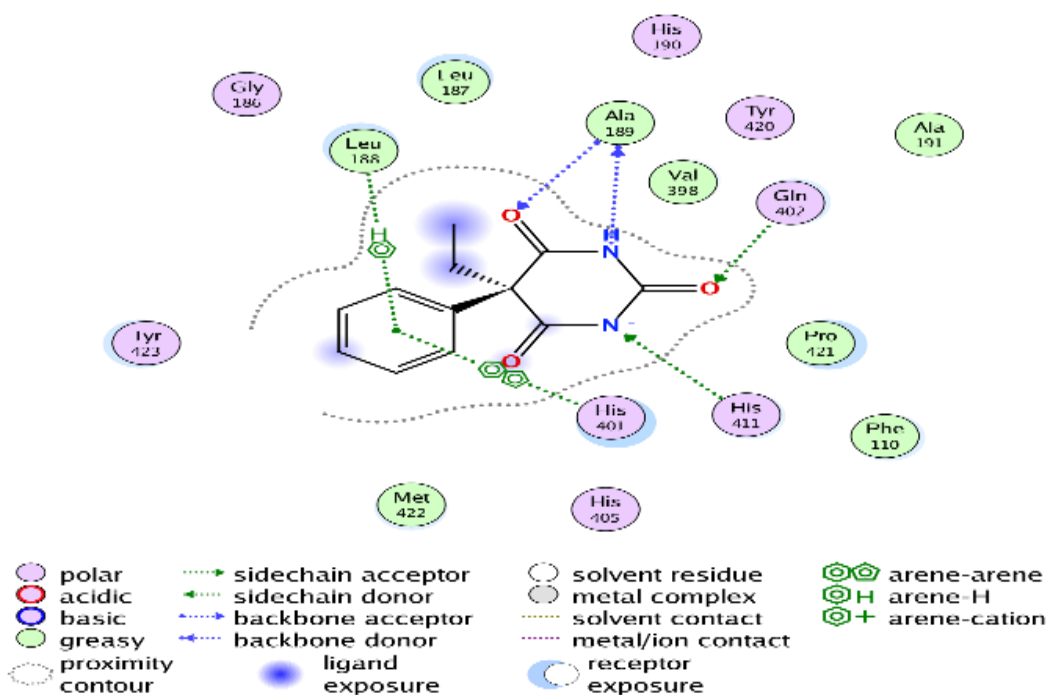


Figure 7.4. (A) Native ligand interaction, (B) Phenobarbital interaction

When we compared Phenobarbital interaction inside the pocket with the native ligand in figure 7-3 there was a similar connection with crucial amino acids (Alanine 189), (Histidine 401, 411), (Glycine 407) and (Leucine 188) by hydrogen bond donor and acceptor with amine and carboxyl groups. This pose showed the lowest energy (S value = -6.0191) and (RMSD value = 1.0836) which represented the correlation distance between the original ligand and the Phenobarbital inside the pocket, the smaller distance indicates that the binding site of them is almost the same and thus the effectiveness is better., consequently the least S value refers to the most stable pose inside the pocket as shown in figure 7-4.

### **7.1.2. ADMET Analysis**

ADMET data is considered as an essential part of discovering and developing new drugs based on evaluation of the pharmacokinetic profile of small molecules. The profile includes multiple parameters like drugs' bioavailability, oral absorption, clearance, volume of distribution, as well as the penetration through the blood–brain barrier (BBB). We used (<http://www.swissadme.ch/index.php>) as a prediction tool for our APIs.

Bioavailability radar has been used to assess Pipenzolate MBr whether it was drug-like or not as shown in figure 7-5. The radar plot of our molecule has to fall entirely inside pink region to be considered drug-like and suitable physicochemical space for oral bioavailability.

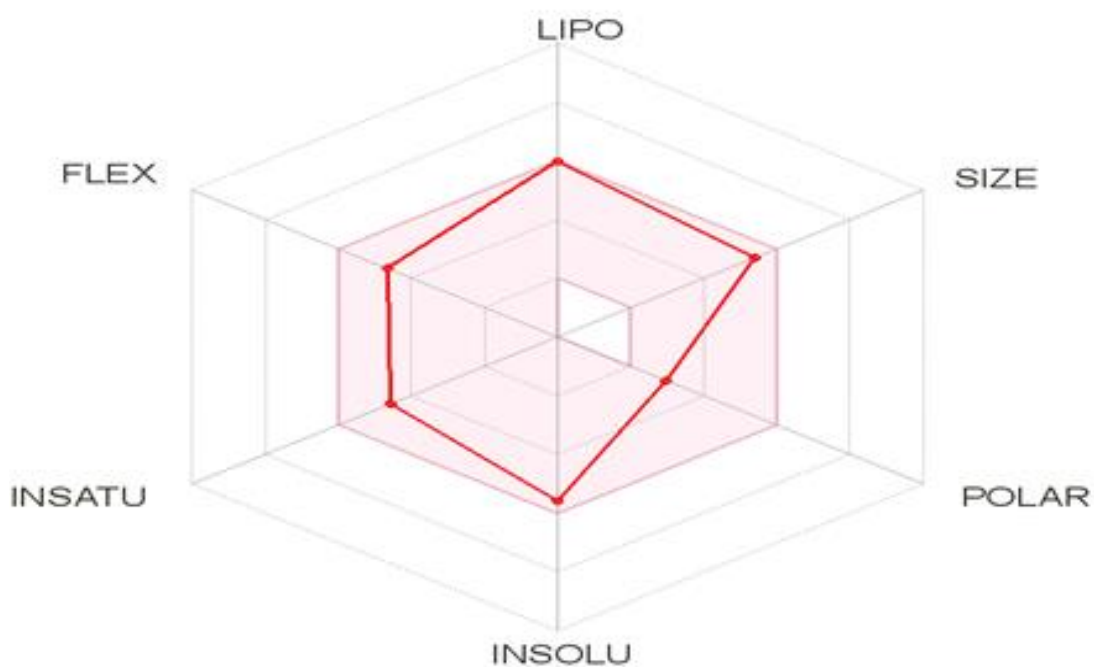


Figure 7.5. Radar plot of Pipenzolate MBr

The physicochemical properties included lipophilicity, size, polarity, flexibility, insolubility and saturation.

Lipophilicity is described by partition coefficient ( $\text{Log } P_{o/w}$ ) which is predicted by five models (iLOGP, XLOGP3, WLOGP, MLOGP and SILICOS-IT), lipophilicity equaled to 1.18. ( $\text{Log } P$  between -0.7 and +5.0)

Insolubility was measured by ( $\text{log } S$ ) which refers to oral administration drugs influencing absorption. It predicts by three models ( $\text{Log } S$  (ESOL),  $\text{Log } S$  (Ali) and  $\text{Log } S$  (SILICOS-IT)). Insolubility values was more than 6 which refers that Pipenzolate MBr is free soluble in water. ( $\text{log } S$  not more than 6)

Polarity is calculated by measured polar surface area (PSA) by using fragmental technique called topological polar surface area (TPSA) which can be used to estimating properties regards to biological barrier crossing like blood brain barrier (BBB). TPSA equaled to  $46.53 \text{ \AA}^2$ . (TPSA between 20 and  $130 \text{ \AA}^2$ )

Flexibility is calculated based on rotatable bonds number which must be not exceeded to 9 bonds.

Size refers to molecular weight of the compound. MW equaled to Molecular weight 448.39 g/mol. (MW between 150 and 500)

In saturation equaled to 0.43. (Instu between 0.25 and 1).

## **7.2. RP-HPLC-Based Quantitative Analysis**

In the pharmaceutical industry, analytical method creation is a crucial task. The diversity of column forms, operating parameters, mobile phase composition, diluent, and pH values necessitates the development of an analytical process. To achieve an appropriate chromatographic resolution, various chromatographic conditions were investigated. The chromatographic conditions were optimized in order to provide a good performance for the assay test.

Development and optimization method included the next points:

### **1- Selection of chromatographic parameters**

To choose the most effective solvent system for the separation of both APIs, preliminary experiments with several solvent systems were conducted. The choice of these solvents is influenced by factors such as cost and polarity.

Methanol, isopropyl alcohol, chloroform, and some phosphate buffers were tested at different pH levels, as well as combinations of these solvents. Methanol, acetonitrile, and phosphate buffer were used as the mobile step in various amounts and pH values. The polarities of APIs were taken into consideration when choosing the stationary phase. As the drug molecules are polar or moderately polar, reversed phase stationary phases were tried.

MACHERY-NAGEL-Germany (C18, 5  $\mu$ m, 25 cm x 4.6 mm) column was chosen to minimize the amount of time spent interacting with the stationary process and APIs. This aided in reducing research time by decreasing API preference for the stationary phase and increasing API contact with the mobile phase.

The mobile phase was prepared as previously mentioned to get better UV detection for both APIs in the same injection with separately. A buffer was developed by prepare (10) mM phosphate buffer with different ratios of Methanol

and Acetonitrile. Chosen pH of the mobile phase was determined after many trials to eliminate the overlapping two peaks and get them with separately and simultaneously.

Solution A, Methanol and Acetonitrile (55:10:35) at 5.75 as pH value was optimum for the best separation.

Column oven temperature has been chosen at ambient temperature because of the good separation consequently, it was found no need to increase temperature. Different wavelengths were studied at 220, 230 and 240 nm. It was found that optimum and highest detection response was obtained at 230 nm. The effect of flow rate was investigated in order to increase the chromatographic efficiency of proposed method and the resolution of the eluted peaks. Between (0.8 - 2) mL per minute, the flow rate was performed. A 1 mL per minute flow rate was found to be ideal for achieving better separation in a reasonable period of time.

Table 1 summarizes the final optimum conditions for the developed process.

These conditions resulted in the highest peak resolution and component separation. The chromatograms of standard preparation and Spastal drops were recorded as shown in figure 7-7 and figure 7-8 respectively. The retention time of Phenobarbital and Pipenzolate MBr was about (5.8) min. and (7.6) min. respectively.

## **2- System suitability**

System Suitability solutions for Pipenzolate MBr and Phenobarbital were conducted for HPLC system and analytical procedure to ensure that It has the ability to give thoughtful and coordinated analysis results by five replicate injections of Pipenzolate MBr and Phenobarbital solutions at concentration (0.160) mg/mL and (0.240) mg/mL respectively as shown in Table 2.

## **3- Linearity**

Different concentrations for Pipenzolate MBr and Phenobarbital in the mixture of pharmaceutical product were prepared for linearity studies. The calibration curves obtained by "plotting peak area against concentration" showed linear relationship over the concentration range of (0.080 - 0.256) mg/mL for Pipenzolate MBr and (0.120 - 0.384) mg/mL for Phenobarbital respectively. The "linear regression equations" for Pipenzolate MBr and Phenobarbital were found to be

$$y = 4012431.680885x - 1094.036903 \text{ and}$$

$$y = 8149011.584131x + 19373.673103 \text{ respectively.}$$

The "regression coefficient values (r<sup>2</sup>) " for Pipenzolate MBr and Phenobarbital were 0.999882 and 0.999005 respectively as shown in figure 7-9 and 7-10, these values demonstrated a high degree of linearity.

The "limits of detection (LOD) and limit of quantitation (LOQ)" were calculated independently using a standard calibration curve. The following formulas were employed

$$\text{LOD} = 3.3 \times D/S \quad (7.1)$$

$$\text{LOQ} = 10 \times D/S \quad (7.2)$$

Where, "D is the standard deviation of regression line and S is the slope of the calibration curve". LOD was found to be 1.700 mg/mL and 0.410 mg/mL for Pipenzolate MBr and Phenobarbital respectively.

The LOQ values for Pipenzolate MBr and Phenobarbital were determined to be 5.680 mg/mL and 1.3600 mg/mL, respectively. Small LOD and LOQ values suggest that the proposed approach is highly sensitive. Table (3) summarizes the regression characteristics of the proposed HPLC system.

#### **4- Selectivity**

Selectivity of the current method was demonstrated by good separation of the two active ingredients (Pipenzolate methyl bromide and Phenobarbital). Furthermore, matrix components, e.g., excipients, do not interfere with both APIs peak.

Each chromatographic peak for an active ingredient was found to be due to no more than two components, indicating that the method is selective. In terms of the drop excipients, there were no interfering peaks. The current method's selectivity was demonstrated by the good resolution of both API peaks, as shown in figure 7.7 and 7.8.

#### **5- Specificity**

In the sample solution chromatogram, peak purity greater than 99 percent was obtained for both APIs, indicating that the suggested approach was very specific for both APIs under consideration. In the presence of excipients, there were no concurrent peaks in the API retention times. Figures 7.7 and 7.8 display this very clearly in the chromatograms.

## **6- Robustness**

Although the robustness is not a basic parameter in the validation process as per US Pharmacopeia. It is an indicator of its ability to remain unaffected by minor changes in method parameters under normal conditions (Walfish, 2006).

There were no statistically relevant variations between the findings obtained under these modified chromatographic conditions and those obtained under the initial chromatographic conditions. Due to the fact that the variations in robustness had no detrimental effect on the developed method, the developed method demonstrated a high degree of robustness.

## **7- Accuracy**

The recovery percentage for Pipenzolate MBr and Phenobarbital was accepted since its value within (98.0-102.0) % of the true value. Table 4 summarizes the average results of three different concentrations with at least one repeat at each concentration for accuracy studies. The recovery values established that the proposed approach was precise within the proposed range. The chromatogram of Pipenzolate MBr and Phenobarbital in 7-7 and 7-8 demonstrated no intermeddle peaks from excipient components with active ingredient peaks.

## **8- Precision**

Method repeatability and intermediate precision were within the acceptable criteria NMT 2.0% of the prescribed sample concentration as shown in Tables 5 and 6 respectively.

Assay values between (first day) and (second day) NMT 2.0% so assay method has an acceptable precision as shown in Table7.

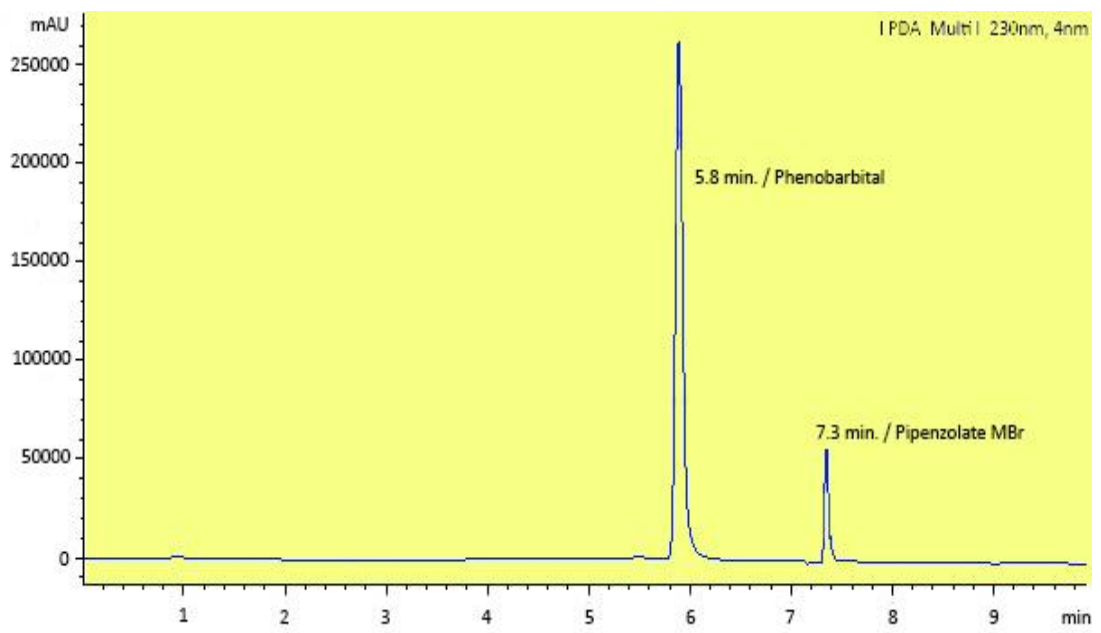


Figure 7.7. Chromatogram of standard solutions for Phen and Pipen

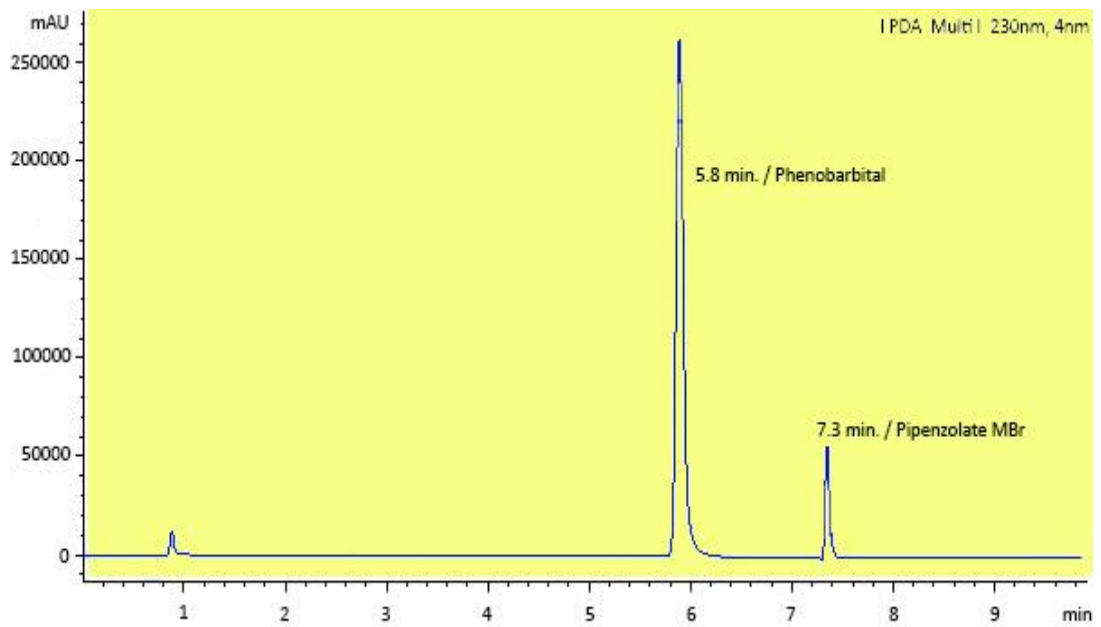


Figure 7.8. Chromatogram of Spastal drops for Phen and Pipen

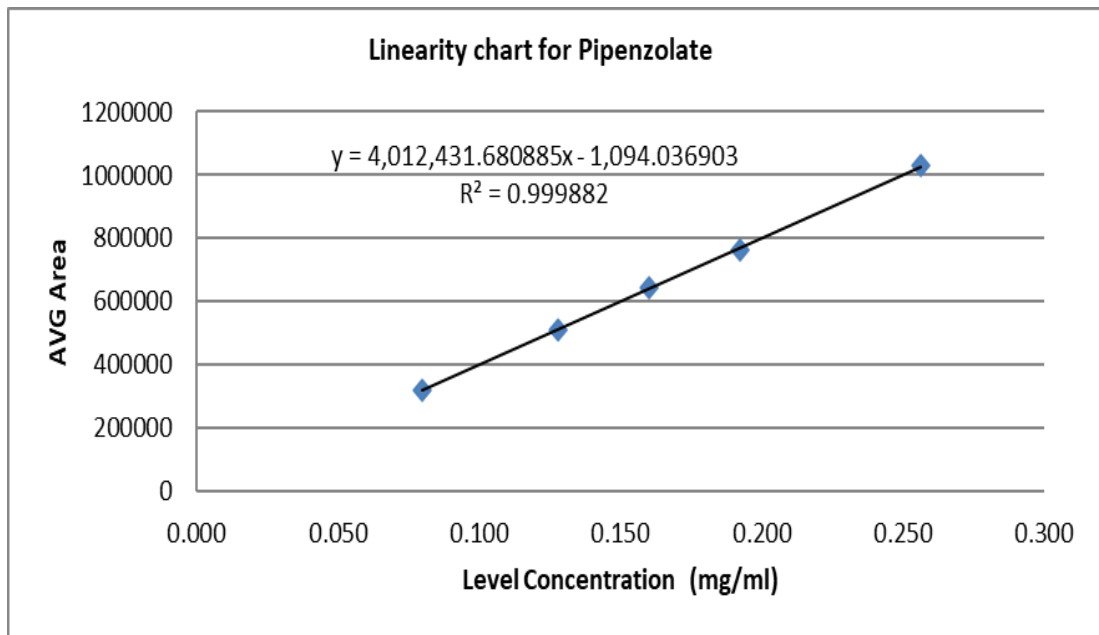


Figure 7.9. Pipenzolate calibration curve over the range of (0.08-0.256) mg/ml

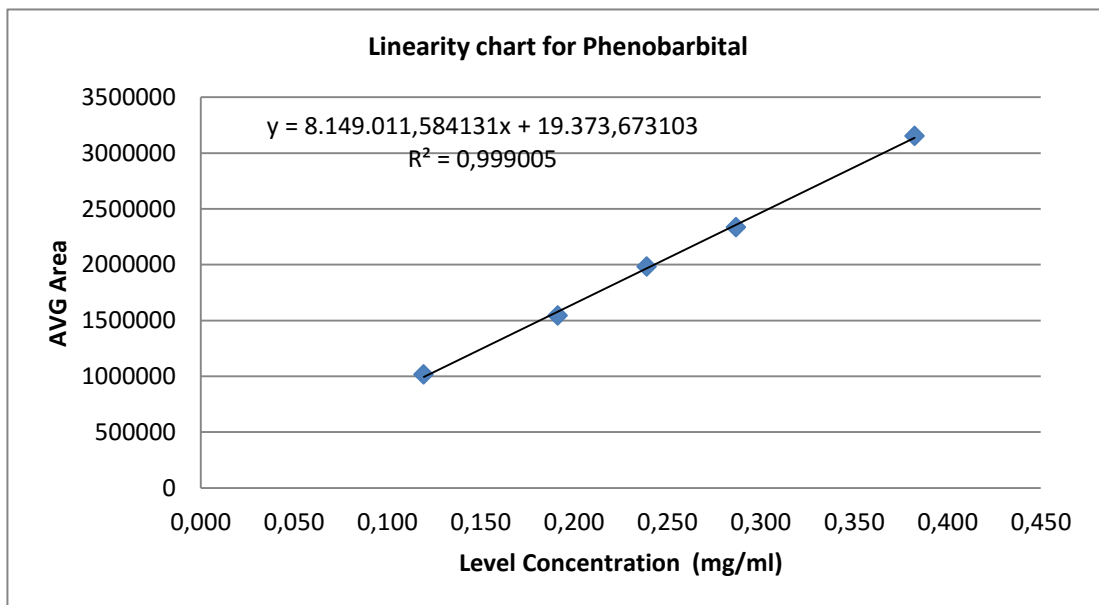


Figure 7.10. Phenobarbital calibration curve over the range of (0.12-0.384) mg/ml

Table 7.1. Chromatographic parameters

<b>Parameter</b>	<b>Details</b>
Column:	(C18,250 X 4.6 mm,5 $\mu$ m) (MN)
Flow rate:	1 ml/min
Detection:	UV PDA detector 230nm
Injection Volume:	20 $\mu$ L
Column oven Temperature	Ambient
Run time:	15 min
Retention Time	Phenobarbital about (5.8) min Pipenzolate MBr about (7.4) min.
System suitability parameters:	Column efficiency: NLT 2000 theoretical plates
For standard solution: (5 injection replicates)	Tailing factor: NMT 2.0 Relative standard deviation: NMT 2.0% Resolution between Phenobarbital and Pipenzolate methyl bromide NLT 3.

Table 7.2. System suitability data for piperzolate methyl bromide and Phenobarbital

System suitability data for piperzolate MBr target concentration: (0.16) mg /mL & Phenobarbital target concentration: (0.24) mg /mL												
System suitability parameters Limits	Retention time Pipen (t <sub>R</sub> ) RSD ≤ 1 %	Retention time Pheno (t <sub>R</sub> ) RSD ≤ 1 %	Response (AUC) Pipen RSD ≤ 2%	Response (AUC) Pheno RSD ≤ 2%	Tailing factor Pipen T < 1.5	Tailing factor Pheno T < 1.5	Theoretical plate Pipen (N) N ≥ 2000	Theoretical plate Pheno (N) N ≥ 2000	Assymet. *Pipen ≤ 2	Assymet. *Phen ≤ 2	Resolution (Rs) Pipen Rs ≥ 2 between the peak of interest and the closest eluted peak 6.478	Resolution (Rs) Pheno Rs ≥ 2 between the peak of interest and the closest eluted peak 19.574
Average of 5 replicate injections Mean recovery	7.3	5.8	638150	1956068	1.2	1.1	84764	93049	1.2	1.1		
n			5	5			5	5	5	5	5	5
SD	0.0	0.0	2455	1526	0.0	0.0						
RSD%	0.0	0.0	0.385	0.078	0.0	0.0						

\*Pipen = Piperzolate methyl bromide

\*Phen = Phenobarbital

Table 7.3. Linearity data for pipenzolate methyl bromide and Phenobarbital

<b>Parameters</b>	<b>Pipenzolate MBr</b>	<b>Phenobarbital</b>
Concentration range	(0.08-0.256) mg/mL	(0.12-0.384) mg/mL
y =	4012431.680885x - 1094.036903	8149011.584131x+19373.673103
Slope =	4012431.680885	8149011.584131
Correlation coefficient (R <sup>2</sup> )	0.999882	0.999005
Intercept	-1094.036903	19373.673103
Regression (R) limit	NLT 0.999	NLT 0.999
LOD	1.70	0.41
LOQ	5.68	1.36

Table 7.4. Accuracy (% recovery) data for Pipenzolate MBr and Phenobarbital

<b>Accuracy results for the assay method</b>						
Ingredient name	Mean recovery at 50%	Mean recovery at 100%	Mean recovery at 150%	Average	SD	RSD
Pipenzolate MBr	98.7	98.8	98.6	98.7	0.077	0.078
Phenobarbital	99.8	99.0	98.0	98.9	0.73	0.738

Table 7.5. Repeatability (intra-day precision) of Pipenzolate MBr and Phenobarbital

	<b>Concentration of Pipenzolate MBr</b>		<b>Concentration of Phenobarbital</b>	
	<b>0.16 mg /mL</b>		<b>0.24 mg /mL</b>	
	Analyte Response	Retention Time	Analyte Response	Retention Time
Average of 6 replicate injections	655171	7.3	2050508	5.8
SD	2246	0.0	5136	0.0
RSD	0.343	0.000	0.250	0.000
Limit	RSD (Area) <1%	RSD (RT) <1%	RSD (Area) <1%	RSD (RT) <1%

Table 7.6. Intermediate precision (inter-day precision) of Pipenzolate MBr and Phenobarbital

	<b>Concentration of Pipenzolate MBr 0.16 mg /mL</b>		<b>Concentration of Phenobarbital 0.24 mg /mL</b>	
	First day	Second day	First day	Second day
Average of 6 replicate injections	101.7	100.7	100.8	101.5
SD	0.279	0.2	0.2	0.2
RSD	0.274	0.199	0.198	0.197
Limit	RSD ≤ 2.0%	RSD ≤ 2.0%	RSD ≤ 2.0%	RSD ≤ 2.0%

Table 7.7. Intermediate precision (inter-day precision) of Pipenzolate MBr and Phenobarbital

Parameters	Assay values			
	Concentration of Pipenzolate MBr		Concentration of Phenobarbital	
	0.16 mg /mL	0.24 mg /mL	0.16 mg /mL	0.24 mg /mL
	First day	Second day	First day	Second day
Average of 6 replicate injections	100.8	101.5	100.8	101.5
SD	0.207	0.172	0.2	0.2
RSD	0.205	0.169	0.198	0.197
Assay average 2 days	101.2		101.1	
SD Assay value between 2 days	0.580		0.440	
R&D Assay value between 2 days	0.573		0.435	
Limit	RSD ≤ 2.0%	RSD ≤ 2.0%	RSD ≤ 2.0%	RSD ≤ 2.0%

### **7.3. Nanodrugs Production, Characterization and Kinetic Dissolution Study**

#### **7.3.1. Optimization of Antisolvent Crystallization Process**

According to single factor method, the optimum crystallization process was set under the following conditions:

- Drug concentration was (Pipenzolate MBr 125mg/ml and Phenobarbital 40mg/ml).
- The solvent to antisolvent volume ratio was 1:3
- Mixing speed 700 rpm
- Temperature was 25 °C.

Based on the conditions above, better crystals of both APIs were gained at micro and nanoscale. Thus, it feasible to prepare Pipenzolate MBr and Phenobarbital crystals via antisolvent crystallization Process.

The formation of crystals and colloidal particles of both Pipenzolate MBr and Phenobarbital decreased with the increase of temperature because increasing the temperature leads to increasing the crystal size. High temperature leads to large crystals while the low temperature will decrease the solubility in higher supersaturation and decrease the diffusion and growth kinetics consequently small particles will be obtained. Thus, 25 °C was considered an optimum temperature for the antisolvent crystallization process.

The solvent-Antisolvent ratio is an important factor. The formation rate of crystals and colloidal particles of both Pipenzolate MBr and Phenobarbital will increase with a larger amount of antisolvent. Also, the diffusion distance will increase with a higher solvent amount.

High drug concentration leads to an increase in the nucleation rate, this means massive nuclei formation and increase the number of crystals consequently smaller crystal size. Drug particle size decreases with increases in drug concentration. Nucleation rate increases with the increase of the drug concentration. Over concentration leads to agglomerate crystals and poor distribution, also it leads to the increase of the drug solution viscosity and hinders the drug diffusion between solution (solvent) and antisolvent consequently non-uniform and particles agglomeration will produce. Smaller particles are produced at the high stirring speed, increase the stirring speed will decrease the particle size (Ramisetty et al., 2013 and Teng et al., 2017).

In a solvent/antisolvent combination, the stabilizer must have a high affinity for drug particles, a quick diffusion rate, and strong adsorption onto the drug particle surface (Pouretedal, 2014).

### 7.3.2. Scanning Electron Microscopy (SEM)

A snapshot image was taken at a scale of 100 nm and 30KX magnification; the pipenzolate MBr nanoparticles were clearly visible at this stage in figure 7.11 (a). With 100K X magnification in figure 7.11 (b), the dimensions of the synthesized colloidal Pipenzolate MBr particles can be measured easily. These images were obtained from colloidal solution without stabilizer. The selected particles area was consisting of 203 nanoparticles and the diameters between (2.1–84.3) nm with average size 31.864nm.

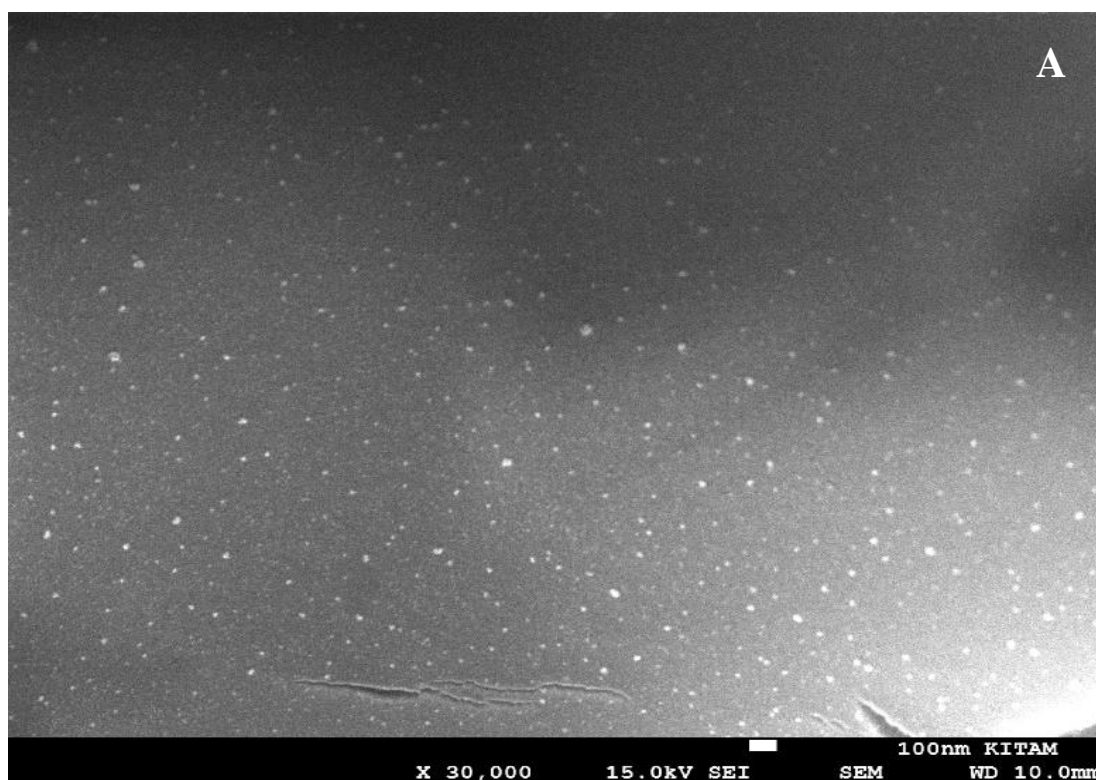


Figure7.11. SEM image of (A) Pipenzolate MBr nanoparticles at 30 KX

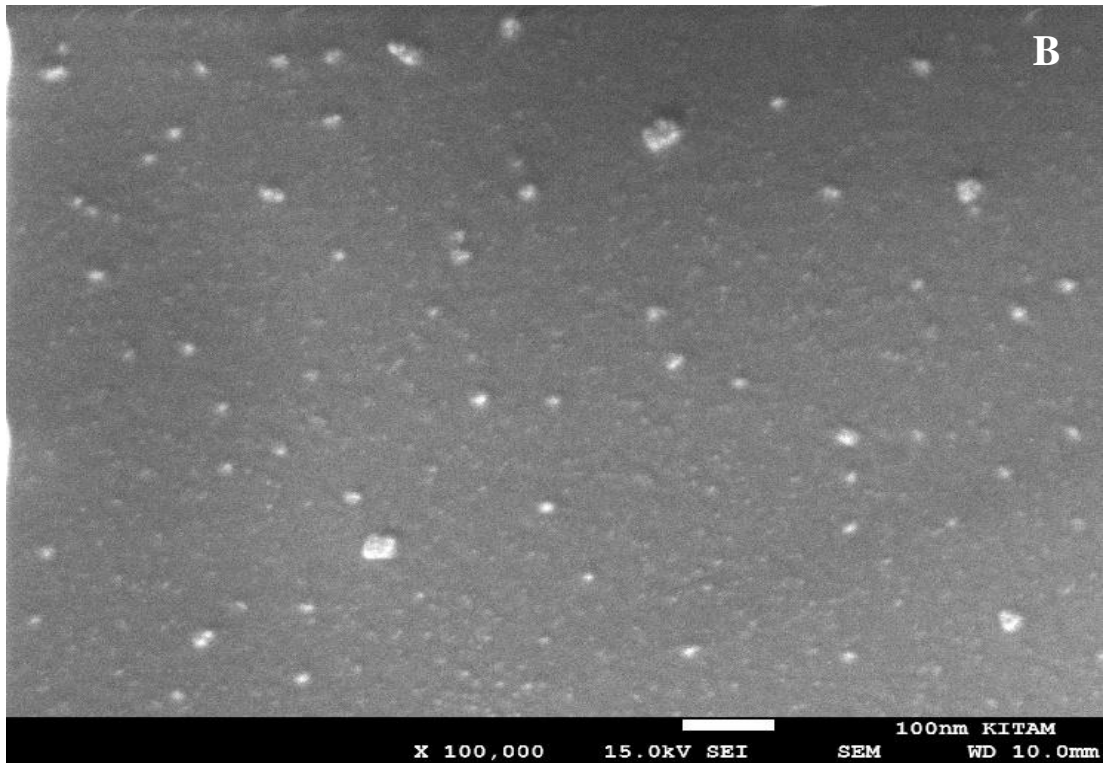


Figure7.11. SEM image of (B) Pipenzolate MBr nanoparticles at 100 KX

The other three solutions of Pipenzolate MBr with stabilizer produced micro particles because of low affinity between the drug and stabilizers (Tween 20, PVP and HPMC E6) as shown in figure 7.12.

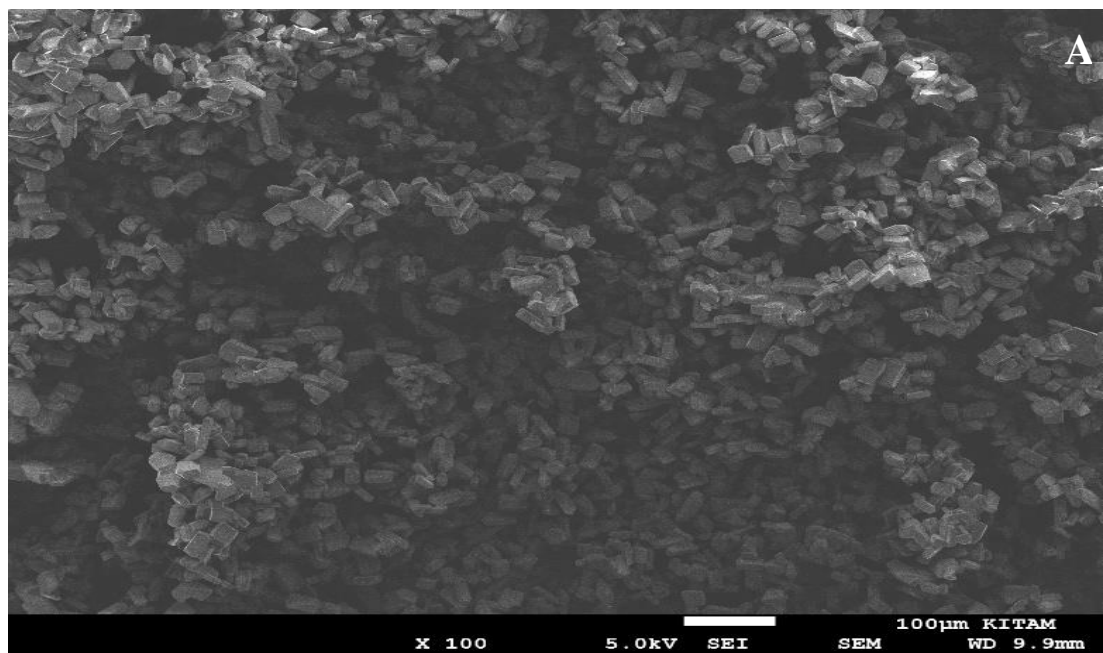


Figure7.12. SEM image of (A) Pipenzolate MBr microparticles at 100 X (Tween 20)

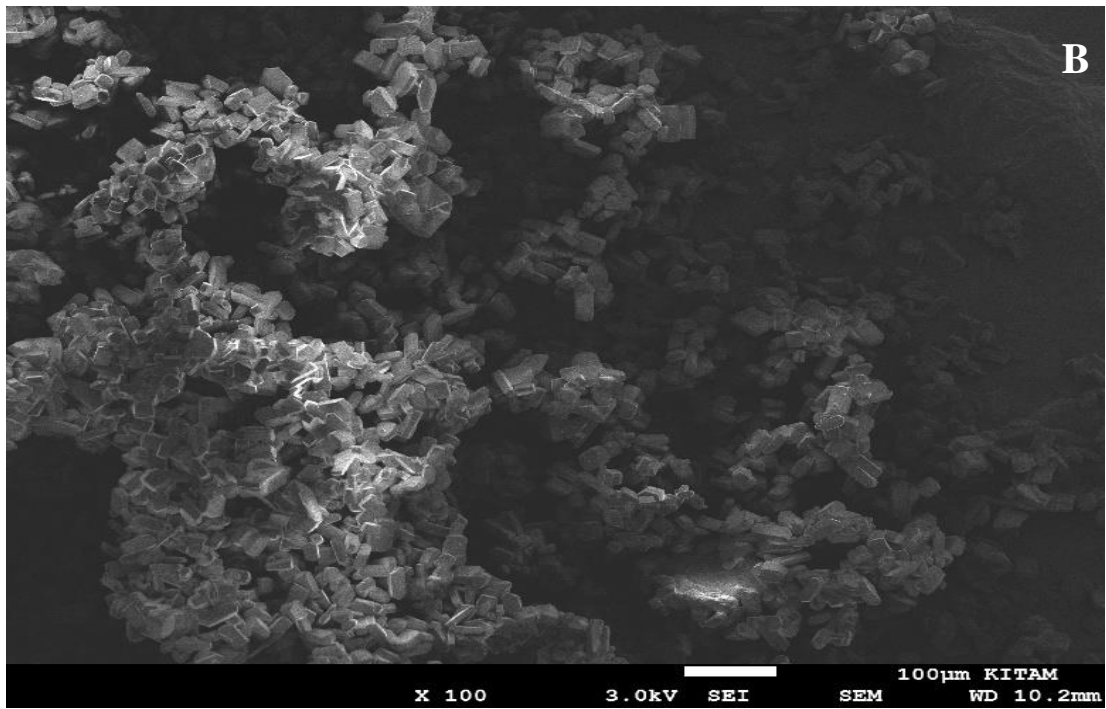


Figure7.12. SEM image of (B) Pipenzolate MBr microparticles at 100 X (PVP)

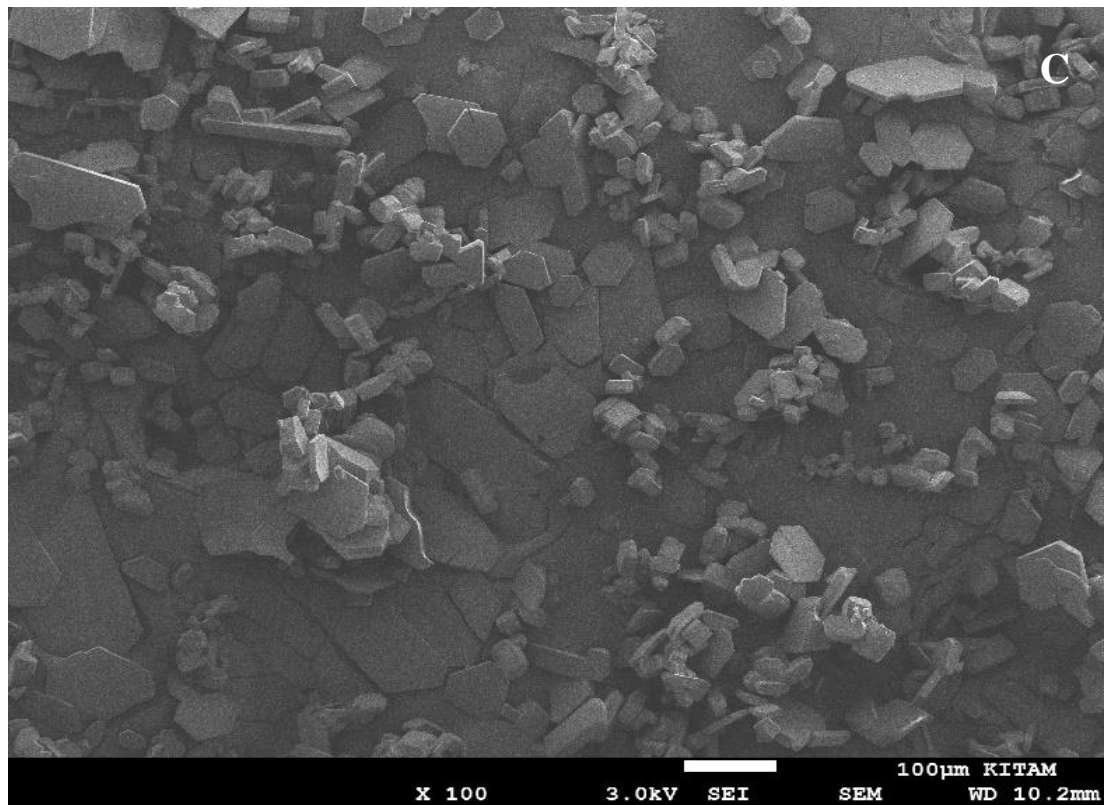


Figure7.12. SEM image of (C) Pipenzolate MBr microparticles at 100 X (HPMC E6)

A snapshot image was taken at a scale of 100 nm and 30KX magnification; in figure 7.13, the nanoparticles of Phenobarbital were clearly visible at this stage (a). With a magnification of 50KX in figure 7.13 (b), the dimensions of the synthesized colloidal Phenobarbital particles can be measured easily. These images were obtained from colloidal solution without stabilizer. The selected particles area was consisting of 657 nanoparticles and the diameters between (0.24–97.3) nm with average size 11.363nm.

The other three solutions of Phenobarbital with stabilizer produced micro particles because of low affinity between the drug and stabilizer as shown in figure 7.14.

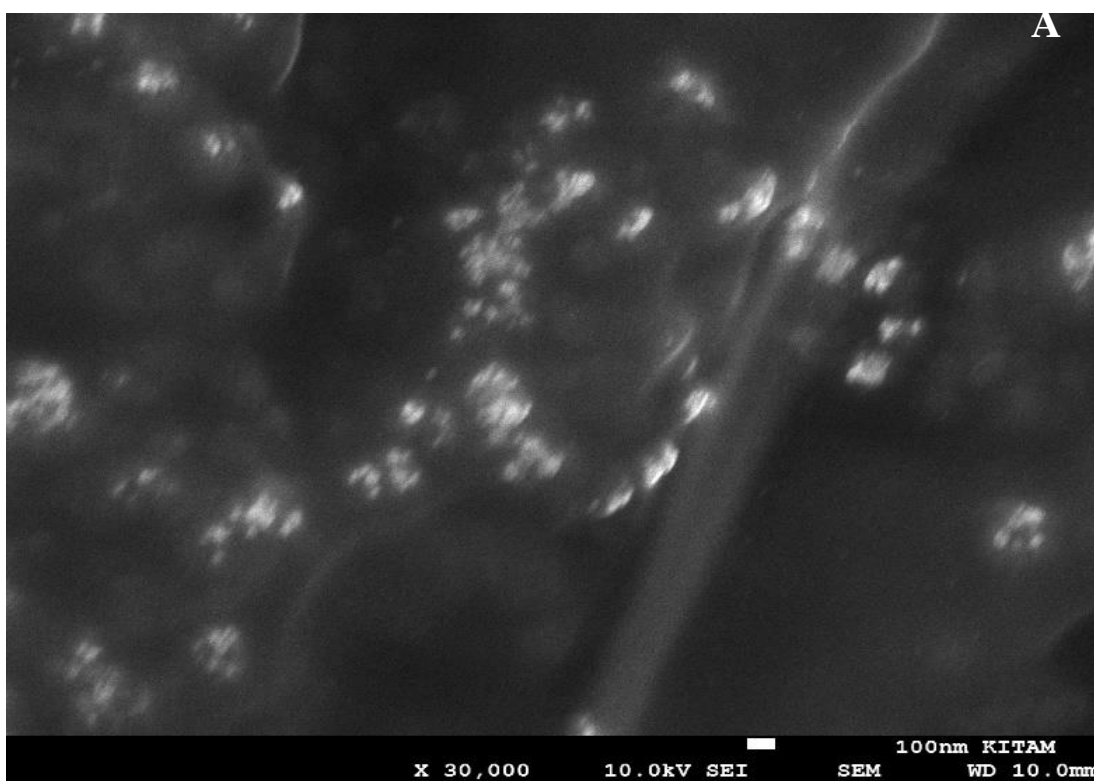


Figure 7.13. SEM image of (A) Phenobarbital nanoparticles at 30 KX

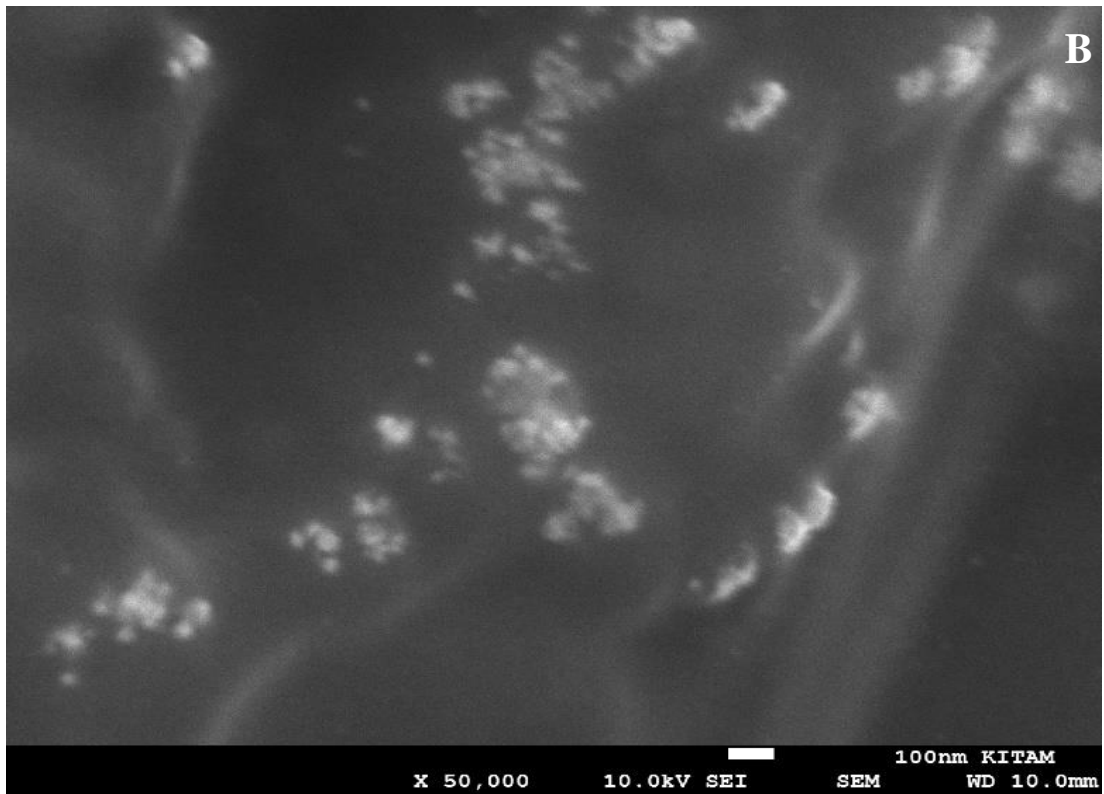


Figure7.13. SEM image of (B) Phenobarbital nanoparticles at 50 KX

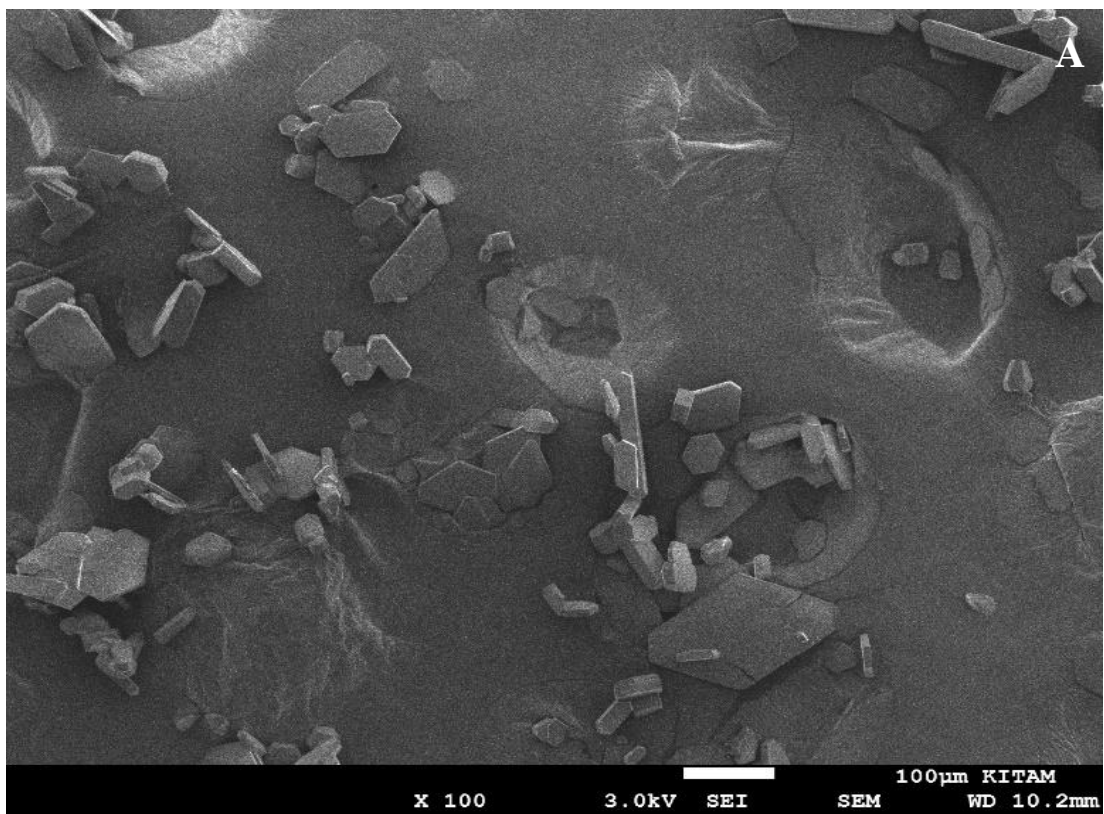


Figure7.14. SEM image of (A) Phenobarbital microparticles at 100 X (Tween 20)

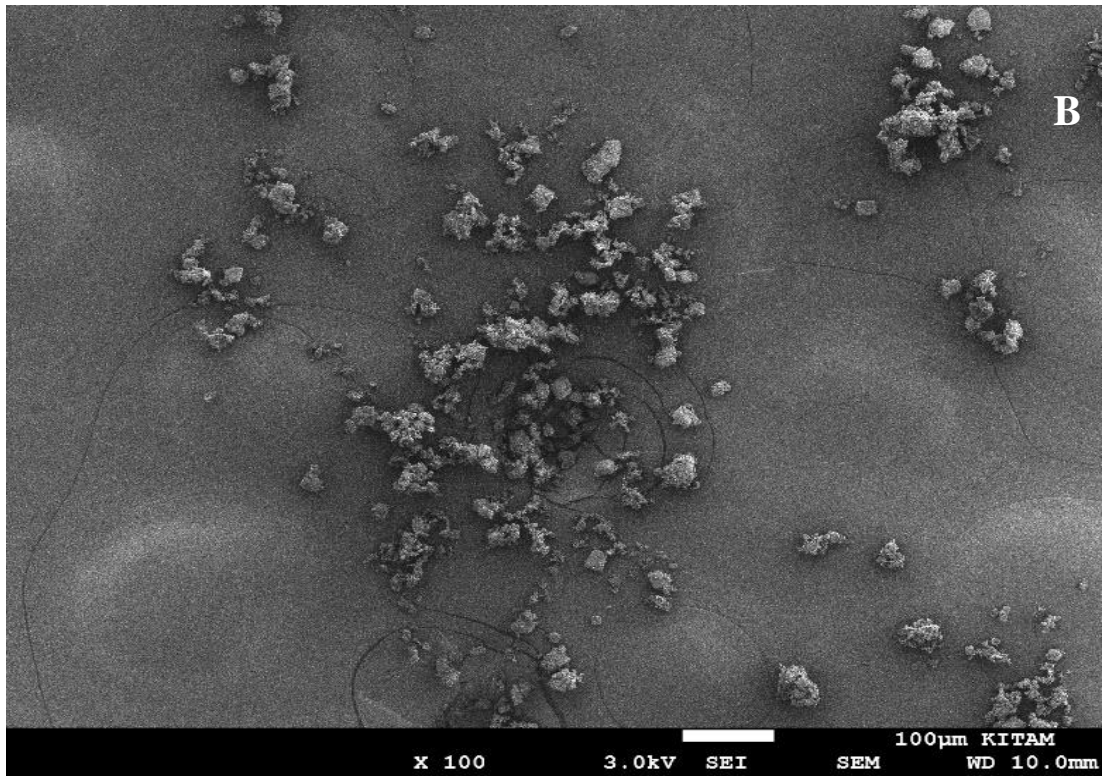


Figure7.14. SEM image of (B) Phenobarbital microparticles at 100 X (PVP)

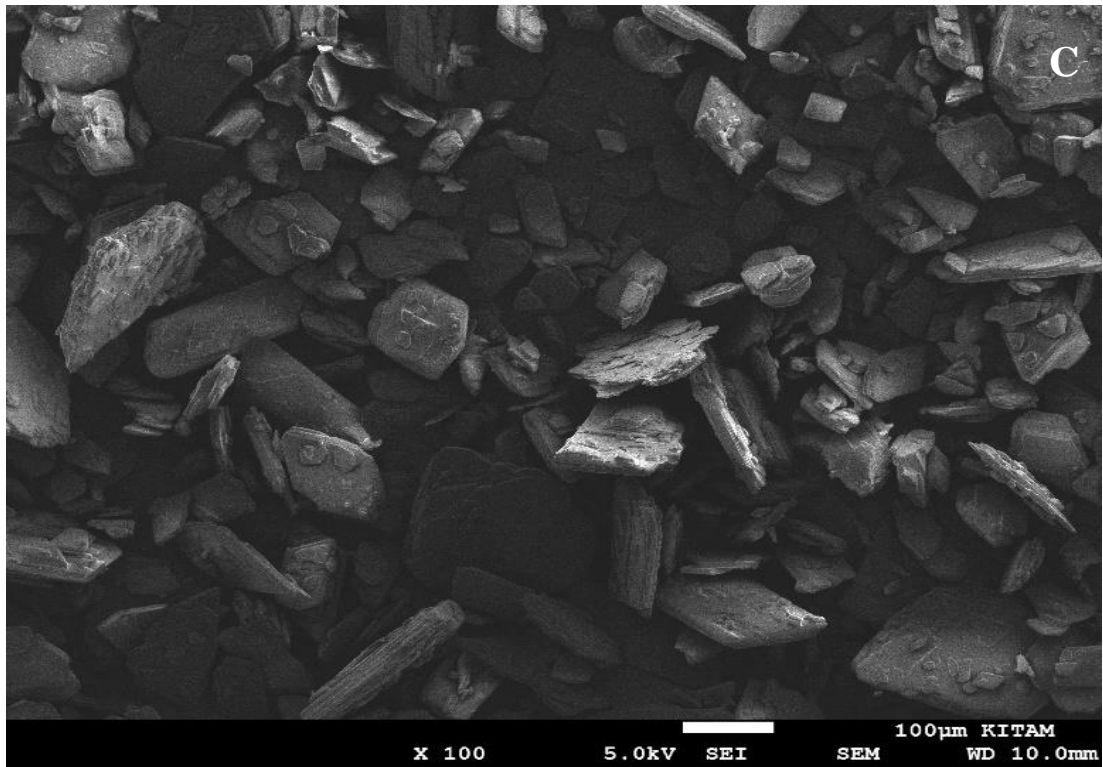


Figure7.14. SEM image of (C) Phenobarbital microparticles at 100 X (HPMC E6)

### 7.3.3. XRD Analysis

The spectra in the figure 7.15 (a) and (b) showed fifteen diffraction peaks of Pipen raw and recrystallized at  $7.17^\circ$ ,  $9.64^\circ$ ,  $12.18^\circ$ ,  $14.14^\circ$ ,  $15.94^\circ$ ,  $16.72^\circ$ ,  $19.84^\circ$ ,  $21.74^\circ$ ,  $22.65^\circ$ ,  $23.45^\circ$ ,  $24.59^\circ$ ,  $26.36^\circ$ ,  $28.59^\circ$ ,  $30.92^\circ$  and  $38.94^\circ$ .

The spectrum of major diffraction intensity peaks of Pipen raw and recrystallized nanoparticles were at  $14.14^\circ$ ,  $22.65^\circ$ ,  $19.84^\circ$  and  $24.59^\circ$  as shown in figure 7.15.

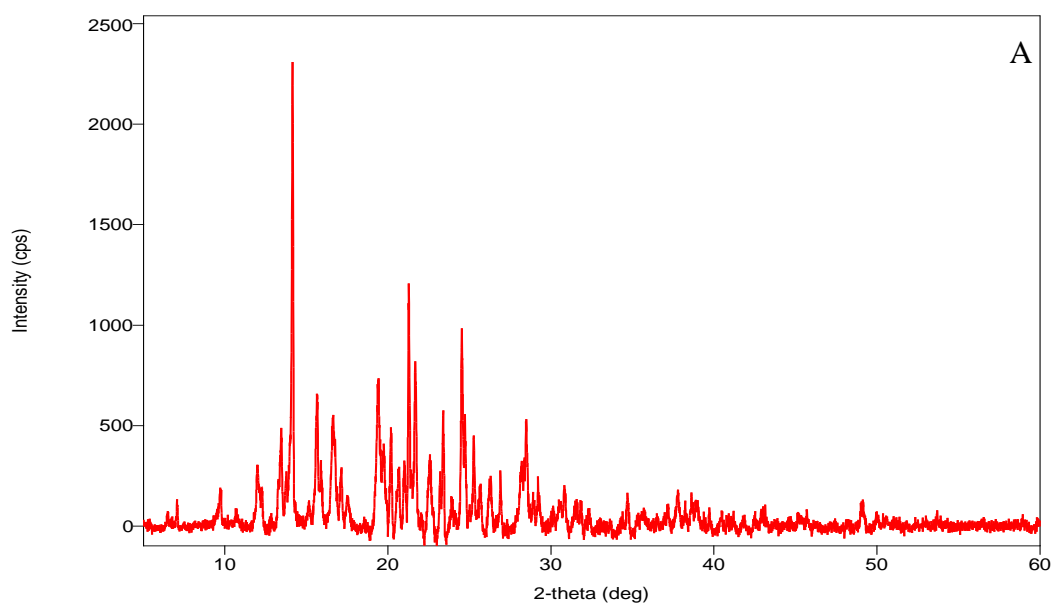


Figure 7.15. XRD pattern of (A) Pipenzolate MBr raw material

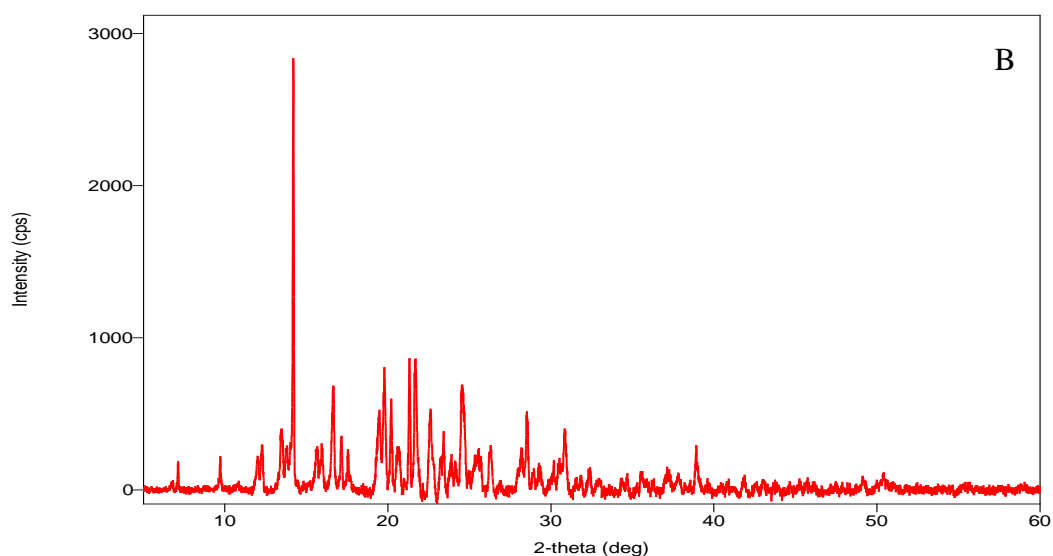


Figure 7.15. XRD pattern of (B) Pipenzolate MBr re-crystallized

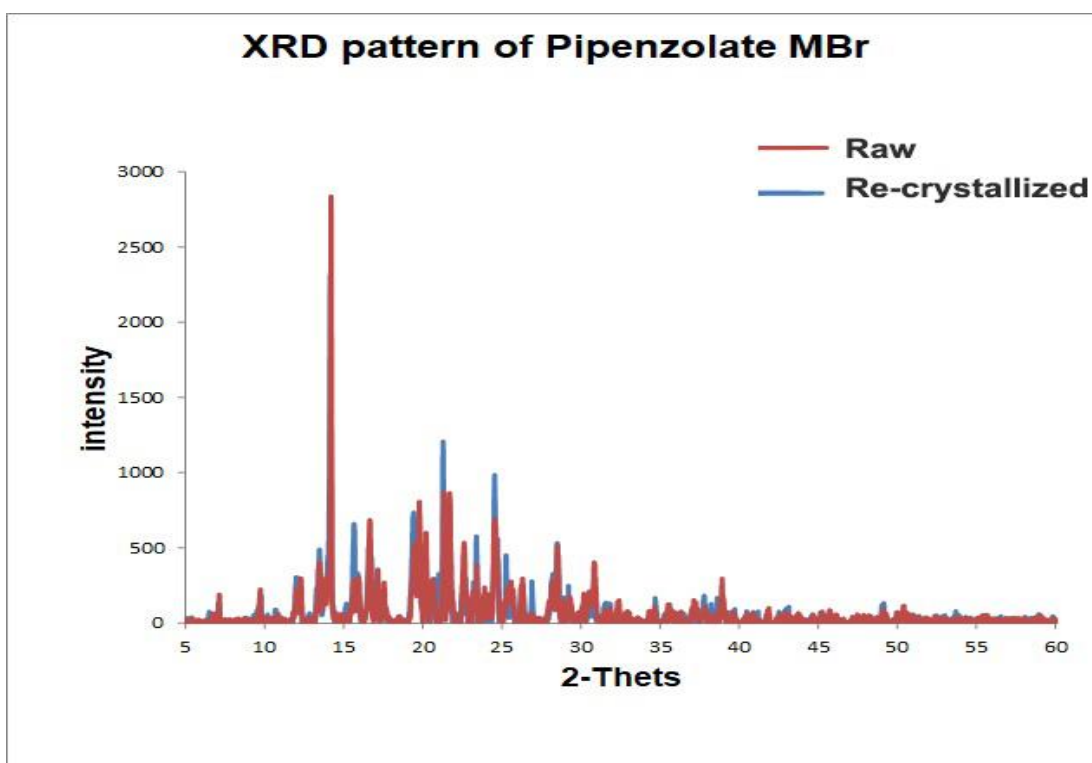


Figure 7.16. The comparison plot between XRD patterns of Pipenzolate MBr

The spectra in the figure 7.17 showed sixteen major diffraction peaks of Phenobarbital at  $7.4^\circ$ ,  $11.19^\circ$ ,  $13.83^\circ$ ,  $15.46^\circ$ ,  $17.42^\circ$ ,  $18.63^\circ$ ,  $20.92^\circ$ ,  $21.58^\circ$ ,  $22.68^\circ$ ,  $23.75^\circ$ ,  $24.78^\circ$ ,  $25.61^\circ$ ,  $26.42^\circ$ ,  $27.52^\circ$ ,  $28.38^\circ$ , and  $35.24^\circ$ .

The spectrum of major diffraction intensity peaks of Pipen raw and recrystallized nanoparticles were at  $7.4^\circ$ ,  $15.46^\circ$ ,  $18.63^\circ$  and  $22.68^\circ$  as shown in

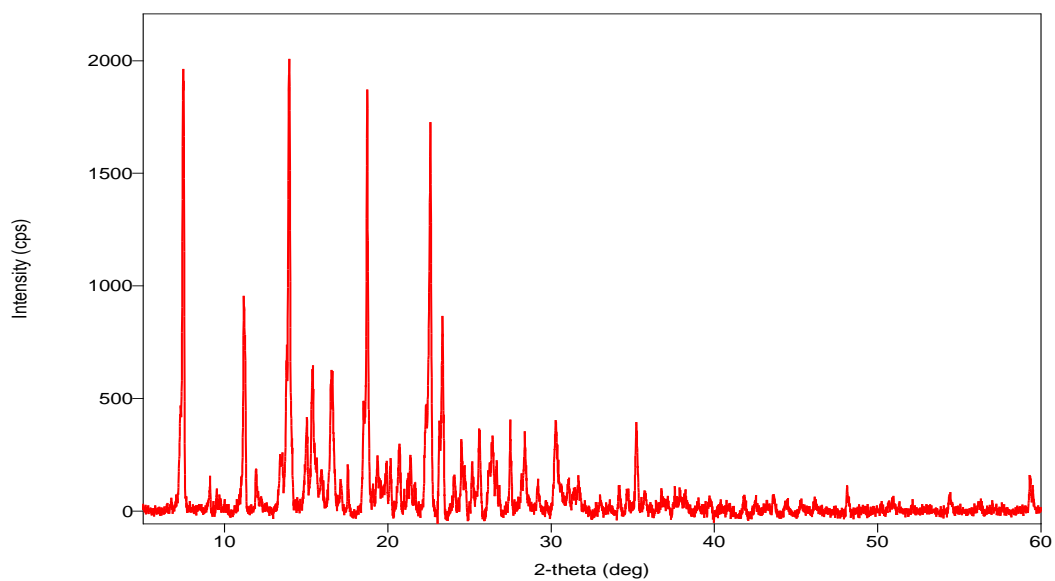


Figure 7.17. XRD pattern of (A) Phenobarbital raw material

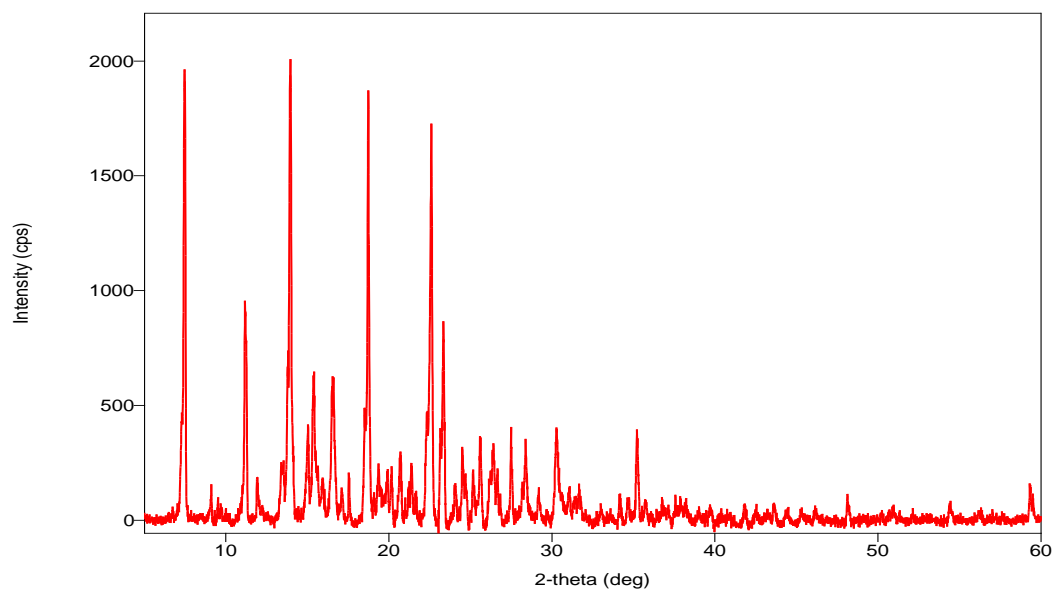


Figure 7.17. XRD pattern of (B) Phenobarbital recrystallized

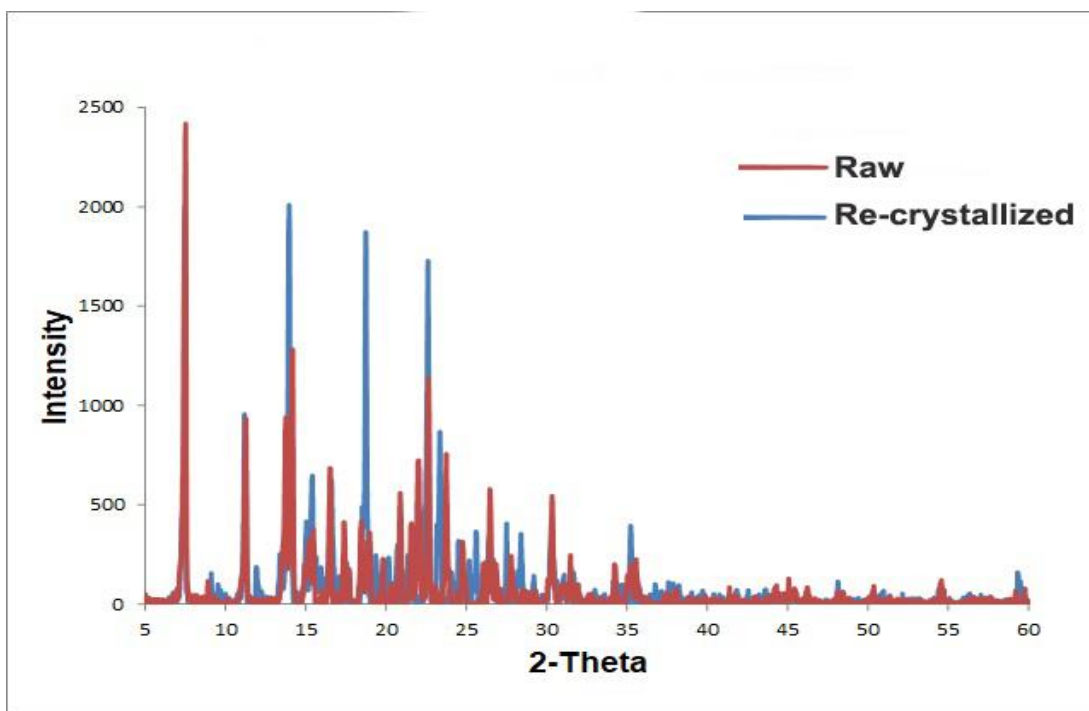


Figure 7.18. The comparison between XRD patterns of Phenobarbital

According to the comparison between XRD patterns for raw and re-crystallized powder of both Pipenzolate MBr and Phenobarbital, there was no significantly different diffractogram for Pipenzolate MBr as shown in figure 7.16, also there was no significantly changes between two phases for Phenobarbital as shown in 7.18. This result indicates that the Pipenzolate MBR and Phenobarbital particles' crystal structures are not modified during the antisolvent crystallization process.

#### 7.3.4. FTIR Analysis

The FTIR spectra of raw and re-crystallized powders for Pipenzolate MBr and Phenobarbital have been performed as shown in the next four figures. Both powders have identical absorption peaks with a frequency range of 400–4000, suggesting that the functional group structures of raw and re-crystallized powders are very similar.

For Pipen the major peak is 1735.93 which represent Aldehyde group and (1226.73, 1246.02) which represent carboxylic acid group as shown in figure 7.19.

For Phen the major peak is 1705.07 which represent Aldehyde group and (1300.02, 1224.80) which represent carboxylic acid group as shown in figure 7.21(B).

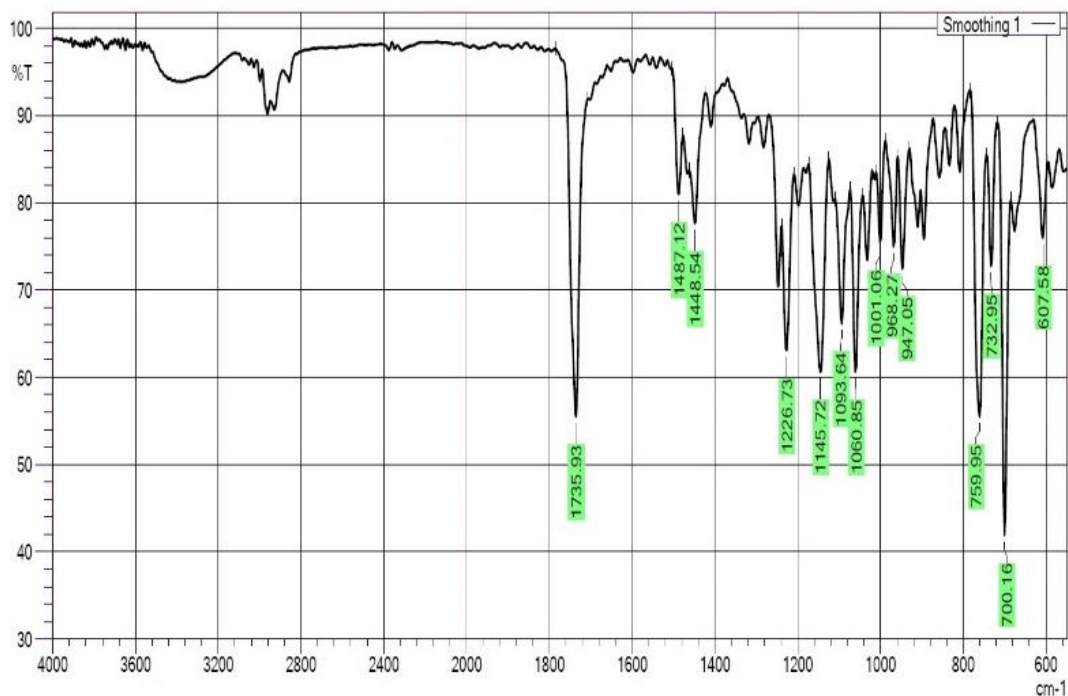


Figure 7.19. IR chart of (A) Pipenzolate MBr raw

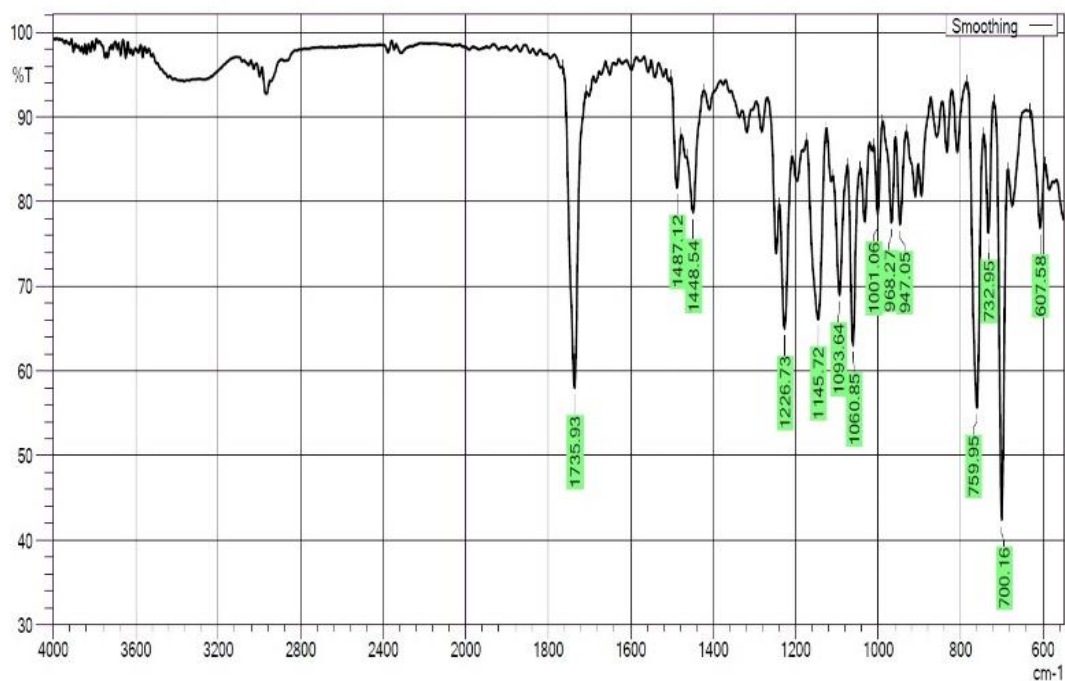


Figure 7.19. IR chart of (B) Pipenzolate MBr re-crystallized

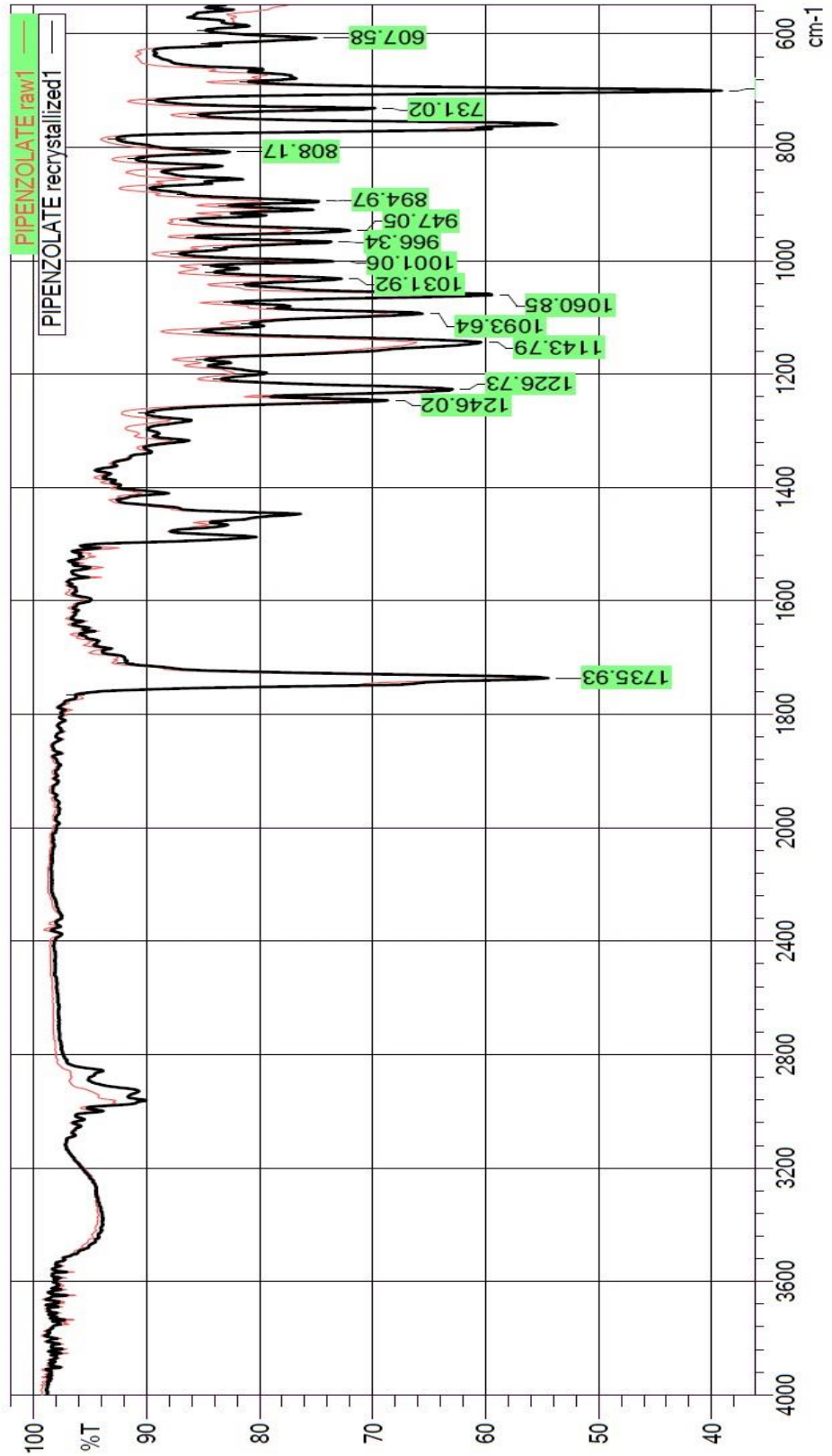


Figure 7.20. IR comparison chart between raw and re-crystallized Pipenzolate MBr

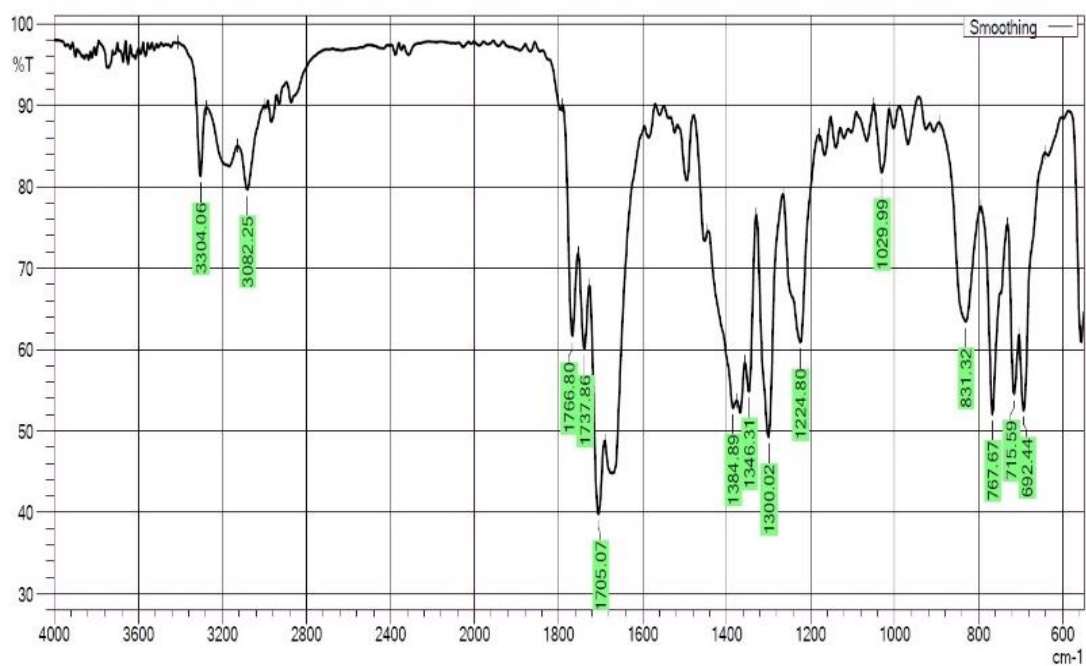


Figure 7.21. IR chart of (A) Pipenzolate MBr raw material

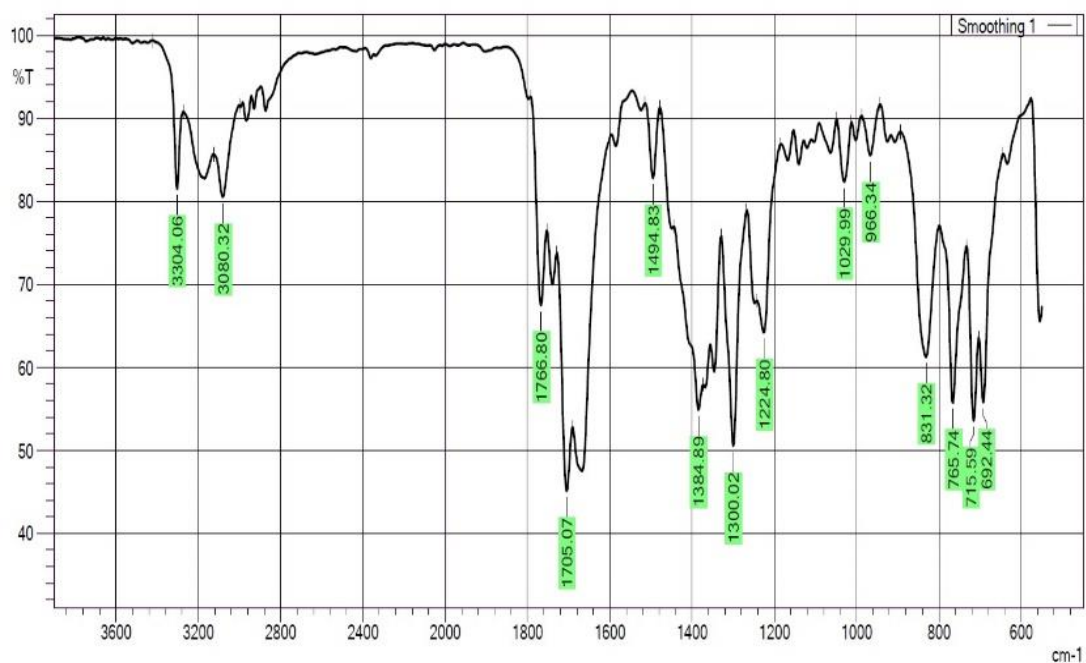


Figure 7.21. IR chart of (B) Pipenzolate MBr re-crystallized

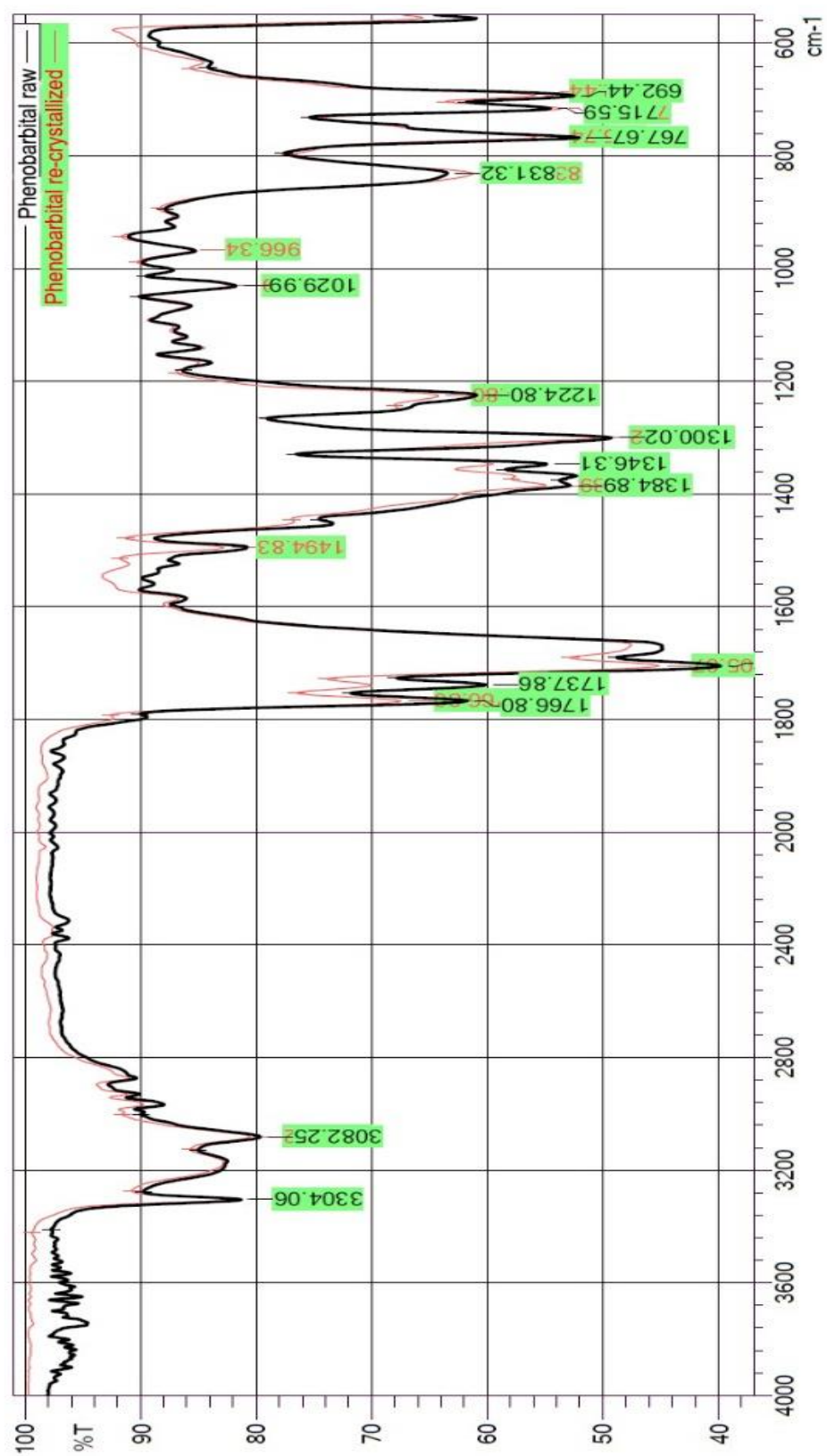


Figure 7.22. IR comparison chart between raw and re-crystallized phenobarbital

### 7.3.5. Thermo-Gravimetric Analysis (TGA)

According to the TG curves in figures (7.23 for Pipen and 7.24 for Phen), when the temperature of raw and re-crystallized API powders increased from 40 to 225 °C, almost no weight loss occurs, but weight loss occurs rapidly above 225 °C. Both raw and re-crystallized powders lost about the same amount of weight. These findings indicate that both types of materials exhibit a high degree of thermal stability (below 225 °C).

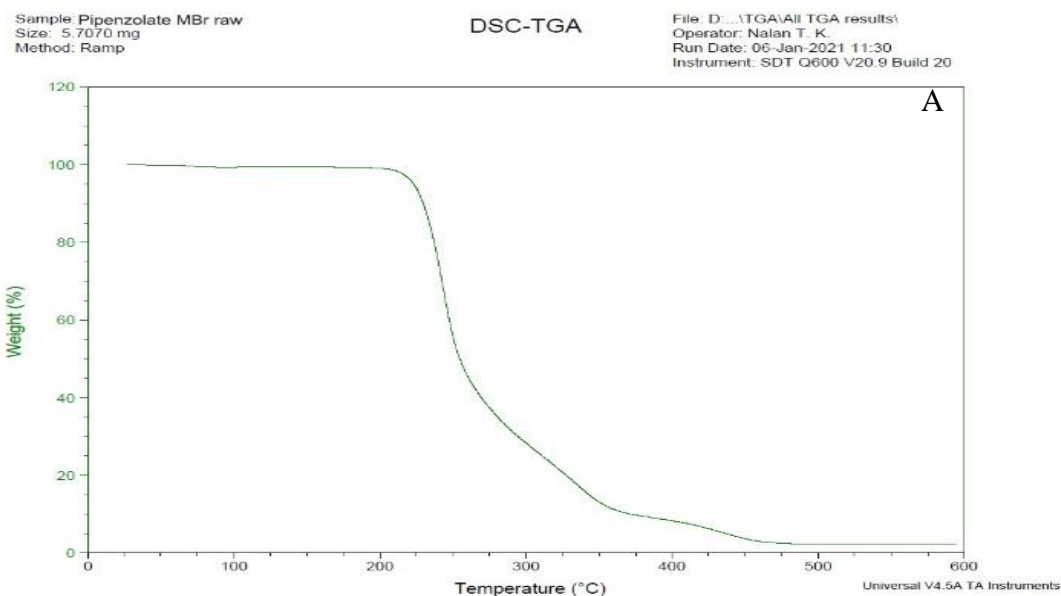


Figure 7.23. TG curve of (A) Pipenzolate MBr raw material

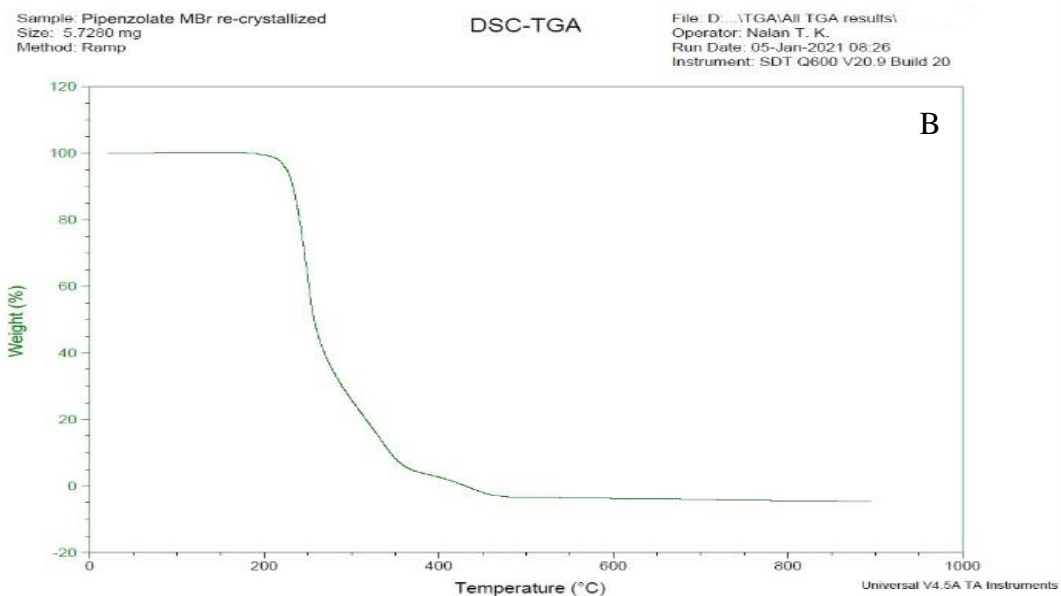


Figure 7.23. TG curve of (B) Pipenzolate MBr re-crystallized

Sample: Phenobarbital raw  
Size: 6.7870 mg  
Method: Ramp

DSC-TGA

File: D:\...TGA\All TGA results\  
Operator: Nalan T. K.  
Run Date: 06-Jan-2021 08:37  
Instrument: SDT Q600 V20.9 Build 20

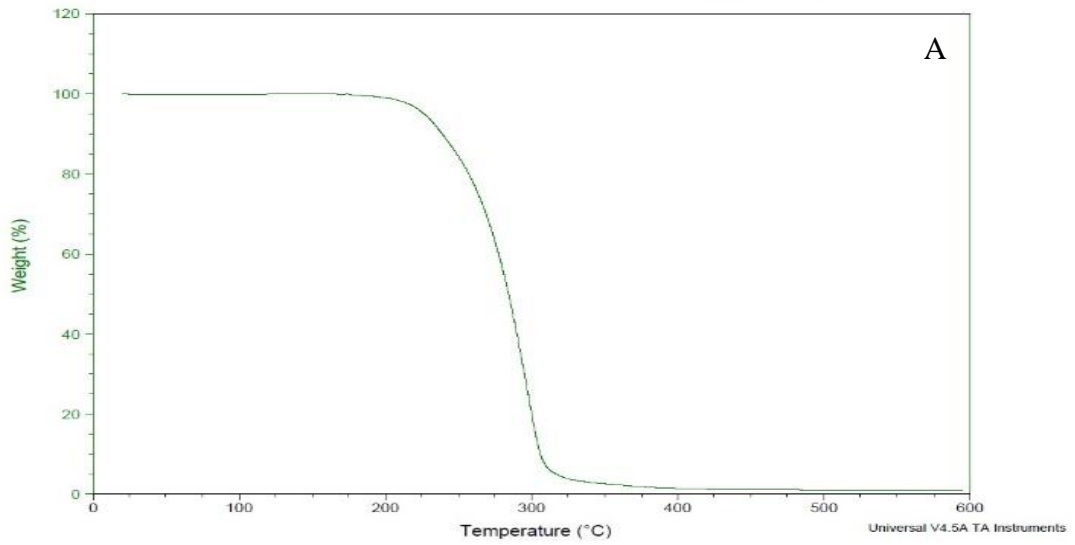


Figure 7.24. TG curve of (A) Phenobarbital raw material

Sample: Phenobarbital re-crystallized  
Size: 6.6340 mg  
Method: Ramp

DSC-TGA

File: D:\...TGA\All TGA results\  
Operator: Nalan T. K.  
Run Date: 05-Jan-2021 11:31  
Instrument: SDT Q600 V20.9 Build 20

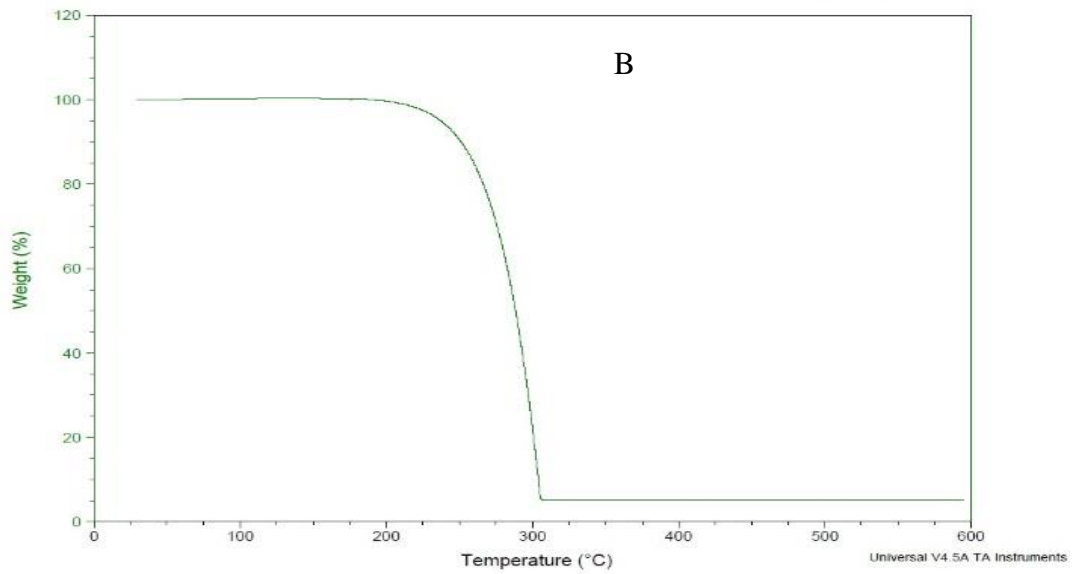


Figure 7.24. TG curve of (B) Phenobarbital re-crystallized

### 7.3.6. Differential Scanning Calorimetry (DSC) Analysis

The DSC technique is used to determine the temperature and energy differences at phase transitions, which are related to the degree of crystallinity and stability of the drug's solid state. As shown in figure 7.25, the DSC thermogram of Pipenzolate MBr (raw and re-crystallized powders) revealed one exothermic peak at 187.5 °C, while Phenobarbital (raw and re-crystallized powders) revealed one exothermic peak at 175 °C, both of which were attributed to melting and decomposition as shown in figure 7.26. This phenomenon was supported by XRD results, which revealed that the re-crystallized structure of Pipenzolate MBr had changed, while Phenobarbital's structure remained unchanged.

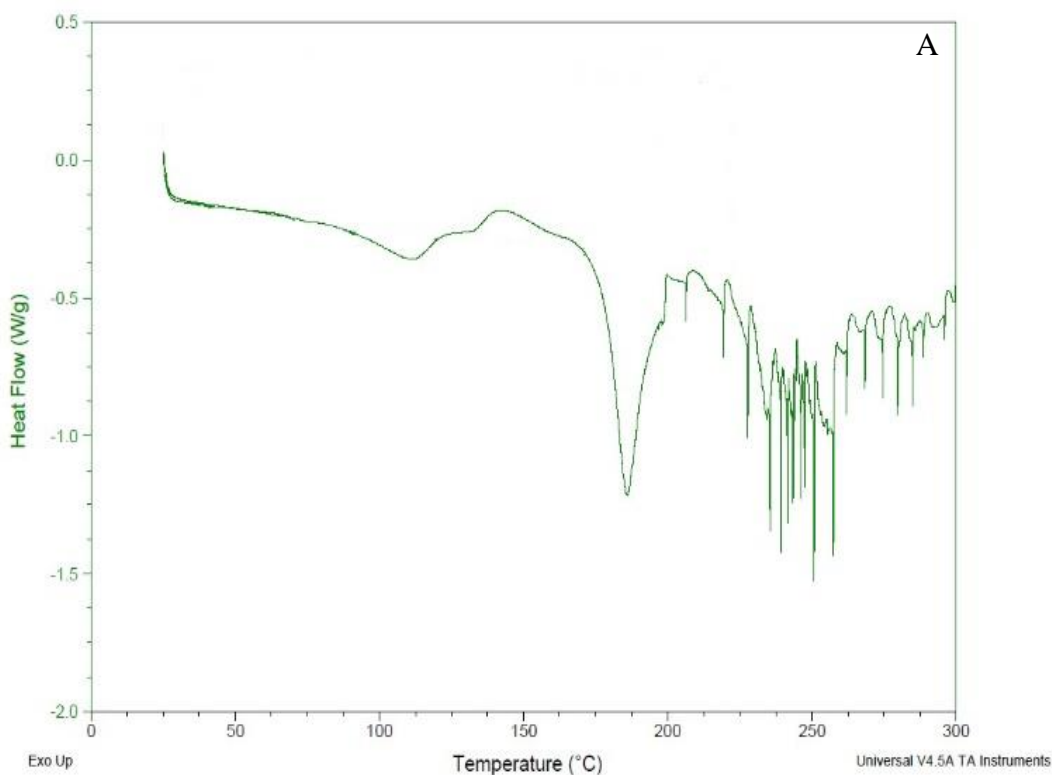


Figure 7.25. DSC curve of (A) Pipenzolate MBr raw material

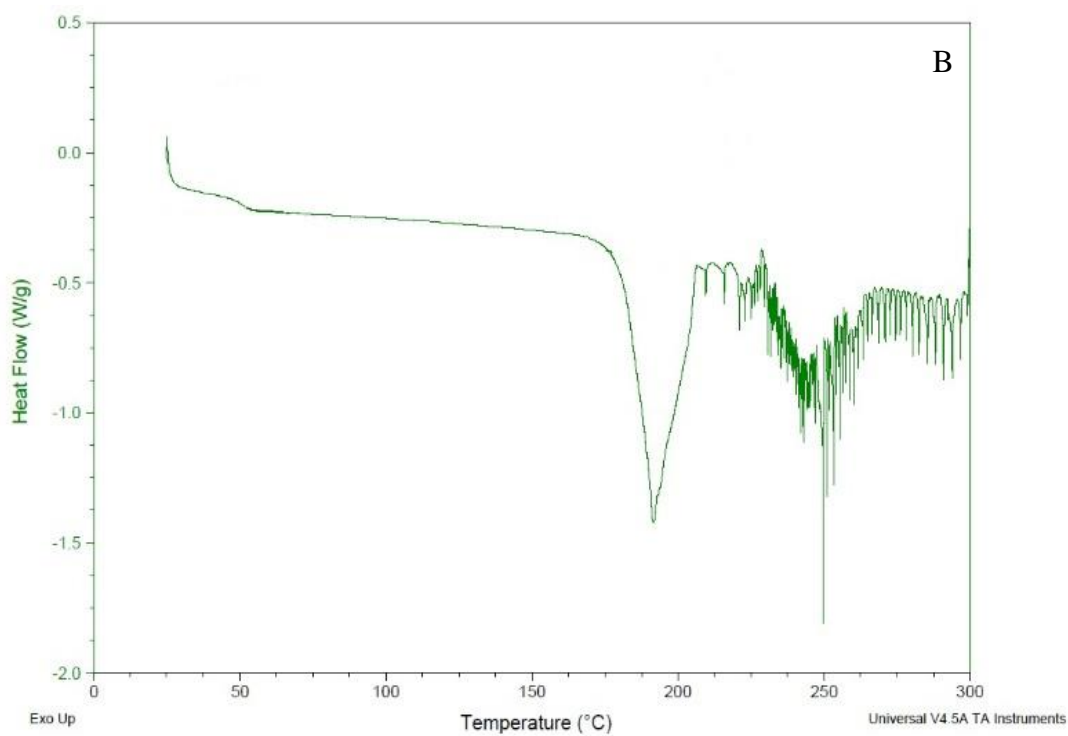


Figure 7.25. DSC curve of (B) Pipenzolate MBr re-crystallized

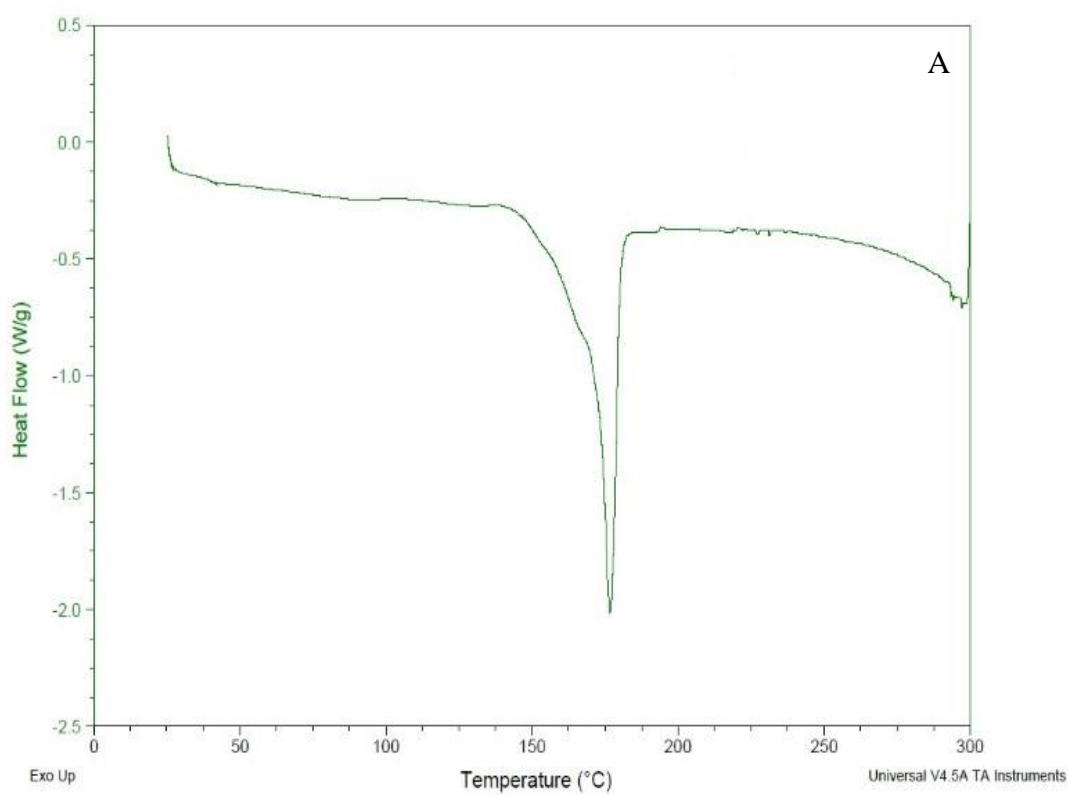


Figure 7.26. DSC curve of (A) Phenobarbital raw material

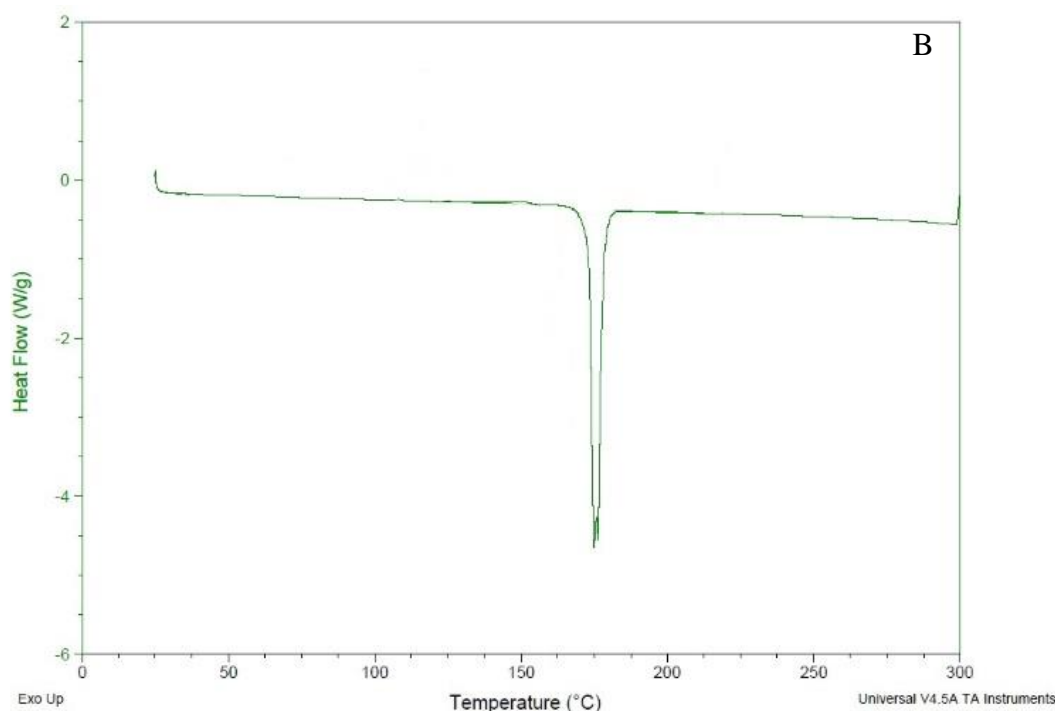


Figure 7.26. DSC curve of (B) Phenobarbital re-crystallized

### 7.3.7. Kinetic Dissolution Study

The dissolution results of Pipenzolate MBr as per figure 7.27 showed that the solubility of re-crystallized powder was increased by twice as compared with raw powder. Thus, it is feasible to prepare Pipenzolate powder at micro and nano-scale via antisolvent crystallization method to improve and enhance its dissolution rate in water.

The dissolution results of Phenobarbital as per figure 7.28 showed that the solubility of re-crystallized powder was increased by three times as compared with raw powder. Thus, it is feasible to prepare Phenobarbital powder at micro and nano-scale via antisolvent crystallization method to improve and enhance its dissolution rate in water.

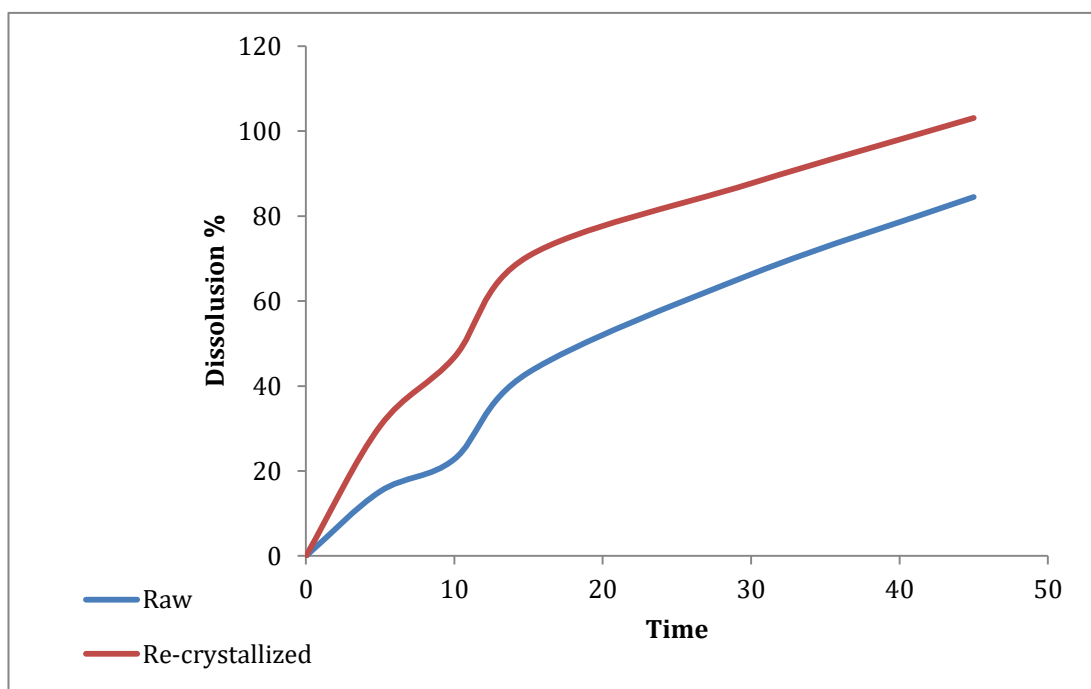


Figure 7.27. Comparison dissolution profile of raw versus re-crystallized of Pipenzolate MBr.

Table 7.8. The percentage raw and re-crystallized Pipenzolate MBr release versus time

Time	Raw	Re-crystallized
0	0	0
5	15.2 %	30.6%
10	22.8%	46.8%
15	43.2%	70.6%
30	66.3%	87.7%
45	84.5%	103.1%

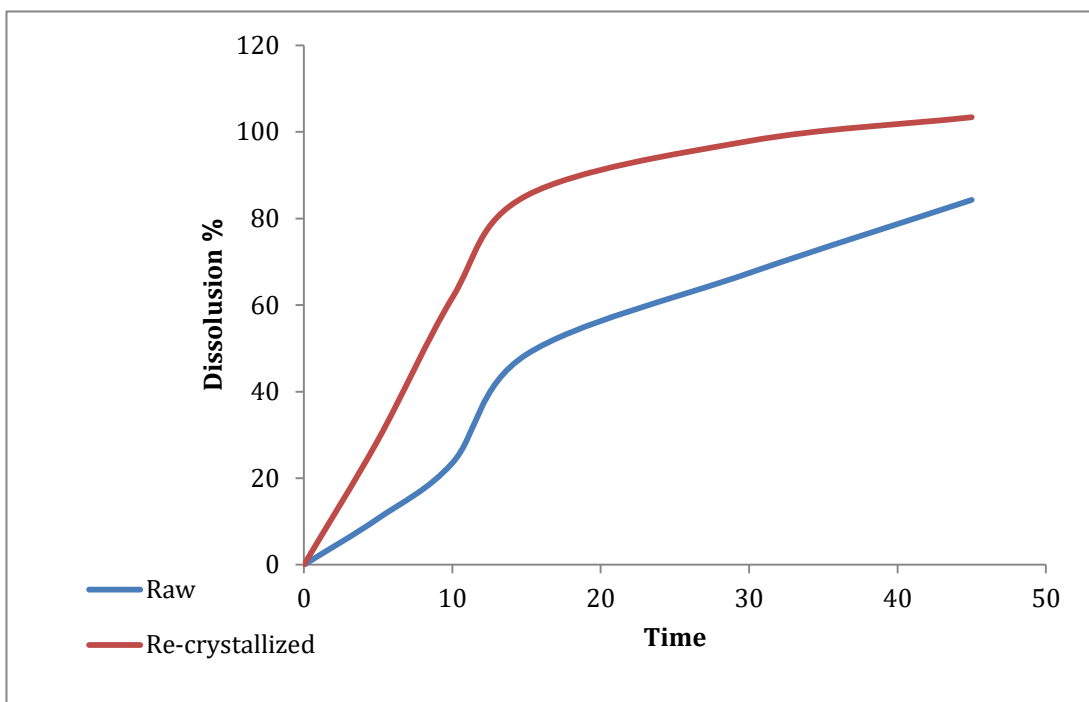


Figure 7.28. Comparison dissolution profile of raw versus re-crystallized of Phenobarbital.

Table 7.9. The percentage raw and re-crystallized Pipenzolate MBr release versus time

Time	Raw	Re-crystallized
0	0	0
5	10.7	28.9
10	23.5	61.7
15	48.6	85.3
30	67.4	97.9
45	84.3	103.4

## 8. CONCLUSION

- Pipenzolate methyl bromide and Phenobarbital nano-drugs were successfully synthesized by Antisolvent Crystallization technique.
- Pipenzolate was prepared by an optimum parameter (Drug concentration: 125 mg/mL, 700 rpm under 25°C).
- Phenobarbital was prepared by an optimum parameter (Drug concentration: 40 mg/mL, 700 rpm under 25°C).
- Antisolvent Crystallization technique appeared unique properties of particle size in terms of controlling the drug concentration and stirring speed at room temperature.
- Particle size of produced nano-drugs were obtained within nano-scale.
- A new proposed HPLC method exhibits that it was simple, reliable and validated method for routine work in quality control department.
- In antisolvent crystallization the selection of solvent and antisolvent must be done precisely as possible as due to their miscibility.
- It would be useful to find another compatible stabilizer to get more nanodrugs quantity.
- Antisolvent crystallization conserved the structure of Pipenzolate MBr and Phenobarbital during fabrication process based on XRD, FTIR, TGA and DSC analysis.

## REFERENCES

- Abo-Talib, N. F., & El-Ghobashy, M. R. (2009). Simultaneous determination of pipenzolate bromide and phenobarbitone in pharmaceutical preparations by HPLC method.
- Abrams, P., Andersson, K. E., Buccafusco, J. J., Chapple, C., De Groat, W. C., Fryer, A. D., & Wein, A. J. (2006). Muscarinic receptors: their distribution and function in body systems, and the implications for treating overactive bladder. *British journal of pharmacology*, 148(5), 565-578.
- Aguilar, M. I. and Hearn, M. T. W. (1996) High resolution reversed phase high performance liquid chromatography of peptides and proteins. *Meth. Enzymol.* 270, 3–26.
- Ahmad, N. R., & Sulyman, E. Z. Development of Kinetic Spectrophotometric Determination of pipenzolate methyl bromide in Pharmaceutical Preparations.
- Ahuja, S., & Rasmussen, H. (Eds.). (2011). HPLC method development for pharmaceuticals. Elsevier.
- Balaban, A. T. (Ed.). (2006). *From chemical topology to three-dimensional geometry*. Springer Science & Business Media.
- Betle Broth, P. (2012). Phytofabrication and characterization of silver nanoparticles from Piper betle broth. *Research Journal of Nanoscience and nanotechnology*, 2(1), 17-23.
- Birdsall, N. J., & Lazareno, S. (2005). Allosterism at muscarinic receptors: ligands and mechanisms. *Mini reviews in medicinal chemistry*, 5(6), 523-543.
- Bleeker, E. A. J., Cassee, F. R., Geertsma, R. E., de Jong, W. H., Heugens, E. H. W., Koers-Jacquemijns, M., ... & Wijnhoven, S. W. P. (2012). Interpretation and implications of the European Commission's definition on nanomaterials.
- Borman, P., & Elder, D. (2018). ICH Quality Guidelines: An Implementation Guide.
- Carmine, A. A., & Brogden, R. N. (1985). Pirenzepine. *Drugs*, 30(2), 85-126.
- Caulfield, M. P., Birdsall, N. J., & International Union of Pharmacology. (1998). XVII. Classification of muscarinic acetylcholine receptors. *Pharmacol Rev*, 50, 279-290.
- Chandra, R., & Sharma, K. D. (2013). Quantitative determination of paracetamol and caffeine from formulated tablets by reversed phase-HPLC separation technique. *Int J Chromatogr Sci*, 3(2), 31-34.
- Cheng, F., Li, W., Liu, G., & Tang, Y. (2013). In silico ADMET prediction: recent advances, current challenges and future trends. *Current topics in medicinal chemistry*, 13(11), 1273-1289.
- Cho, E., Cho, W., Cha, K. H., Park, J., Kim, M. S., Kim, J. S., ... & Hwang, S. J. (2010). Enhanced dissolution of megestrol acetate microcrystals prepared by antisolvent precipitation process using hydrophilic additives. *International journal of pharmaceutics*, 396(1-2), 91-98.

- Colvin, V. L., Schlamp, M. C., & Alivisatos, A. P. (1994). Light-emitting diodes made from cadmium selenide nanocrystals and a semiconducting polymer. *Nature*, 370(6488), 354-357.
- Daniel, M. C., & Astruc, D. (2004). Gold nanoparticles: assembly, supramolecular chemistry, quantum-size-related properties, and applications toward biology, catalysis, and nanotechnology. *Chemical reviews*, 104(1), 293-346.
- Farwell, J. R., Lee, Y. J., Hirtz, D. G., Sulzbacher, S. I., Ellenberg, J. H., & Nelson, K. B. (1990). Phenobarbital for febrile seizures—effects on intelligence and on seizure recurrence. *New England Journal of Medicine*, 322(6), 364-369.
- Ferreira, L. G., Dos Santos, R. N., Oliva, G., & Andricopulo, A. D. (2015). Molecular docking and structure-based drug design strategies. *Molecules*, 20(7), 13384-13421.
- Ferreira, L. L., & Andricopulo, A. D. (2019). ADMET modeling approaches in drug discovery. *Drug discovery today*, 24(5), 1157-1165.
- Fleming, N. (2018). Computer-calculated compounds. *Nature*, 557(7707), S55-S57.
- Gao, L., Zhang, D., & Chen, M. (2008). Drug nanocrystals for the formulation of poorly soluble drugs and its application as a potential drug delivery system. *Journal of Nanoparticle Research*, 10(5), 845-862.
- González-Medina, M., Naveja, J. J., Sánchez-Cruz, N., & Medina-Franco, J. L. (2017). Open chemoinformatic resources to explore the structure, properties and chemical space of molecules. *RSC advances*, 7(85), 54153-54163.
- Hadad, G. M. (2008). Validated, Stability-Indicating LC Method for Analysis of Pipenzolate Bromide and Its Hydrolysis Products. *Chromatographia*, 68(3), 207-212.
- Hansch, C., Sammes, P. G., & Taylor, J. B. (1990). Computers and the medicinal chemist. *Comprehensive medicinal chemistry*, 4, 33-58.
- Homayouni, A., Sadeghi, F., Varshosaz, J., Garekani, H. A., & Nokhodchi, A. (2014). Promising dissolution enhancement effect of soluplus on crystallized celecoxib obtained through antisolvent precipitation and high-pressure homogenization techniques. *Colloids and Surfaces B: Biointerfaces*, 122, 591-600.
- Ibrahim, H. (2020). Nanotechnology and Its Applications to Medicine: an over view. *QJM: An International Journal of Medicine*, 113(Supplement\_1), hcaa060-008.
- Kakran, M., Sahoo, N. G., Tan, I. L., & Li, L. (2012). Preparation of nanoparticles of poorly water-soluble antioxidant curcumin by antisolvent precipitation methods. *Journal of Nanoparticle Research*, 14(3), 1-11.
- Kakran, M., Sahoo, N. G., Tan, I. L., & Li, L. (2012). Preparation of nanoparticles of poorly water-soluble antioxidant curcumin by antisolvent precipitation methods. *Journal of Nanoparticle Research*, 14(3), 1-11.
- Karelson, M. (2000). *Molecular descriptors in QSAR/QSPR*. Wiley-Interscience.
- Karthikeyan, M., & Vyas, R. (2014). Chemoinformatics approach for the design and screening of focused virtual libraries. In *Practical Chemoinformatics* (pp. 93-131). Springer, New Delhi.

- Kitchen, D. B., Decornez, H., Furr, J. R., & Bajorath, J. (2004). Docking and scoring in virtual screening for drug discovery: methods and applications. *Nature reviews Drug discovery*, 3(11), 935-949.
- Kumalo, H. M., Bhakat, S., & Soliman, M. E. (2015). Theory and applications of covalent docking in drug discovery: merits and pitfalls. *Molecules*, 20(2), 1984-2000.
- Kurup, M., & Arun, R. R. (2016). Antisolvent crystallization: a novel approach to bioavailability enhancement. *European Journal of Biomedical and Pharmaceutical Sciences*, 3(3), 230-4.
- Li, C., Li, C., Le, Y., & Chen, J. F. (2011). Formation of bicalutamide nanodispersion for dissolution rate enhancement. *International journal of pharmaceutics*, 404(1-2), 257-263.
- Liu, Y., Sun, C., Hao, Y., Jiang, T., Zheng, L., & Wang, S. (2010). Mechanism of dissolution enhancement and bioavailability of poorly water-soluble celecoxib by preparing stable amorphous nanoparticles. *Journal of Pharmacy & Pharmaceutical Sciences*, 13(4), 589-606.
- Livanainen, M., & Savolainen, H. (1983). Side effects of phenobarbital and phenytoin during long- term treatment of epilepsy. *Acta Neurologica Scandinavica*, 68, 49-67.
- Lonare, A. A., & Patel, S. R. (2013). Antisolvent crystallization of poorly water-soluble drugs. *International Journal of Chemical Engineering and Applications*, 4(5), 337.
- London, N., Miller, R. M., Krishnan, S., Uchida, K., Irwin, J. J., Eidam, O., & Taunton, J. (2014). Covalent docking of large libraries for the discovery of chemical probes. *Nature chemical biology*, 10(12), 1066-1072.
- Lu, P. J., & Weitz, D. A. (2013). Colloidal particles: crystals, glasses, and gels. *Annu. Rev. Condens. Matter Phys.*, 4(1), 217-233.
- Lu, Y., Chen, Y., Gemeinhart, R. A., Wu, W., & Li, T. (2015). Developing nanocrystals for cancer treatment. *Nanomedicine*, 10(16), 2537-2552.
- Lu, Y., Li, Y., & Wu, W. (2016). Injected nanocrystals for targeted drug delivery. *Acta Pharmaceutica Sinica B*, 6(2), 106-113.
- Macdonald, R. L., & Greenfield Jr, L. J. (1997). Mechanisms of action of new antiepileptic drugs. *Current opinion in neurology*, 10(2), 121-128.
- Matsuoka, H., Ise, N., Okubo, T., Kunugi, S., Tomiyama, H., & Yoshikawa, Y. (1985). "Ordered" structure in dilute solutions of biopolymers as studied by small- angle x- ray scattering. *The Journal of chemical physics*, 83(1), 378-387.
- McEvoy, G., Snow, E., & Miller, J. (2008). American society of health system pharmacists. Bethesda AHFS drug information. 1st ed. USA: AHFS Drug Information.
- Meng, X. Y., Zhang, H. X., Mezei, M., & Cui, M. (2011). Molecular docking: a powerful approach for structure-based drug discovery. *Current computer-aided drug design*, 7(2), 146-157.
- Moffat, A. C., Osselton, M. D., Widdop, B., & Watts, J. (2011). Clarke's analysis of drugs and poisons (Vol. 3). London: Pharmaceutical press.

- Mukesh, B., & Rakesh, K. (2011). Review on Molecular docking. *Ijrap*, 2(6), 1746-51..
- Neels, H. M., Sierens, A. C., Naelaerts, K., Scharpe, S. L., Hatfield, G. M., & Lambert, W. E. (2004). Therapeutic drug monitoring of old and newer anti-epileptic drugs. *Clinical Chemistry and Laboratory Medicine (CCLM)*, 42(11), 1228-1255.
- Özkan, S. A., Erk, N., & Sentürk, Z. (1999). Simultaneous determination of two-component mixtures in pharmaceutical formulations containing chlordiazepoxide by ratio spectra derivative spectrophotometry.
- Park\*, M. W., & Yeo, S. D. (2010). Antisolvent crystallization of roxithromycin and the effect of ultrasound. *Separation Science and Technology*, 45(10), 1402-1410.
- Park, M. W., & Yeo, S. D. (2012). Antisolvent crystallization of carbamazepine from organic solutions. *Chemical Engineering Research and Design*, 90(12), 2202-2208.
- Paulino, A. S., Rauber, G., Campos, C. E. M., Maurício, M. H. P., De Avillez, R. R., Capobianco, G., ... & Cuffini, S. L. (2013). Dissolution enhancement of Deflazacort using hollow crystals prepared by antisolvent crystallization process. *European Journal of Pharmaceutical Sciences*, 49(2), 294-301.
- Pharmacopeia, U. S. (2016). National Formulary [current revision]. Rockville, MD: US Pharmacopeial Convention.
- Pouretedal, H. R. (2014). Preparation and characterization of azithromycin nanodrug using solvent/antisolvent method. *International Nano Letters*, 4(1), 103.
- Pramanick, S., Singodia, D., & Chandel, V. (2013). Excipient selection in parenteral formulation development. *Pharma Times*, 45(3), 65-77.
- Ramisetty, K. A., Pandit, A. B., & Gogate, P. R. (2013). Ultrasound-assisted antisolvent crystallization of benzoic acid: effect of process variables supported by theoretical simulations. *Industrial & Engineering Chemistry Research*, 52(49), 17573-17582.
- Rangaraju, A., & Rao, A. V. (2013). A review on molecular docking: Novel tool in drug design and analysis. *J Harmon Res Pharm*, 2, 215-21..
- Ren, X., Qi, J., Wu, W., Yin, Z., Li, T., & Lu, Y. (2019). Development of carrier-free nanocrystals of poorly water-soluble drugs by exploring metastable zone of nucleation. *Acta pharmaceutica sinica B*, 9(1), 118-127.
- Sawyer, M., & Kumar, V. (2003). A rapid high-performance liquid chromatographic method for the simultaneous quantitation of aspirin, salicylic acid, and caffeine in effervescent tablets. *Journal of chromatographic science*, 41(8), 393-397.
- Segall, M. (2014). Advances in multiparameter optimization methods for de novo drug design. *Expert opinion on drug discovery*, 9(7), 803-817.
- Semah, F., Gimenez, F., Longer, E., Laplane, D., Thuillier, A., & Baulac, M. (1994). Carbamazepine and its epoxide: an open study of efficacy and side effects after carbamazepine dose increment in refractory partial epilepsy. *Therapeutic drug monitoring*, 16(6), 537-540.
- Seybold, P. G., May, M., & Bagal, U. A. (1987). Molecular structure: Property relationships. *Journal of Chemical Education*, 64(7), 575.

- Shegokar, R., & Müller, R. H. (2010). Nanocrystals: industrially feasible multifunctional formulation technology for poorly soluble actives. *International journal of pharmaceutics*, 399(1-2), 129-139.
- Sinha, B., Müller, R. H., & Möschwitzer, J. P. (2013). Bottom-up approaches for preparing drug nanocrystals: formulations and factors affecting particle size. *International journal of pharmaceutics*, 453(1), 126-141.
- Skoog, D. A., West, D. M., Holler, F. J., & Crouch, S. R. (2013). *Fundamentals of analytical chemistry*. Nelson Education.
- Sweetman, S. C., & Blake, P. S. (2011). *Martindale. The complete drug reference*, 33.
- Teng, H., Chen, L., & Lee, W. Y. (2017). Anti-Solvent Crystallization of L-Alanine and Effects of Process Parameters and Ultrasound. *Food Science and Technology Research*, 23(4), 495-502.
- Thorat, A. A., & Dalvi, S. V. (2012). Liquid antisolvent precipitation and stabilization of nanoparticles of poorly water-soluble drugs in aqueous suspensions: Recent developments and future perspective. *Chemical Engineering Journal*, 181, 1-34.
- Todeschini, R., & Consonni, V. (2009). *Molecular descriptors for chemoinformatics: volume I: alphabetical listing/volume II: appendices, references* (Vol. 41). John Wiley & Sons.
- Tripathi, A., & Misra, K. (2017). Molecular Docking: A structure-based drug designing approach. *JSM Chem*, 5(2), 1042-1047.
- Tripathi, A., & Misra, K. (2017). Molecular Docking: A structure-based drug designing approach. *JSM Chem*, 5(2), 1042-1047.
- Tropsha, A., Gramatica, P., & Gombar, V. K. (2003). The importance of being earnest: validation is the absolute essential for successful application and interpretation of QSPR models. *QSAR & Combinatorial Science*, 22(1), 69-77.
- Twyman, R. E., Rogers, C. J., & Macdonald, R. L. (1989). Differential regulation of  $\gamma$ -aminobutyric acid receptor channels by diazepam and phenobarbital. *Annals of Neurology: Official Journal of the American Neurological Association and the Child Neurology Society*, 25(3), 213-220.
- Vardanyan, R. (2017). *Piperidine-based drug discovery*. Elsevier.
- Viçosa, A., Letourneau, J. J., Espitalier, F., & Re, M. I. (2012). An innovative antisolvent precipitation process as a promising technique to prepare ultrafine rifampicin particles. *Journal of crystal growth*, 342(1), 80-87.
- Walfish, S. (2006). Analytical methods: a statistical perspective on the ICH Q2A and Q2B guidelines for validation of analytical methods. *BioPharm International*, 19(12), 1-6.
- Wang, Z., Chen, J. F., Le, Y., Shen, Z. G., & Yun, J. (2007). Preparation of ultrafine beclomethasone dipropionate drug powder by antisolvent precipitation. *Industrial & engineering chemistry research*, 46(14), 4839-4845.
- Waring, M. J., Arrowsmith, J., Leach, A. R., Leeson, P. D., Mandrell, S., Owen, R. M., ... & Weir, A. (2015). An analysis of the attrition of drug candidates from four major pharmaceutical companies. *Nature reviews Drug discovery*, 14(7), 475-486.

- Wójciak-Kosior, M., Skalska, A., & Matysik, A. (2006). Determination of phenothiazine derivatives by high performance thin-layer chromatography combined with densitometry. *Journal of pharmaceutical and biomedical analysis*, 41(1), 286-289.
- Xie, Y., Shi, B., Xia, F., Qi, J., Dong, X., Zhao, W., ... & Lu, Y. (2018). Epithelia transmembrane transport of orally administered ultrafine drug particles evidenced by environment sensitive fluorophores in cellular and animal studies. *Journal of Controlled Release*, 270, 65-75.
- Yetisgin, A. A., Cetinel, S., Zuvun, M., Kosar, A., & Kutlu, O. (2020). Therapeutic nanoparticles and their targeted delivery applications. *Molecules*, 25(9), 2193.
- Zhang, Z. B., Shen, Z. G., Wang, J. X., Zhao, H., Chen, J. F., & Yun, J. (2009). Nanonization of megestrol acetate by liquid precipitation. *Industrial & engineering chemistry research*, 48(18), 8493-8499.
- Zhang, Z. B., Shen, Z. G., Wang, J. X., Zhao, H., Chen, J. F., & Yun, J. (2009). Nanonization of megestrol acetate by liquid precipitation. *Industrial & engineering chemistry research*, 48(18), 8493-8499.

## **BACKGROUND**

MARWA OBAID KHALAF was born in Iraq. After graduated from High school Samarra in (2003-2004), she graduated from Tikrit University-Engineering Faculty- Chemical Engineering department in (2007-2008). She entered Ondokus Mayis University – Nanoscience and Nanotechnology department - Master's program (English) in (2019). She is working as a chemical analyst in a pharmaceutical company in Iraq since graduation, speaks English at a good level. Basic interests include reading, cooking and decoration (25-6-2021).

### **Contact information**

STUDENT NO. : 19211551

ORCID ID : <https://orcid.org/0000-0002-2520-4195>.